DETERMINATION OF STABILITY CONSTANTS OF Eu^{3+} ION WITH AMINO ACIDS BY SPECTROPHOTOMETRIC TITRATION AND THE HYPERSENSITIVE TRANSITION INTENSITIES IN THESE COMPLEXES

A Thesis Submitted
In Partial Fulfilment of the Requirements
for the Degree of
DOCTOR OF PHILOSOPHY

by
SHASHI JAIN

to the
DEPARTMENT OF PHYSICS
INDIAN INSTITUTE OF TECHNOLOGY, KANPUR
APRIL, 1983

CERTIFICATE

Certified that the work presented in this thesis is the original work of Shashi Jain carried out under our supervision.

This work has not been submitted elsewhere for a degree.

R.C. Srivastava
Professor
Department of Physics
I.I.T., Kanpur.

P. Gupta Bhaya
Assistant Professor
Department of Chemistry
I.I.T., Kanpur.

ACKNOWLEDGEMENTS

I express my deep indebtedness to my supervisors Dr. R.C. Srivastava of the Department of Physics and Dr. P. Gupta Bhaya of the Department of Chemistry, I.I.T., Kanpur for their affectionate guidance throughout the course of this work.

I would like to thank Dr. G.K. Lal, Dr. Y.R. Waghmare, Dr.(Mrs.) P. Sharma for inspiration and for providing me a sense of direction, Dr. N. Satyamurthi and Shri T. Joseph for the CURVEFIT programme, Dr. P. Gans of Sheffield University for sending instructions regarding MINIQUAD programme, Dr. U.C. Agarwala and Dr. S. Chandrasekharan for advice, Dr. H.D. Bist, Dr. V.N. Sarin, Dr. S.C. Sen for making the key to the Cary 17D room available at odd hours, Shri R.K. Jain for his affectionate understanding and able assistance regarding Cary 17D Spectrometer use, Shri V. Manuja for ably maintaining Cary 17D, Shri R.M. Jha and Shri Imran Khan for repairs of Cary 17D at crucial moments, Shri Vishal Saxena for helping out at difficult moments with help in various matters including Cary 17D, Shri Joginder Singh for, among other things, keeping the balance in good shape, Shri Amrit Lal Gupta and Shri D.R. Kakkar for keeping the lab going, Shri Panna Lal and Shri R.K. Gupta for help in many ways, Shri Y. Kamalakara Rao for help in preparation of the thesis at the last moment, Shri Ashok Srivastava for advice on the computer programme,

Shri J.P. Gupta for efficient typing and Shri H.K. Panda for able cyclostyling.

Last but not least, I thank my parents, parents-in-law and my husband, Anil, for their encouragement. My children bore my long absence from home with patient understanding.

SHASHI JAIN

CONTENTS

LIST OF TABLES AND FIGURES

Chapter 3

Chapter 4

LIST OF FIGURES

SYNOPSIS

DETERMINATION OF STABILITY CONSTANTS OF Eu^{3+} ION WITH AMINO ACIDS BY SPECTROPHOTOMETRIC TITRATION AND THE HYPERSENSITIVE TRANSITION INTENSITIES IN THESE COMPLEXES

Shasi Jain
Ph.D. Thesis
Department of Physics
Indian Institute of Technology, Kanpur, India

The first part of the thesis describes the details of a spectrophotometric technique for the determination of the stability constants of association equilibria of amino acids and Eu^{3+} ion. The concentration of free metal ion in the presence of a definite concentration of metal and ligand is determined by measuring spectrophotometrically the displacement of a metal-dye (in particular murexide) equilibrium by ligand binding to metal. The displacement occurs because the metal-ligand equilibrium is coupled to the metal-dye equilibrium. The titration data i.e. the concentration of free metal ion in the presence of varying concentration of metal and ligandare analysed by a versatile computer programme. The computer programme identifies the species and calculates the values of the respective equilibrium constants, which give ''best fit'' with the experimental data. The measurement of free metal ion concentration requires accurate values of stability constants for metal-murexide equilibrium. The literature values were obtained in the presence of buffer,

but the values were not properly corrected for binding of buffer to metal. Since Eu^{3+} binds buffer sufficiently strongly, these values needed serious correction. The extinction coefficient of murexide as a function of temperature and at two pH's were determined, as well as the values of $\Delta \varepsilon$, the difference in molar extinction coefficient of metal-murexide complex and murexide at the experimental pH and temperature. The metal-murexide equilibrium constants were redetermined by direct adjustment of pH in the cuvette without any buffer. The values differ considerably from published values and are highly reproducible.

In the metal-ligand titration experiments, one would need metal-buffer binding constants and one prefers a buffer that weakly binds metal ions. ''Good buffers'' are obvious choices. Binding constants of Eu^{3+} to ''Good buffers'' (in particular TES) are determined by titrating TES solution with Eu^{3+} in the presence of murexide, the Eu^{3+}-murexide stability constant being already known. For experiments at pH 5, acetic acid-sodium acetate buffer is used, since Good buffers which do not bind Eu^{3+} strongly are not available at this pH. In this case the correct value of metal-buffer equilibrium constant is even more important. The correction is large and a significant error in a large correction factor can introduce substantial error in the quantities that are ''fitted'' by the binding parameters in the computer programme. Binding constant of Eu^{3+}-acetate equilibrium, reported in the

literature had acceptable precision but low accuracy. This quantity was redetermined by spectrophotometric titration in the presence of murexide.

The stability constants of Eu^{3+} with Aspartic acid, Glutamic acid, Glutamine and Aspargine at 15°C, 25°C, 35°C and at fixed pH's 5.0 and 6.5 are determined using these data. The experimental details and discussion of errors are presented in detail. Discussion on the choice of technique and experimental conditions, with appropriate reference to literature is presented. The details of the programme are also given.

In the second part of the thesis the enhancement of the absorption intensity of the ''hypersensitive'' band between 464 nm-466 nm in the amino acid complexes of Eu^{3+} are reported. With the known values of equilibrium constants, one calculates the enhancement per mole of the complexes.

The observed hypersensitive absorption band is a superposition of absorption bands arising out of a maximum of five different transitions, slightly shifted in frequency from each other. The hypersensitive band of Eu^{3+} (aquo) and the Eu^{3+}-amino acid complexes are analysed in terms of overlapping Gaussians by a computer programme. This allows a measurement of the differential enhancement of transition probability of individual absorption transitions. The Gaussian at the longest wavelength is clearly enhanced more

significantly relative to the others. It is also shifted to shorter wavelength more significantly. There is a clear difference in line shape between spectra at pH 5.0 and at pH 6.5. The data on total enhancement of oscillator strength per mole and lineshape analysis of Eu^{3+}-Amino Acid complexes are discussed. Oscillator strength of Eu^{3+}(aquo) ion changes with temperature. It is interpreted in terms of an equilibrium between different aquated species in solution.

The thesis is divided in five chapters. In Chapter I we provide the background for the research described in later chapters. The use of lanthanide ions as probe in Ca^{2+} binding biological molecules is discussed. The reports in literature are mostly on application of fluorescence and NMR spectroscopy to Eu^{3+}-doped biomolecules. The possible use of absorption spectroscopy of doped lanthanide ions in structural studies on biomolecules is discussed. Literature reports on use of hypersensitive bands to structure elucidation of small lanthanide complexes in solution are summarized. The techniques of determination of equilibrium constant are discussed. The relevance of the work presented in the later chapters is highlighted. In Chapter II we describe the details of the determination of Eu^{3+}-murexide equilibrium constant. In Chapter III we describe the details of the determination of Eu^{3+}-Amino Acid equilibrium constants. The literature reports on the determination of stability constants of Eu^{3+}-Amino Acid equilibrium and on the NMR spectroscopic

investigations of the structure of these complexes are discussed critically. In Chapter IV, the experimental details of the measurement of molar enhancement of oscillator strength and the results of lineshape analysis are summarized. In Chapter V, we summarize the conclusions and point towards future developments.

CHAPTER 1

Introduction

The importance of metal ions such as Na^+, K^+, Ca^{2+}, Mg^{2+}, Cu^{2+}, Mn^{2+}, Fe^{2+}, Fe^{3+} ions in biological processes is firmly established and well documented in physiological literature [1]. Ca^{2+} ion plays an important role in the activity of neurotransmitter substances [2]. Mg^{2+} and Ca^{2+} ions influence the contraction of striated muscle in a variety of ways [3,4]. Only trace amounts of Ca^{2+} ion is needed for the control of contracticle behaviour. Of all the ions in blood, only Ca^{2+}, when injected intracellularly can turn on the muscle [5]. Thus, the processes have high specificity. Calcium is intimately involved in mitochondrial function [6]. In many systems, in which a stimulus, electrical or chemical elicits a secretory response, Calcium is a necessary component in the external medium. The intracellular Calcium levels rise following stimulation. Often, the level of cyclic AMP is coupled with Calcium level. Nearly all membranes maintain a Ca^{2+} ion concentration gradient. Following a stimulus, the membrane must allow the passage of a pulse of Calcium ions [6]. Many of these processes are incompletely understood.

On the molecular level, a large number of Calcium binding proteins have been isolated and characterized by physical and chemical techniques. Structure determination of several of them have been completed using X-ray crystallography.

Spectroscopic techniques have also been extensively applied to study their properties in solution. X-ray structure clearly establish the existence of specific sites for Ca^{2+} ion binding to proteins. The sites distinguish between metal ions of differing size and differing chemical and stereochemical demands [7,8].

Calcium ion does not give many easily observed spectroscopic signals. Some studies have used, for example Ca^{43} NMR [9], but a much larger number of studies have used an isomorphous replacement of Ca^{2+} ions by lanthanide ions. The latter shift and broaden NMR signals and shorten magnetic relaxation times of nuclei spatially close to them. Structural information is derived from the measurement of the shift, line broadening and relaxation enhancement [10-18, 20,21,30]. They also emit radiation, whose characteristics give structural information about the sites [8, 22, 24-29]. Thus, biologically irrelevant lanthanide ions occupy a significant part of biochemical literature.

The choice of lanthanide ions is based on their similarity to Ca^{2+} ion in size and in preference for ionic bonding to ligands. Many of them are trivalent, but this does not seem to make a significant difference in their preference for the same site. Mn^{2+} has a similar size, but in its preference for more polarizable ligands e.g. nitrogen, in preference to oxygen, it resembles Mg^{2+} more closely than Ca^{2+} [7]. The size of lanthanide ions vary along the series.

It is established that metal binding sites of the protein transferrin are so size-specific that they bind the smaller ions in the lanthanide group, but not the larger ones [8].

Replacement of Ca^{2+} by lanthanide ions sometimes leads to preservation of biological activity. α-amylase of B-subtilus [10,11] porcine trypsin [12] and thermolysin [13] are active in presence of either Ca^{2+} or lanthanides, particularly those having ionic radius closer to that of Ca^{2+}. t-RNA is active in presence of Mg^{2+} or Eu^{3+} [14]. Staph nuclease is competitively inhibited by several lanthanides [15,16]. It is interesting to note, in this connection that Ca^{2+} in the nuclease is at the active site, whereas it is not so in trypsin and thermolysin [6].

Trivalent Lanthanide ions, with the exception of $Gd^{(III)}$ have anisotropic magnetic susceptibility. Their electron spin systems relax so rapidly ($\ll 10^{-12}$ seconds) that their EPR spectra are not observable in solution at room temperature. They lead to large dipolar (or pseudo-contact) shift, but do not broaden lines significantly. Gd(III) has isotropic magnetic susceptibility and consequently the electron spin system relaxes more slowly ($\sim 10^{-10}$ sec). It gives an observable ESR signal and affects the relaxation of nuclei near it. Thus Eu(III) is a ''shift probe'' and Gd(III) is a relaxation probe [17]. In the transition series, Fe(III) is a ''shift probe'' and Mn(II) is a ''relaxation probe''. Ofcourse Fe(III) naturally occurs in many proteins. The Fe(III) induced NMR

shift nas been used in the study of the haemoglobin problem [18]. Cu(II) is in between the two extremes. It has anisotropic magnetic susceptibility, but its ESR spectrum is also observable.

Campbell and co-workers [19,20] have used the fact that Gd(III) binds to the active site of lysozyme and inhibits the enzyme. From a study of the difference NMR spectrum arising out of broadening by Gd(III), they have measured the distance of the various residues near the Gd(III) binding site from the Gd(III) ion. The basic principle is that the dipolar coupling between Gd(III) and the proton being observed is dependent on distance and is responsible primarily for relaxation. Theoretical equations relating the relaxation enhancement of the proton being observed and the distance between Gd(III) and the proton are known. Thus the magnitude of relaxation enhancement is a ''spectroscopic ruler''.

Con-A exists either as a dimer or as a tetramer, depending on pH. Each sub-unit has a transition metal binding site and one calcium binding site. Both metal sites must be occupied for Sugar binding to occur. Derivatives of Con-A in which Zn(II), Mn(II) or Co(II) ions occupy the transition metal binding site have equal ability to bind sugar. Using relaxation enhancement in Mn(II)-Con-A., Brewer and co-workers [21] were able to measure distances between the metal ion and each carbon nucleus of the bound sugar using ^{13}C NMR.

The dipolar shift caused by trivalent lanthanide ions other than Gd(III), for example, Eu(III) ion, depends on the distance between the Eu(III) ion and the observed nucleus, as well as on the angular orientation of the vector joining Eu(III) ion and the nucleus. Thus, the interpretation of the shift data requires the distance information from Gd(III) induced relaxation enhancement experiments. Campbell and co-workers [20] first obtained the resonances perturbed by Gd(III) by paramagnetic difference spectroscopy and then shifted these perturbed resonances by shift probes, to obtain information about angular orientation. A combination of shift and broadening data combined with a thorough computer search identified the lanthanide ion binding site in cyclic AMP [22] to be one of two possibilities. The final choice was made on the basis of a Nuclear Overhausser Effect experiment.

A significant amount of work has been done using shift and line broadening techniques using lanthanide ions to determine stability constants and structure of lanthanide-amino acid complexes. This is discussed in Chapter III of this thesis.

Relaxation of water molecules bound to a paramagnetic ion, e.g. Mn(II) or Gd(III), is enhanced to very different extents in aquo ion in bulk water as compared to aquo ion bound to a large macromolecule with a much slower tumbling rate. Eisinger and co-workers [23,24] measured the relaxation

enhancement of water molecules when a macromolecule, such as DNA, is added to an aqueous solution of Mn^{2+} ions. This quantity can be used to monitor metal ion binding, as well as to measure molecular motion parameters relating to water in the metal binding site. The latter is possible, because relaxation enhancement of water bound to metal ions on a macromolecule depends not only on the overall tumbling rate of the macromolecule, but also on the local mobility of the site.

Burton et al. [25] measured the frequency dependence of water proton relaxation rates in IgG-Gd(III) system and concluded that the metal binding site has a large internal mobility. The rotational correlation time of the metal-binding part of IgG has a rotational correlation time of 0.4 to 40 nsec, whereas that of the whole IgG molecule, determined by nanosecond fluorescence depolarization experiments, is 168 nsec [26]. A later experiment [27], based on the measurement on IgG-Gd(III) system in 50% H_2O/50% D_2O mixtures, of relaxation rates of both ^1H and ^2D nuclei, has smaller error and establishes the conclusion of firmer grounds.

Some experiments use two relaxation probes, e.g. a nitroxide spin label and a paramagnetic ion, Mn(II) or Gd(III), and measure the quenching of the ESR signal of the spin label by the paramagnetic ion. The FV fragment of the dinitrophenyl (DNP) binding IgA myeloma protein 315 has one lanthanide ion binding site. Using a series of DNP-nitroxide

spin labels of varying size Sutton and co-workers [28] probed the dimension of the binding site by ESR mobility mapping. The observation of the ESR spectrum of the spin labels also enabled them to monitor the interaction with the lanthanide binding site. The quenching of the ESR signal by Gd(III) over and above that observed for La(III) was used to calculate the distance between the two sites. In order to locate the metal ion unequivocally, the authors had to make the experiment considerably complicated. In addition to using both the optical isomers of a chiral spin label of hapten I and hapten II, they needed data on relaxation enhancement of the protons on the DNP ring (without nitroxide, which would broaden NMR lines to make an NMR experiment impossible) by the Gd(III) ion.

Andersson and co-workers [9] studied the binding of Na^{+} and Ca^{2+} ions to Panulirus interruptus hemocyamin by ^{23}Na and ^{43}Ca NMR spectroscopy. ^{43}Ca nucleus has a quadrupole moment. Relaxation is relatively inefficient in the aquo ion and narrow NMR signal is observed. The relaxation is enhanced when Ca^{2+} binds to a macromolecule and ^{43}Ca NMR is too broad to be observed. When exchange is rapid, a weighted average relaxation rate is measured. The measured relaxation rate allowed the determination of metal-protein stability constants. It was established that two classes of sites are present - strong and weak. The value of pH determines the extent of binding and binding, in turn, determines relaxation

rate of ^{43}Ca nucleus. Thus pH dependence of relaxation rate led to the determination of the pK of the calcium binding groups. It has been suggested that carboxylate groups bind Ca^{2+} ion. Correlation time of ^{43}Ca bound to the weak sites indicate considerable internal motion present at these sites.

Early studies on the application of Fluorescence Spectroscopy of lanthanide ions to biological molecules relied on the transfer of excitation energy from a chromophore in the macromolecules to the lanthanide ion, followed by emission from the latter. Lanthanide ions being very poor absorbers, the study of their fluorescence on direct excitation came later, particularly after lasers were more widely available.

Luk [8] determined the number of lanthanide ions bound to the protein transferrin by ultravoilet difference spectroscopy and showed that the number is two for Tb^{3+}, Eu^{3+}, Er^{3+} and Ho^{3+}, but only one for Nd^{3+}, Pr^{3+}. Thus the size sensitivity of the sites is established and the size is effectively ''measured''. Tb^{3+} fluorescence was enhanced by a factor of 10^5 when excited at 295 mμ, i.e. when the tyrosinate in the protein is the absorber. No enhancement was observed when Tb^{3+} was directly excited at 352 mμ. The lifetime of Tb^{3+} fluorescence was increased marginally from 0.432 msec to 1.27 msec, when bound to transferrin. The non-proportional increase in intensity and lifetime is thought

to be the result of transfer of excitation energy of the protein to the bound Tb^{3+} ion. Excitation spectrum of Transferrin is identical to the UV difference spectrum of the metal-protein complex. The author establishes that the energy transfer from Tyrosinate in the protein to Tb^{3+} is 100% efficient. Thus Tb^{3+} must be directly bound to the Tyrosinate group. The small deuterium solvent effect on the Tb^{3+} fluorescence in the complex indicates that very few water molecules are bound to Terbium. Tb^{3+} fluorescence is virtually unquenched by the presence of a quencher ion, Fe^{3+} bound to the other site. Thus the two sites are at a distance where Förster energy transfer is of negligible magnitude. This leads the author to put the distance between the two metal binding sites at greater than 43 A^{o}. Thus effect of energy transfer on lanthanide ion fluorescence is used as a ''spectroscopic ruler''.

Wolfson and Kearns [29] have used the enhancement of Eu^{3+} fluorescence by very efficient energy transfer from 4-thiouridine, a naturally occurring base in E-coli t-RNA. The authors establish the proximity of the first 3-4 Eu^{3+} binding sites to the thiouridine residue from the efficiency of energy transfer, and determine their binding constants. Excitation spectrum shows 4S-U absorbs light at 340 nm and transfers energy to Eu^{3+}, which emits at 618 nm. t-RNA without 4S-U does not give this fluorescence. If 4S-U is cross linked by photolysis to a nearby cytosine, Eu^{3+} emission is

quenched. Competition experiments suggest that the strong binding sites are the same for Mg^{2+} and Eu^{3+}. Unfractionated t-RNA and purified t-RNA f-Met are similar in their above mentioned spectroscopic properties. This indicates that the strong binding sites are nearly the same for a large group of t-RNA molecules. Two different lifetimes of the ^5D_o state are resolved. The authors conclude that, in addition to the strong sites, weak Eu^{3+} binding sites exist.

Yonuschot and Mushrush [30] showed that Tb^{3+} reacted with DNA and chromatin to form a complex in which Tb^{3+} acted as a sensitive fluorescence probe. By measuring the narrow line emission of Tb^{3+} when DNA is selectively excited, the relative amount of Tb^{3+} bound to the DNA can be calculated. Tb^{3+} was bound to DNA until one Tb^{3+} was present for each phosphate group. After this point, no more Tb^{3+} was bound. Terbium was bound to chromatin in a linear manner until approximately 0.48 $TbCl_3$ was added for each phosphate group in the chromatin - DNA solution. The authors conclude that 52% of the phosphate groups in chromatin were unavailable for binding.

Ferri and Grazi [31] find that six Tb^{3+} ions bind to monomeric actin molecule and fluoresce strongly at 545 nm when excited at 285 nm, i.e. when the protein is the absorber. Actin polymerizes in the presence of salt. In $MgCl_2$ and KCl solutions, two different polymeric forms are observed. The association constants and number of binding sites in the two

forms are different and are determined by measurement of Tb^{3+} fluorescence.

Horrocks and co-workers [32] studied the fluorescence of lanthanide ions resulting from the direct excitation of Eu^{3+} and Tb^{3+} ions by a laser. In the case of Eu^{3+} ion, the particular transition studied by them very briefly, in this short communication is the $^7Fo \longrightarrow {}^5D_2$ transition studied by us in absorption spectroscopy in this thesis. The life-time is considerably shorter in $Eu(H_2O)_n$ ion in comparison to $Eu(D_2O)_n$ ion. This is related to the phenomenon of electronic relaxation by energy transfer between electronic and vibrational degrees of freedom. OH oscillators act independently of other ligands in dessipating energy. Thus number of H_2O molecules co-ordinated to the metal ion can be found. These authors find that two water molecules are co-ordinated to Eu(III) and Tb(III) ions substituted in Calcium site I of the protein thermolysin.

Wang and co-workers [33] showed that two of the four Ca^{2+} binding sites of calmodulin bind Tb^{3+} strongly and the other two bind Tb^{3+} weakly. The same preference in binding applies to Ca^{2+} also. With Calmodulin selectively nitrated (nitrotyrosines do not fluoresce) at either of the two tyrosine groups can transfer energy to the bound Tb^{3+}, the fluorescence of only Tyr-138 is sensitive to metal-binding. Eu^{3+} ion fluorescence is observed following direct excitation of $^7F_o \longrightarrow {}^5D_o$ line of Eu^{3+} ion at 579 nm by a laser. The

emission ($^5D_o \longrightarrow {}^7F_2$) is observed at 612 nm. The transition being excited has the feature that under any ligand field, neither the ground nor the excited state (being singly degenerate) split. Thus, the fact that the excitation spectrum of the fluorescence remains a single peak at 579.3 nm, and only increases in intensity during a titration suggest strongly that the four ion binding sites have identical microenvironment.

The same group [34] find in their study of Troponin-C that the excitation spectrum of Eu^{3+} fluorescence on direct excitation by a laser has two closely spaced overlapping, but clearly resolvable, peaks at around 579 nm. Thus the microenvironment of Ca^{2+} ion binding sites are different. Fluorescence of Tb^{3+} and Eu^{3+}, sensitized by energy transfer from the protein and the change of fluorescence of the tyrosine chromophore of the protein on metal-binding are used to monitor metal ion binding to protein. The existence of two classes of metal binding sites is established.

These workers use the relationship between the difference in lifetime of $Eu(H_2O)_n^{3+}$ and $Eu(D_2O)_n^{3+}$ and the number of co-ordinated water molecules [34] to show that the number of co-ordinated water molecules at the strong sites of Troponin-C [34] is two and that at the weak sites is three. In Calmodulin [33] all four sites show the number to be 1.38, i.e. number of H_2O molecules at each site fluctuate but the average value is identical.

Krebs and Carafoli [35] studied Ca^{2+} induced conformational change of Calmodulin under a variety of conditions by PMR techniques. The Phenylalanine residue responsible for resonances at 6.47 ppm (Ca^{2+} free form) and 6.64 ppm (Ca^{2+} saturated form) respectively are shown to be located close to the Ca^{2+} binding site by a combination of Gd^{3+} induced NMR line broadening experiments and a Nuclear Overhausser enhancement of Phenylalanine residues on irradiation of the metal-binding Tyrosine resonances.

Thus the application of NMR and Fluorescence spectroscopy has yielded very detailed structural information about metal-binding biological molecules. In contrast, absorption spectroscopy of lanthanide ions has not been applied in Biochemistry at all. The state of art in the field of application of absorption spectroscopy of lanthanide ions to the determination of structure of co-ordination compounds in solution has recently been reviewed by Yatsimirskii and Davidenko [36].

The absorption spectra of lanthanide ions have low intensity, complex fine structure and are relatively inert towards changes in the lanthanide ion environment. In solution, the lines are broadened by the coupling between the electronic degrees of freedom of the ion and the vibrational degrees of freedom of the solvent. Of the various absorption transitions in lanthanide ions, there is one class, which is exceedingly sensitive ("hypersensitive") to

microenvironment, The absorption is very weak on an absolute scale, but its enhancement factor varies widely in going from one micro-environment to another. Henrie and co-workers [37] have reviewed the field of hypersensitivity in the electronic transitions of lanthanide and actinide complexes.

Since hypersensitive transition intensity of an ion is sensitive to its microenvironment, absorption spectroscopy of lanthanide ions is potentially a very useful tool for the biochemist. Our experience with the Eu^{3+}-amino acid systems (Chapter 4) shows that with the absorption spectrometers now available, one should be able to measure the weak hypersensitive absorption spectrum of Eu^{3+} ions bound to proteins with good accuracy if one uses long path length cells as well as the repititive scanning accessory to carry out time averaging. Since the absorption line intensities can be measured accurately, one must study the more well defined simpler systems in detail to appreciate the structural information obtainable from various features of the absorption spectra. It is unfortunate that Fourier transform spectroscopy has not revolutionized the field of UV and Visible spectroscopy in the same way as it has influenced the field of Infrared and NMR spectroscopy. Nonetheless, even without FT techniques, absorption spectrum of lanthanide ions as a probe for Ca^{2+} binding sites in biological molecules, will receive more attention in the years to

come. Whether the information content and their interpretability will match those in fluorescence and NMR, is too early to assess, but at the very worst, information gathered from absorption spectroscopy will complement those from fluorescence and NMR.

A considerable amount of work has been done on the quantitative understanding of the oscillator strength of lanthanide ions placed in different environments in crystals as well as isolated complexes. The oscillator strength of transitions between states arising from f^n configuration is particularly interesting. In a few cases, the transitions derive their intensity wholly or partially by magnetic-dipole mechanism. The selection rules for magnetic dipole transition are $\Delta J \leq 1$, (but not $0 \leftrightarrow 0$), $\Delta L = 0$, $\Delta S = 0$ and $\Delta \ell = 0$ in the Russell Saunders Coupling scheme. Strong spin-orbit coupling weakens the constraints on L and S, but the constraint on J is rigorous. The second important mechanism is electric dipole in character. Static and dynamix crystal field perturbation mix excited state wave functions of a parity different from that of f^n states to the wave function of f^n states. Thus a ''parity forbidden'' electric dipole transition becomes ''weakly allowed''. Judd [38] and Ofelt [39] have derived theoretical equations assuming the ''forced electric dipole mechanism''. Under certain approximations the equation assumes a simple form with only three parameters,

$$P = \sum_{\lambda=2,4,6} \bar{\nu}\, T_\lambda \langle f^n \psi J \,|\, u^{(\lambda)} \,|\, f^n \psi' J' \rangle$$

$|f^n \psi J\rangle$ and $|f^n \psi' J'\rangle$ are eigenvectors of the initial and final states arising from f^n configuration. These are unperturbed wave functions. $\bar{\nu}$ is the wave number of the baricenter of the absorption band. Equations for T_λ depend on the perturbation mechanism. If it is static crystal field, theoretical expression for T_λ contains static crystal field parameters, refractive index of the medium and integrals involving perturbed radial wave function of the metal ion. If the perturbation mechanism is dynamic crystal field, the expression contains derivatives of crystal field parameters with respect to normal coordinates of vibration, matrix elements $\langle n | Q_i | n' \rangle$ where $|n\rangle$ and $|n'\rangle$ are initial and final vibrational eigenstates and Q_i is the normal coordinate of vibration, population of initial vibrational state, in addition to refractive index and appropriate radial integrals. The theory predicts that for P to be non-zero $|\Delta J| \leqslant 6$, $|\Delta L| \leqslant 6$, $|\Delta S| = 0$ and if either J or J' = 0, $|\Delta J|$ must be even. For the matrix elements of $u^{(2)}$ to be non-zero $|\Delta J| \leqslant 2$, $|\Delta L| \leqslant 2$ and $|\Delta S| = 0$ and if either J or J' = 0 $|\Delta J|$ must be 2. The constraints on $|\Delta J|$ are expected to be fairly rigorous, while those on $|\Delta L|$ and $|\Delta S|$ will be less so, because of strong spin-orbit coupling in lanthanides [66]. The condition for non-zero $u^{(2)}$ is the same as the selection

rules for quadrupolar transition. The hypersensitive transitions, of interest in this thesis, have large values for $u^{(2)}$ matrix elements. In the Judd-Ofelt equation for P, T_2 is the coefficient of $u^{(2)}$ matrix elements. Thus if T_2 is environment sensitive, P will change by large magnitudes in going from one environment to another taking advantage of the large value of $u^{(2)}$. The fact that hypersensitive transitions obey quadrupolar selection rules, owes its origin to the theoretical result that the conditions for non-zero values of $u^{(2)}$ is the same as quadrupolar selection rules. In this model, hypersensitive transition is "forced electric dipole" in nature.

To give an example, the hypersensitive transitions in Nd^{3+} are $({}^4G_{5/2}, {}^2G_{7/2}) \leftarrow {}^4I_{9/2}$ and ${}^4G_{7/2} \leftarrow {}^4I_{9/2}$ ($|\Delta J| \leq 2$) located at $\sim 7300\ cm^{-1}$ and $19200\ cm^{-1}$ respectively. The $u^{(2)}$ matrix elements of Nd^{3+} are substantial (-0.2580 for ${}^2G_{7/2}$, -0.9471 for ${}^4G_{5/2}$ and 0.2529 for ${}^4G_{7/2}$), whereas they are close to zero for the other transitions (e.g., 0 for ${}^2L_{15/2}$, ${}^4D_{1/2}$) the largest being 0.0986 for ${}^2H_{9/2} \leftarrow {}^4I_{9/2}$ [38

Jorgensen and Judd [40] proposed an alternative model, which assumes that the hypersensitive transitions are basically electric quadrupole in nature. The expression of the oscillator strength due to electric quadrupole mechanism is [66]

$$P = \frac{4\pi mc}{3h} \chi \sum \Omega_2 \left\langle f^n \psi J \middle| u^{(2)} \middle| f^n \psi' J' \right\rangle$$

where

$$\Omega_2 = (2J+1)\frac{56\pi^2}{225}\,\bar{\nu}^2\,\langle 4f|r^2|4f\rangle^2$$

The form of this equation is identical to the first term of Judd-Ofelt equation, with the important difference that T_2 (quadrupole) is dependent on the frequency of radiation. The experimental oscillator strengths of hypersensitive transitions are 10^2 to 10^5 times larger than that predicted the equation given above [41], and the Ω_2 parameter does not show the $\bar{\nu}^2$ dependency required by this equation. Ω_2 in a number of Er(III) complexes show a ratio of oscillator strengths of the two hypersensitive transitions between 1 and 1.3, whereas the equation given above predicts a ratio of 1.92 [41]. Thus a pure quadrupolar transition mechanism arising from the coupling of quadrupole moment of the electronic charge distribution with the electric field gradient of the radiation field at the ion is clearly insufficient to account for experimental oscillator strengths. Jorgensen and Judd [40] proposed that inhomogeneity of dipoles induced by electromagnetic field in molecules-ligands or solvent molecules around the metal ion, enhances the electric field across the metal ion. They are able to account for the magnitude of intensity in Nd^{3+} and Er^{3+} aquo ions by a semiquantitative estimate within a factor 30. This mechanism also does away with the frequency dependence of Ω_2, because the primary source of electric field gradient is no longer the spatial dependence of the electric field of the radiation [41].

More recently, Mason, Peacock and Stewert have developed a theory, which originates from the idea of Fajans that the phenomenon of metal-ligand perturbation is reciprocal, i.e., the electric field of the ligand affects the metal and that of the metal polarizes the ligand [41]. This idea has been formulated in the form of a formal mathematical theory. For a metal-ion transition with a vanishing zero-order electric-dipole moment, the expression for the first order electric dipole moment of the perturbed metal ion transition has terms over and above that given in the crystal field theory. The additional terms represent the coulombic correlation of transient electric dipole moments in the ligands by the transitional charge distribution of the metal ion. The leading term in the transitional charge distribution for hypersensitive transition is the electric quadrupole. The expression derived by Mason, Peacock and Stewert [41] for oscillator strength (the mechanism is electric-dipole) is

$$P = \frac{8\pi^3 mc}{3h}\,\nu\,\Omega_2 \left\langle f^n \psi\, J \left| u^{(2)} \right| f^n \psi'\, J' \right\rangle^2$$

where

$$\Omega_2 = \frac{28}{5}(2J+1)\left\langle 4f \left| r^2 \right| 4f \right\rangle^2 \sum_{m=0}^{3} (2-\delta_{m,0})$$

$$\sum_L \left| R_L^{-4}\, \bar{\alpha}\,(L)\, C_m^{(3)}\,(L) \right|^2$$

$\bar{\alpha}(L)$ is the mean polarizability of the ligand L at the f electron transition frequency. R_L is the radial coordinate of the ligand atom L in a coordinate system, where metal ion is at the origin. $Cm^{(3)}$ (L) depends on the angular orientation θ_L, ϕ_L of the ligand L. An interesting point about the equation is that it has the form of the first term of the Judd-Ofelt equation.

Oscillator strength of absorption bands of many lanthanide ions in a variety of environments in crystals as well as isolated complexes in solution have been fitted remarkably well (Typical r.m.s. error $\sim$ 10% of the oscillator strengths) with the three parameter Judd-Ofelt theory. Carnall, Fields and Wybourne, and Carnall, Fields and Rajnak [42], find that oscillator strength of transitions of several lanthanide aquo ions (in dilute acid solution) anhydrous lanthanide nitrate in anhydrous acetic acid solution and in molten nitrate melts can be fitted with three parameters only. The only glaring exception is Pr^{3+} (r.m.s. error in fit $\sim$ 100%). For most bands (ΔJ greater than 2), T_4 and T_6 are sufficient, but T_2 is necessary for hypersensitive bands. T_2 is found to be most sensitive to the environments studied by these workers. They point out that crystal field theory predicts the order of environment sensitivity as $T_6 > T_4 > T_2$. This order is not observed. The failure to account for oscillator strength in Pr^{3+} ion is not surprising. The assumption that difference in energy

between terms of different configurations is much larger than the transition energy which leads to the three parameter Judd-Ofelt theory, breaks down in the case of Pr^{3+} ion. But on this basis, it is surprising that Judd-Ofelt theory accounts for oscillator strength of Tb^{3+}. The approximation holds even less accurately for Tb^{3+}. The excellent agreement for all the ions, even in near-ultraviolet, where this assumption is less valid owes its origin to the fact that if L-S coupling is not seriously violated, only terms of the same spin can interact substantially. In Tb^{3+}, even though the lowest term of the excited configuration is closer to the ground state than it is in Pr^{3+}, the first term of the same spin is separated from the ground state term by a large magnitude of energy. The success of the Judd-Ofelt theory, however does not prove any mechanism, because the form of the equations of oscillator strength for the Judd-Ofelt forced electric dipole, the Jorgensen-Judd forced electric quadrupole, the Mason-Peacock-Stewert dynamic coupling as well as the pure quadrupole mechanism are identical in form.

Peacock [43] pointed out that if one excludes one of the two hypersensitive oscillator strengths from the data, while determining T_λ parameters of a lanthanide ion with two hypersensitive transitions, one gets a much better fit (i.e. r.m.s. error is smaller). The value of T_2 is higher if one uses the higher energy transition in data-fitting.

Thus the oscillator strengths are better parametrized in terms of T_4, T_6 (equal for all the transitions) and one T_2 parameter per hypersensitive transition. In cases, where removing all but one hypersensitive transitions from data fitting leads to a ''much better fit'' T_4 and T_6 alter as well, because of the interdependence of the parameters when determined empirically. Peacock considered the possibility that the failure of the three parameter fit is due to the approximation made in the Judd-Ofelt theory that $E(\psi, J) - E(n', \ell', \psi'', J'')$ and $E(\psi', J') - E(n', \ell', \psi'', J'')$ are equal is not valid. $E(\psi, J)$, $E(\psi', J')$ and $E(n', \ell', \psi'', J'')$ are the energies of the ground and excited states of the $f \leftrightarrow f$ transitions and of the perturbing manifold respectively. But the trend predicted by such a cause on the dependence of T_2 on the energy of transition is not experimentally observed. In addition, it does not explain why T_4 and T_6 should not vary in a way similar to T_2. The frequency dependence of T_2 is not accounted for in the Judd-Ofelt mechanism, but is explained by the dynamic coupling model of Mason et al. [41]. Peacock points out [43] that if only the nonhypersensitive transitions are used in data fitting, T_2 is ill defined, often assumes the disallowed negative values, and is merely a fitting parameter without any physical meaning. The ''real value'' of T_2 is obtained only if the oscillator strength of at least one hypersensitive transition is included in the data to be fitted.

The Judd-Ofelt theory predicts that forced electric dipole mechanism will be of significant importance in symmetries, where expansion of crystal field potential contains Y_{Km} with odd K. In particular, sites with a center of inversion among their symmetry elements will not give rise to enhancement. However Y_{1m} was not allowed in the crystal field potential, because unlike all Y_{Km} with $K > 1$, they possess nonvanishing derivatives at the origin, namely the nucleus of the rare-earth ion. This implies the existence of an electric field at the nucleus and hence that the rare-earth ion and its complex are not in equilibrium [44]. The exclusion of Y_{1m} did not allow the crystal field model to explain the experimental observation that in going from one environment to another, T_2 alters significantly, whereas T_4 and T_6 largely remains unaltered. Varying amplitudes of Y_{1m} from one microenvironment to another alters T_2 alone (there is no T_0), that of Y_{3m} alters T_2 and T_4, and that of Y_{5m} alters T_4 and T_6.

Judd [44] argued, that electrons of the rare-earth ion may also produce an electric field at the nucleus, that exactly cancels that coming from neighbouring ions. The asymmetrical electronic distribution within the rare earth ion can be regarded as being produced by the external electric field. He has listed the 32 point groups of Ci and C_{nv} symmetry which allow the inclusion of such terms. The terms Y_{1m} in combination with the dipole operator reduces to an

effective quadrupole operator within the 4f shell. This explains the quadrupolar selection rule for the hypersensitive transitions. Restriction on the symmetry of the site that allows hypersensitivity exists in the ''dynamic coupling'' theory of Mason, Peacock and Stewert also [41]. Point groups D_p and C_{pv}, with p unrestricted, C_{3h}, D_{3h}, T_d and their subgroups allow hypersensitivity. The dynamic coupling mechanism is forbidden where there is inversion symmetry or a S_p axis with $p \geqslant 5$. Thus the Mason-- Peacock - Stewert theory [41] is less restrictive about symmetry than the crystal field theory [44].

The equations for the T_λ parameters for the static and dynamic crystal field show that if the latter has a significant contribution, the oscillator-strength should be temperature dependent. Change of temperature changes the population of vibrational states, a quantity that appears in expressions for T_λ.

The influence of site symmetry on hypersensitive intensities is well documented in literature. Bukietynska and Choppin [45] measured hypersensitive intensity of Nd^{3+} ion in a nitrate and a sulfate complex and in a $t_n\alpha$ - picolinate complex in aqueous solution. Analysis in terms of T_λ parameters show that T_2 changed most significantly in going from one microenvironment to another. The authors infer that Nitrate complex of Nd^{3+} has low symmetry about the metal ion. The α-picolinate complex is inferred to have a symmetry

not higher than some of the C_{nv} groups. The experimental values of T_2 is in the following order: nitrate > α-picolinate > aquo complex, showing T_2 increases with decreasing symmetry.

Blasse, Bril and Nieuwpoort [46] measured the fluorescence spectra of Eu^{3+} ion in several host lattices. In Ba_2GdNbO_6, the site symmetry of Eu^{3+} is strictly O_h. The emission originates mainly from magnetic dipole and vibronic transitions. In O_h symmetry, electric dipole mechanisms of all transitions - hypersensitive and non-hypersensitive - are forbidden. Vibronic transitions involving noncentrosymmetric vibrations will however be weakly allowed in the Judd-Ofelt model. In $YAl_3B_4O_{12}$, the site symmetry of Eu^{3+} is D_3 and the emission is predominantly electric dipole. The ratio of the intensities of electric and magnetic dipole emission increases strongly with increasing deviation from inversion symmetry achieved by changing chemical composition. These authors point out that in rutile, the polarizability of the oxide anion in the Ti_3O plane present in the structure differ strongly from that perpendicular to this plane [47]. Thus, the Jorgensen-Judd inhomogeneous dielectric model may have contribution to hypersensitive transition intensity of Eu^{3+} in oxide lattices [46].

Kislink, Krupke and Gruber [48] examined spectra of Er^{3+} ion in single crystal of Y_2O_3 in absorption and fluorescence. Of the two inequivalent cation sites C_2 and C_{3i},

the authors demonstrate that only the site without inversion symmetry (C_2) gives rise to the entire observed spectrum.

Rackestraw and Dieke [49] studied Y^{3+} in YCl_3. The point symmetry is approximately octahedral. The small deviation gives substantial intensity to $^2H_{11/2} \leftarrow {}^4I_{15/2}$, $^4G_{11/2} \leftarrow {}^4I_{15/2}$ and $^4I_{11/2} \leftarrow {}^4I_{15/2}$ transitions (the first two are known to be hypersensitive, the third one obeys the selection rule $\triangle J = 2$), while other absorption bands are largely unaffected (excepting one or two transitions to individual ligand field split states in a term). Thus hypersensitive band intensities respond more sensitively to small deviations of symmetry.

Ryan and Jorgensen [50] studied lanthanide hexachloride and hexabromide complexes in nonaqueous solvents and in solid phase. They found that the intensities of the non-hypersensitive transitions of $LnCl_6^{3-}$, $LnBr_6^{3-}$ and $Ln(SCN)_6^{3-}$ are an order of magnitude lower than those of aquo ions, whereas the hypersensitive transition intensities remain either unchanged or increase. The authors observe that the electronic lines are still prominent and weak distortions perhaps exist. Henrie, Fellows and Choppin [37] based on the data of Ryan and Jorgensen [50], Ryan [51] and Henrie and Henrie [52], pointed out that the order of intensities for the non-hypersensitive transitions is $LnCl_6^{3-} > LnBr_6^{3-} > LnI_6^{3-}$, whereas the order is reversed for hypersensitive transitions. The first observation indicates that the hexaiodo complex is the

least distorted of all, from Oh symmetry. The second observation indicates that a small deviation from O_h symmetry enhances hypersensitive transition more significantly. From known trends, covalency is expected to be in the order iodide > bromide > chloride. If one now postulates that covalency enhances hypersensitive intensity, then intrinsically iodide complex will have a higher hypersensitive intensity. The smaller deviation from O_h symmetry is against hypersensitivity in LnI_6^{3-}, but the aid of covalency more than offsets this and leads to the observed order. Covalency enhances hypersensitive intensity by mixing ligand wave function with wave function of metal and thus destroying the odd parity of the $4f^n$ state. In the theoretical expression for T_λ, covalency modifies the radial integrals. Temperature dependent studies find that the intensity of bands (including hypersensitive band) of $NdCl_6^{3-}$ remain unaltered in going from room temperature to 77°K (53). This rules out any aignificant contirbution from vibronic mechanism. It has however been suggested([37], W.T. Carnall, private communication to R.L. Fellows) that one needs to lower the temperature further to rule out vibronic contribution.

In order to give rise to hypersensitivity, covalency should be able to modify T_2 parameter more significantly than T_4 and T_6. There is difference of opinion on this point. Henrie and Choppin [54] in their study of hypersensitivity in $Nd(acac)_3$ and $Nd(EDTA)^-$ showed that the oscillator strength

of hypersensitive transition increases with increase in the nephelauxetic ratio ($\bar{\nu}_{AV}$ complex/ $\bar{\nu}_{AV}$ aquo), which is thought to be a measure of covalency [67]. Using the formula of Jorgensen and Judd [40], these authors get an order of magnitude agreement between observed T_2 and that calculated for vibronic contribution. The correlation with nepheleuxetic ratio leads them to conclude that covalency modifies the radial integrals and thus aids the vibronic contribution. They give semiquantitative arguments to show that the effect of covalency will alter T_2 more significantly than T_4 and T_6. Peacock [55] has also briefly considered the covalent model, but he concludes that T_4 ought to be the most sensitive parameter to covalency. Henrie and Choppin [54] assume that the static crystal field, with or without covalency, has no role to play in hypersensitivity because of the results on hexahalo complexes of lanthanide ions. Their contention that vibronic effect, aided by covalency, leads to hypersensitivity, lacks the very necessary support of data on temperature-dependent oscillator strength.

Krupke and Gruber [56] investigated the intensities of Tm^{3+} ethylsulfate and Krupke [57] reported data on Pr^{3+}, Nd^{3+}, Eu^{3+}, Er^{3+}, Tm^{3+} ions in Y_2O_3 host and Pr^{3+} and Nd^{3+} in LaF_3 host. They find that T_4 and T_6 (which occour in the expression of intensity for nonhypersensitive transitions) cannot be calculated with reasonable agreement assuming only a static

mechanism. There is also some evidence that both parameters are temperature dependent for Tm^{3+} ethylsulfate. However T_2 could be calculated with at least an order of magnitude agreement allowing only a static perturbation. It will be of interest to know if the goodness of fit changes on recalculation (following Peacock [43]) of T_λ parameters taking one hypersensitive transition at a time. Nd^{3+} hypersensitive transition shows a sharp decrease in intensity in going from Y_2O_3 to a site of different symmetry in LaF_3 lattice. Since T_2 is accountable by static mechanism, Krupke considers hypersensitivity in Nd^{3+} due to site geometry alone.

Henrie, Fellows and Choppin [37] have reinterpreted Krupke's data. They point out the possibility that the decrease in Nd^{3+} hypersensitive transition intensity in going from Y_2O_3 to LaF_3 could originate in stronger covalent interaction with oxide (as compared to fluoride). The site symmetry of Y_2O_3 as Krupke observes, also favours a larger intensity. Thus, the reinterpretation stands as follows : Covalent interaction aids the effect of site symmetry. Temperature dependence of intensity was not studied. This is a necessity before ruling out vibronic effect. We like to point out, following Blasse, Bril and Nieuwpoort [46] that one should not overlook the possibility of inhomogeneous dielectric effect of Jorgensen and Judd [40] in oxide lattices. The Mason theory [41] can also account for this effect.

Peacock [58] studied $([LnW_{10}O_{35}]^{7-}$ with Ln = Ho^{3+}, Pr^{3+}. He, in contrast to Henrie and Choppin [54] does not observe, any correlation between nephelauxetic effect and hypersensitive oscillator strength in the Ho^{3+} complexes. Peacock further reports in this paper that the ratio of the oscillator strength (hypersensitive/nonhypersensitive) is the same in solution and in powder reflectance (after appropriate correction) and hypersensitivity is observed even though, the lanthanide is not exposed to solvent. He assumes that inhomogeneous dielectric effect can originate from solvent molecules alone and concludes that the Jorgensen-Judd mechanism (forced electric quadrupole) does not contribute significantly. We point out that inhomogeneous dielectric effect can originate from polarization of the ligand atoms also. This has been often ignored in discussions in literature.

Gruen and Dekock [59] studied oscillator strength of hypersensitive absorption bands of NdI_3 and $NdBr_3$. They find that the oscillator strengths of hypersensitive transitions are 10-15 times larger than the corresponding quantity in Nd^{3+} aquo ion, while nonhypersensitive bands are in general less intense. The authors reject crystal field induced electric dipole mechanism, because the planar D_{3h} symmetry is not in Judd's list of symmetries that cause hypersensitivity. They also reject the inhomogeneous dielectric model of Jorgensen and Judd [40]. The Jorgensen-Judd formula for the ratio of the gradient of electric field created by the induced dipoles

of the ligand atoms to the electric field gradient due to the electromagnetic field alone is

$$\xi_f = \frac{15}{4\pi^2} \frac{n^2-1}{n(n^2+2)} \left(\frac{a}{R}\right)^3 \left(\frac{\lambda}{R}\right),$$

where a is the lattice constant, R is nearest neighbour distance, λ is wavelength of light, n the bulk refractive index. Jorgensen and Judd found ξ_f to be sufficiently large to account for the hypersensitive intensity enhancements in Nd^{3+} and Er^{3+} aquo ions by taking n = 1.5, a = R = 2.5 A^o, λ = 5000 A^o, ξ_f, then is $\simeq$ 75. The ratio of T_2 is proportional to ξ_f^2. Gruen and Dekock [59] used n = 1.001 appropriate for the bulk refractive index of $NdBr_3$ and NdI_3. The factor $(n^2-1)/n(n^2+2)$ is then smaller by a factor of 10^3. Thus inhomogeneous dielectric effect estimated in this manner fails by a factor of 10^6 to account for hypersensitivity of gaseous NdI_3 and $NdBr_3$. The authors calculate the contribution of vibronic mechanism to T_2 using the formula derived by Jorgensen and Judd [40]

$$T_2^{vib} \sim 7 \left[N(\rho'')^2 a_o^4/(\rho')^6\right] \times 10^{-17} \text{ Sec.}$$

N is a dimensionless factor of the order of 10, ρ' is the radius of the oscillating complex containing the lanthanide ion and its immediate neighbours, ρ'' the amplitude of the oscillation. Using $\rho'' \sim 0.1$ A^o and $\rho' \sim 1$ A^o, they find T_2^{vib} is sufficient to explain most of the hypersensitivity

observed. The agreement is to a great extent due to the use of an unrealistic value of $\rho' = 1$ A^{o}, because in the vapor Nd-X (Br, I) distances are 2.72 and 2.94 A^{o}. Thus, $\rho' \simeq 3$ A^{o} is more appropriate. This would make the agreement go off by a factor of $\simeq 10^{3}$. Jorgensen and Judd [40] found the vibronic contribution to T_2 is too small because they used a realistic value of $\rho' \simeq 4$ A^{o} for Nd^{3+} and Er^{3+} aquo ions.

These authors also point out the possible role of covalency, even though the nature of the orbitals involved in covalent bond formation is only qualitatively discussed. The covalency modifies the radial integrals in the expressions for T_2 and enhances its magnitude. The reasons for proposing that the role of covalency is significant is two fold. NdI_3 has a higher hypersensitive intensity than $NdBr_3$. It is known that the order of tendency to form covalent bond is I $>$ Br. Secondly, the bond length decreases and hypersensitive intensity increases in going from solid NdI_3 to the vapour phase. Decrease in bond length by $\sim 12\%$ indicates a substantial increase in covalency. Thus, it is proposed that increase in covalency aids the increase in hypersensitive transition intensity by vibronic mechanism. The proposal of vibronic mechanism however lacks the necessary support of data confirming temperature dependence of oscillator strength.

Gruen and Dekock [59] reject the inhomogeneous dielectric model by using the bulk refractive index of the gas in

the Jorgensen-Judd equation. NdI_3 molecule may as a whole, be in a homogeneous dielectric. But Nd^{3+} ion definitely would sense any electric field gradient across the Nd^{3+} ion set up by the dipoles induced in I^- ions by the electromagnetic field. The D_{3h} symmetry may make this effect disappear, for this static structure. Vibrational motion of certain types may however make this effect non-zero. An evaluation of this effect has not yet been done properly.

The theory of Mason, Peacock and Stewert [41] however registers a major triumph by quantitatively accounting for the hypersensitive intensity in Nd-trihalides. The $^4G_{5/2} \leftarrow {}^4I_{9/2}$ transition intensity of Nd(III) near 17000 cm^{-1} has the oscillator strength ($10^{-6}P$) of 5.6 for NdF_3 in the LaF_3 crystal [57] compared with a value of 530 for NdI_3 in vapor phase [59]. Highlighting the role of polarizabilities the theory quantitatively accounts for this variation of oscillator strength over two orders of magnitude. It also quantitatively accounts for the substituent effects observed in the lanthanide tri β-dicarbonyl chelate complexes. As stated earlier, it also accounts for the frequency dependence of T_2.. However, even though it predicts small polarizability dependent red shift of the transition frequency, of the order of 5 cm^{-1}, it cannot quantitatively account for the nephelauxetic red shift.

There is one piece of experimental evidence that argues against the Jorgensen-Judd forced electric quadrupole mechanism.

Blanc and Ross [60] studied polarized absorption in the $^5D_2 \leftarrow {}^7Fo$ hypersensitive transition and emission in the $^5D_o \rightarrow {}^7F_2$ hypersensitive transition of Eu^{3+} ion in an organic chelate, in crystalline phase. Both sets of transitions consist of three lines, two polarizing strongly perpendicular to the crystallographic C-axis, the third polarizing parallel to this axis. On the basis of quadrupolar selection rules, the number of allowed transitions for almost all of the appropriate symmetries is expected to be greater than three. Complete polarization is also not to be expected of quadrupolar transitions.

We stated earlier that the proposal for vibronic mechanism for $Nd(acac)_3$, $Nd(EDTA)^-$ [54], and for Nd-trihalides [59] lack the necessary support of data regarding temperature dependence of oscillator strength. Peacock [61] has reported the absorption spectra of solid glasses of $K_{13}[Eu(SiW_{11}O_{39})_2]$ and $K_{13}[Ho(SiW_{11}O_{39})_2]$ at 295 ^oK and 80 ^oK. He finds that the spectra are temperature independent. Gruber, Menzel and Ryan [53] also find temperature independence of spectral line intensities in $[(C_6H_5)_3PH]_3NdCl_3$. Lanthanide tricyclopentadienides show large temperature variation of the oscillator strengths when cooled at 4 ^oK [62]. This observation was made in crystalline phase. Peacock [61b] in a critical survey of the possible role of vibronic contribution to hypersensitive oscillator intensity concludes that in isolated complexes in solution, there is no evidence of vibronic mechanism. There

is some evidence, in its favour, in crystals [56,57,62]. This can be understood if the important vibrations are low frequency lattice modes. Such vibrations would not be available in molecular complexes [41].

The temperature range available for establishing significant temperature dependence of T_λ parameters of complexes in solution may be small [37]. The only evidence of temperature dependence of oscillator strength in solution comes from the work of Bell, Thompson and Helton [63] whose measurements range from 25°C to 356°C. The 5754 A° line of Nd^{3+} increases in intensity by a factor of 5 with increase of temperature. The area under the band and its position change linearly with temperature with changes in slope at 90° and 240°. Temperature dependence is interpreted to be due to vibronic interaction. Increase in temperature, the authors argue, should destroy the inhomogeneity of the dielectric. Thus if the latter was the cause of hypersensitive intensity, increase in temperature should have decreased the intensity. The change in slope indicates that water molecules are displaced from the hydration sphere. The other bands in Nd^{3+} and Pr^{3+} (non-hypersensitive) either decrease in intensity with rise in temperature or show irregular behaviour. This study is done in aqueous solution above 100°C, under high pressure ($\sim$ vapor pressure of water at each temperature). The temperature dependence may have contribution from pressure induced structural change in aqueous solution. At high temperature hydrolysis also complicates interpretation.

Henrie, Fellows and Choppin [37] have summarized the evidence in support of the role of basicity and polarizability of ligand atoms and perhaps of covalency in oscillator strength of hypersensitive transitions. Covalency in lanthanide complexes is well-known. The quantitative calculation of ligand field parameters yield poor results only if covalency is taken into account [36]. The value of T_2 in a series of complexes of Nd^{3+} and Ho^{3+} with anions of acids of different pKa vary linearly with the value of pKa [37]. This is interpreted by postulating that covalency is more significant in a metal complex with an anion derived from an acid of higher pKa.

We have stated earlier that Krupke [57] concluded that the change of hypersensitive oscillator strength in going from Y_2O_3 to LaF_3 can be interpreted in terms of site symmetry alone. Henrie, Fellows and Choppin [37] reinterpret the data. O^{2-} is more basic than F^- and is higher up in the nephelauxetic series. Thus covalency is thought to be stronger in the O^{2-} lattice. They quote EPR evidence for stronger covalency of Ln^{3+} ions in oxides in comparison with fluorides. Plausible as it is, we like to point out that both the Jorgensen-Judd inhomogeneous dielectric mechanism [40] and the theory of Mason, Peacock and Stewert [41] may also be able to account for the effect. O^{2-} is more polarizable than F^-.

There is evidence for increase of T_2 with decreasing Ln-O bond distance [64]. Henrie, Fellows and Choppin [37] interpret this effect as evidence for increase of T_2 with increase of covalency. However, it may be pointed out that the Jorgensen-Judd model [40] and Mason-Peacock-Stewert theory [41] are equally consistent with the observation. If a more polarizable group is at a shorter distance, all the models predict higher hypersensitivity.

In the same class is the case of higher hypersensitive oscillator strength of solid NdI_3 ($r = 2.38\ A^o$) compared to gaseous NdI_3 ($r = 2.94\ A^o$). Greater covalency definitely accompanies shortening of bond length. But, as stated earlier, Mason theory [41] accounts for it quantitatively. Henrie, Fellows and Choppin [37] point out there is a lot in common between a covalent model and the dynamic coupling model of Mason, Peacock and Stewert [41]. It is perhaps meant that in the two theories, the same effect is partitioned differently under different headings.

Apart from the fact that a more explicit demonstration of equivalence is lacking, we may point out that the symmetry requirement for the effect of covalency to show up in the crystal field theory of the oscillator strength of absorption bands is not identical to the symmetry requirement of the dynamic coupling model of Mason et al. [41]. Low symmetries are however allowed in both the approaches.

We like to point out that when the effect of covalency is included the requirement of symmetry is still necessary and is identical to the requirement in electrostatic point charge model of crystal field theory. Symmetry of the microenvironment determines the symmetry of the combination of ligand orbitals to be used in the formation of molecular orbitals. Covalency affects the oscillator strength only if the parity of f^n states is destroyed through covalency. Thus in the octahedral hexahalo complexes, if the symmetry was a perfect octahedron, covalent interaction would not lead to modification of the oscillator strength. The situation is identical to that of the effect of ligands on the splitting of levels in the crystal field theory and in the molecular orbital theory.

In the early theoretical work on hypersensitive oscillator strength [38] mixing of $4f^{n-1}5d$ configuration with $4f^n$ configuration was considered and gave reasonable agreement with experiments on lanthanide aquo ions. Axe [65] showed that the relative intensities of the electric dipole and the magnetic dipole transitions occurring in the fluorescence spectrum of $Eu(C_2H_5SO_4)_3 \cdot 9H_2O$ can be interpreted by crystal field induced effect. Agreement with experiment was obtained if 5g orbital configuration mixing was assumed to contribute significantly. The factors that decide the contribution of the mixing of some states to oscillator strength is the difference of energy between the perturbing

state and the perturbed state and the magnitude of radial integrals e.g. $\langle 4f | r | 5d \rangle$ or $\langle 4f | r | 5g \rangle$. The increase in ΔE lowers the contribution and the increase in the value of the radial integrals increases it.

An interesting possibility that has attracted attention recently is the role of charge-transfer states in destroying parity of the $4f^n$ states [37,68]. It has been observed [68] that in those host lattices, where the Eu^{3+} ion occupies a site allowing a linear crystal field term (listed by Judd [44]) and the Eu^{3+} charge transfer band is at relatively lower energies, the intensity of hypersensitve $^5D_0 \rightarrow {}^7F_2$ and $^5D_0 \rightarrow {}^7F_0$ (which is not hypersensitive but is electric dipole in mechanism) emission increase compared to $^5D_0 \rightarrow {}^7F_1$ magnetic dipole emission (its intensity is environment insensitive). The intensity of electric dipole emission increases as the energy of the charge-transfer state decreases. In order to be effective the parity of the charge transfer states must be different from that of the f^n states. The 5d state is higher in energy than the charge-transfer state. The mixing of $4f^n$ states with charge-transfer states rather than $4f^{n-1}5d$ states is thus favoured. The frequency dependence of T_2 is accounted for in this model because mixing with charge transfer states is more effective if the excited state is higher in energy [37]. The higher hypersensitivity of Eu^{3+} than Nd^{3+} (e.g. with Cl^-, Eu^{3+} hypersensitive band shows enhancement at a much smaller chloride

concentration) is consistent with the comparatively low lying charge transfer state of Eu^{3+}. Hypersensitive $^5D_0 \longrightarrow {}^7F_2$ emission has been observed even in a D_{2d} site symmetry [68]. This is allowed by the Mason-Peacock-Stewert theory [41], but not by the crystal field model [44].

In ions where $4f^{n-1}5d$ level is comparatively low lying (Ce^{3+}, Pr^{3+}, Tb^{3+}), the mixing of this state with the $4f^n$ state enhances electric dipole emission. Tb^{3+} emission lifetime shows an increase with increase in $4f \longrightarrow 5d$ energy separation (τ = 1 msec. if $\Delta E_{4f \longrightarrow 5d} = 37000\ cm^{-1}$, τ = 9-10 msec. if $\Delta E_{4f \longrightarrow 5d} = 42000\ cm^{-1}$) and τ = 30 msec. in a site with inversion symmetry [68]. The $4f^5 5d$ state is relatively low lying (e.g. in Eu^{3+} ion in CaF_2 host lattice $\Delta E_{4f \longrightarrow 5d}$ is 68500 cm^{-1}, whereas in Tb^{3+} in the same lattice $\Delta E_{4f \longrightarrow 5d}$ is 46500 cm^{-1}). But the mixing is ineffective if the site symmetry has an inversion symmetry

Hypersensitivity to microenvironment can also be explained naturally by consideration of mixing with charge transfer states, because charge transfer transitions are ligand sensitive. But, in order for this explanation to be a general one, one must be able to show that mixing of charge transfer state with the states involving hypersensitive transition is more significant than the mixing with the states involving non-hypersensitive transitions.

It is to be pointed out that charge transfer is an extreme case of polarization (in what is usually called polarization a partial charge is created, in charge-transfer a full charge is created). Thus, the success of the theory of Mason, Peacock and Stewert [41] based on mutual polarization of metal and ligand leads one to believe that a theory that includes mixing of f^n states with charge transfer states will be able to account for hypersensitivity.

It is evident from the above discussion, that the oscillator strength of the hypersensitive transition has structural information. The Mason-Peacock-Stewert equation for the oscillator strength contains, in addition to known quantities such as the matrix elements and ligand polarizabilities, unknown quantities R_L, θ_L, ϕ_L which are the required structural parameters - the coordinates of the ligand atoms. One, however, has more information than the total oscillator strength. All theories, in particular the Mason-Peacock-Stewert dynamic coupling theory, derive formulae for individual $M_J \rightarrow M_J$, transitions between the two J-manifolds each split into a maximum of (2J+1) components of different energy. Resolution of the experimental curve into component curves (assuming some specific band shape; the model about band shape can be varied to discover model-independent conclusions) can yield oscillator strength for individual $M_J \rightarrow M_J$, transitions. The position of each $M_J \rightarrow M_J$, transition is also predicted by the dynamic coupling theory. Even though nephelauxetic

shifts of larger magnitudes cannot be accounted for by this theory smaller shifts for each $M_J \longrightarrow M_J$, transition from the parent frequency (of the order of 5 cm^{-1}) are predicted. In many systems (e.g. the one's studied by us in this thesis) there is no nephelauxetic shift compared to aquo ion as the standard. But the individual $M_J \longrightarrow M_J$, transitions shift by as much as predicted by the dynamic coupling model. Thus one can theoretically compute a spectrum of well defined shape and oscillator strength for a given set of structural parameters, if one makes a definite assumption about band widths (e.g., one can make the simplest assumption that the band widths are equal). Two sets of structural parameters, which give identical oscillator strength may not give identical shape. The structure that gives the ''best fit'' may be accepted as the best average structure (average, because in a small flexible molecule one usually has a mixture of fast interconverting structures). If this is a valid approach to structure determination, one's obvious choice is the $^5D_2 \longleftarrow {}^7F_0$ hypersensitive transition of Eu^{3+} ion. The ground state being singly degenerate, it gives only one state in all ligand fields. Thus the maximum number of transitions are five. This makes the effect of uncertainty (assumptions of band shape and band-width) less. A detailed computer search of this kind has been used in determination of the structure of lanthanide complexes of small molecules by NMR [69,70]. In the case of NMR, there are assumptions of theory,

which are difficult to remove unambiguously. The lack of information about the magnetic susceptibility tensor of complexes formed in solution makes the unambiguous interpretation of data on contact shift difficult. Specific assumption about correlation time is also necessary for line broadening data. A combination of data on hypersensitive line shape and oscillator strength and NMR shift and broadening data will thus be more powerful than either technique on its own.

Researchers studying absorption and emission spectroscopy of lanthanide complexes in solution, however, have not obtained structural information from oscillator strength and line shape of hypersensitive band. In general, workers have demonstrated that oscillator strength is environment sensitive and line shape also changes.

Some workers [36] infer about the structure of complexes by comparison of their spectra with those of compounds of known structure. The similarity of the absorption spectrum of Nd^{3+} (aq) with $Nd(BrO_3)_3 \cdot 9H_2O$ in crystal establishes the coordination number to be 9 and symmetry to be D_{3h} for the Nd(III) aquo ion. Spectrum of Er(III) aquo ion is similar to that of $ErCl_3 \cdot 6H_2O$, but differs from that of $Er(BrO_3)_3 \cdot 9H_2O$. indicating a coordination number of six. The absorption spectrum of Eu(III) aquo ion is different from those of $EuCl_3 \cdot 6H_2O$ and $Eu(BrO_3)_3 \cdot 9H_2O$. Sayre et al. [71] assumed a coordination number of 8 and inferred a D_{2h} symmetry (centre

of inversion) because the $^5D_2 \leftarrow\!\!\!- \; ^7F_0$ (electric dipole) and $^5D_1 \leftarrow\!\!\!- \; ^7F_0$ (magnetic dipole) transitions have similar intensity. Presence of center of inversion in D_{2h} makes the electric dipole transition forbidden. The assignment of a symmetry as high as D_{2h} is consistent with the fact, stated earlier, that T_2 of aquo ion is known to be smaller than a mononitrate complex with perhaps a C_s symmetry [45].

Karakker [72] studied the shape (without detailed curve analysis) of the hypersensitive absorption bands of the β-diketonates of trivalent lanthanide ions. He showed that the spectra of six coordinate trichelates in polar solvents are akin to seven or eight coordinate complexes. Presumably solvent molecules coordinate. Hydrated 8-coordinate chelates in benzene approximate to six or seven coordinate chelates when the solution is dehydrated. The dependence of spectra on coordination number is discussed. Coordination number determines the symmetry of the ion, if liganding atoms are the same.

Fluorescence spectrum of Eu(III) chelates with β-diketones have been extensively studied because of the possibility of application in the development of lasers. Brecher, Samelson and Lempicki [73] studied the emission spectra of the tris and tetrakis forms of β-diketone chelates in solid and in solution. Partial dissociation of the tetrakis form was observed in solution. The fact that $^5D_0 \longrightarrow ^7F_0$ emission should have only one peak if there is an unique species in

solution is used to establish the existence of the products of dissociation. The effective site symmetries are proposed for the tetrakis chelated Eu^{3+} ion in crystalline form and in solution from the number of allowed emission bands. The high environment sensitivity of the hypersensitive $^5D_0 \longrightarrow {}^7F_2$ transition is emphasized. The authors contrast their result to the emission spectrum of Eu^{3+} ion in CdF_2 crystal. The site symmetry in CdF_2 forbids electric dipole emission and the intensity of emission is two orders of magnitude less in CdF_2 than in the chelates. The same group of workers [74] determined equilibrium constants for the dissociation equilibrium of β-diketone chelates of Eu^{3+} in different solvents by measurement of intensity of the peaks assignable to the dissociated and the undissociated species, in particular the $^5D_0 \longrightarrow {}^7F_0$ emission intensity. Site symmetries are also inferred from the number of allowed transitions. Thus in these studies, number of allowed transitions is the main tool for structure elucidation, rather than oscillator strength. Emission intensity is used to determine equilibrium constant.

Choppin et al. [75] measured the oscillator strength of the hypersensitive $(^4G_{5/2}, {}^4G_{7/2}) \longleftarrow {}^4I_{9/2}$ transition of Nd(III) in acetate complexes of 1:1 and 1:2 stoichiometry. The oscillator strength of aquo ion, mono - and diacetate complexes are 7.9, 9.5 and 46 respectively (all in units of 10^{-6}). The two acetate complexes have distinct peaks. The shift for the monoacetate complex is $-20\ cm^{-1}$ with respect

to the aquo ion and that for the diacetate complex is $-60\ cm^{-1}$. The spectrum of monoacetate complex is shifted, but not enhanced and that of the diacetate complex is both shifted and enhanced. Thus if the shift (nephelauxetic) is due to covalency, the enhancement is more due to lack of symmetry than due to covalent effects. The author points out that in the monoacetate complex, perhaps only one H_2O molecule is displaced and the microenvironment of the Nd (III) ion remains almost the same as that in the Nd(III) aquo ion. Presumably in diacetate complex, more than 2 water molecules are expelled. No effort has been made to determine the structure of the complexes. Choppin's data and therefore his conclusions will perhaps change. In order to calculate molar oscillator strength of Nd(III) acetate complexes, he used potentiometric data on Nd(III)-acetate stability constants. It has been shown [76] that artifact of lanthanide hydrolysis introduces large error in these values. If the stability constants are wrong, the values of molar oscillator strength are wrong.

Hypersensitivity has been used to distinguish between inner and outer sphere complexes with chloride ion [77]. Cl^- affects Nd(III) hypersensitive spectrum only at very high (5-6 M) concentration, even though weak complex formation is known to occur at much lower concentration. Choppin et al. conclude that at low concentration, Cl^- forms an outer sphere complex with Nd(III) i.e., Cl^- is separated from Nd(III) by a

hydration layer. At high concentration, inner sphere complex forms, i.e., Cl^- binds directly to Nd(III) without the hydration layer standing in between. It has been stated earlier that Eu^{3+} hypersensitive intensity is affected at lower Cl^- concentration. NO_3^- in sharp contrast forms inner sphere complex and enhances hypersensitive absorption even at a low concentration.

In some pieces of work, the shift of the band position has also been used. Addition of DMF to the solution of lanthanide aquo ions in nitromethane displaces water and shifts the lanthanide absorption band. Thus a titration is carried out and one obtains the coordination number of DMF to be 6 [36]. Shift of the $^3P_0 \leftarrow\!\!- \; ^3H_4$ band in Pr(III) is induced by coordination of carboxylate and hydroxyl groups of the coordinating anion. The shift is additive and carboxylic and hydroxyl groups have their own characteristic shift values [36]. Shift has been correlated with Ln-O distance and coordination number from the study on compounds of known structure [36]. The oxydiacetate complexes of lanthanide ions in particular Eu^{3+} has been studied in detail. The fine structure of $^5D_2 \leftarrow\!\!- \; ^7F_0$ Eu^{3+} transition has been resolved. Symmetry of the microenvironment has been inferred from the number of allowed transitions and coordination number has been inferred to be 9. The similarity of the spectrum of the tris-oxydiacetate complex in solution to that in crystalline phase confirms the conclusion about symmetry and

coordination number [36,77]. Data on oscillator strength or line shape has, however not been used in this effort to determine structure.

Birnbaum and co-workers [78] studied the difference spectrum between Nd(III)-BSA complex and Nd(III) aquo ion and assigned the bands to binding of Nd(III) by carboxylate groups. They find that the difference spectrum is very similar to that observed between Nd(III) - acetate or other simple carboxylates and Nd(III) aquo ion. The difference spectrum of Nd(III) aquo ion with Nd(III) - amino acid (e.g. alanine) complex at a pH of 5.6 is ''different'' according to the authors. The authors do not clearly state the details of the difference. But it appears that they are referring to a difference in intensity and not in shape. They assign the difference to weaker binding with the carboxylate group in the amino acid. The weakness arises from the proximity of the NH_3^+ group to the CO_2^- group. Difference spectrum of Nd(III)-Glutamate at pH 5.6 resembles that of Nd(III) carboxylates. The binding at pH 5.6 is assumed to be through γ-carboxylate group. The NH_3^+ group is now far off to influence the binding strength. The spectrum of Nd(III)-Glutamate complex at pH 3.0 resembles that of Nd(III)-alanine complex and other complexes of Nd(III) with simple carboxylates. The authors interpret the spectral features to be arising out of the binding of Nd(III) to the α-carboxyl group. The γ-carboxyl group is protonated at this pH and is assumed

not to bind. The spectrum of Nd(III)-histidine complex at pH 5.6 is similar to that of the Nd(III)-alanine complex. The authors interpret the data to be arising from the binding of Nd(III) with the carboxylate group. The imidazole is protonated at this pH and is assumed not to bind. At pH 7.0, Nd(III)-histidine complex is different indicating that imidazole, deprotonated at this pH, binds the metal ion. The assumption that a protonated group does not bind a metal ion because of electrostatic repulsion is not necessarily valid. Binding may occur accompanied by deprotonation of the protonated site. Moreover, if the difference in the spectrum is only in intensity and not in shape, then the distinction has to be based on molar oscillator strength data. The weak difference spectrum may arise from smaller equilibrium constant of metal-ligand complex formation. It is only the molar oscillator strength that can tell about the binding site. The paper is a preliminery report. The conclusions are not firmly established.

More examples of similar application are given in a recent review article [36]. No serious effort has been made to use oscillator strength and band shape of the hypersensitive transitions in a quantitative manner on the basis of the existing theoretical models to extract structural information.

An important difficulty arises from the fact that in solution one usually has a mixture of different species There is NMR evidence for a monodentate and bidentate coordination of lanthanide ion to the carboxylate group of an amino acid as well as for the binding of Ln^{3+} ion by the amino group and the carboxylate group in a chelate. As the molecule becomes more complicated, the number of possibilities increase. In aspartic acid, each carboxylate group can bind independently. A chelate may also form with both the carboxylates involved in binding. There may also be complexes of different stoichiometry. Thus in order to get spectral data for each structurally distinct molecular species one must know the concentration of each species in solution. The first step is to obtain overall equilibrium constants (β_i's) for the formation of complexes of different stoichiometry. Resolution is harder within a subgroup of complexes of the same stoichiometry. pH dependence of β_i's can separate out equilibria that release or consume protons from those that do not involve protons. Temperature dependence of β_i's can establish simultaneous presence of an endothermic and an exothermic reaction. Spectral studies are the most powerful techniques of resolving these elementary equilibria.

There has been controversy about the values of the overall equilibrium constants β_i's of lanthanide-amino acid equilibria. Potentiometric data [79] and data from electroreduction experiments [80] indicate strong complexes ($K_d \sim 10^{-3}$

to 10^{-5} M). Recent NMR [81] and solvent extraction data [82] indicate weaker complexes ($K_d \simeq$ 0.1 to 0.3 M). Prados et al. [76] have shown that the earlier data indicating strong binding are incorrect because of the artifact of lanthanide hydrolysis.

The experimental quantities one measures in a titration experiment to obtain equilibrium constants are as many free concentration values as possible in a mixture of a given total concentration of metal ions and ligand molecules. The dependence of the free concentration values of the total concentration values is then parametrized by the parameters β_i's, the overall formation constants. They appear in the mass balance equations (written on the assumption that only complexes of the type ML_i form),

$$[M]_T = [M]_f + \sum_i \beta_i [M]_f [L]_f^i$$

$$[L]_T = [L_f] + \sum_i i \beta_i [M]_f [L_f]^i$$

In a spectral e.g. NMR titration, one determines free ligand concentration in a mixture of free and complexed ligand molecules by measuring the average chemical shift of nuclei in ligand molecules (fast chemical exchange is the usual situation). The determination is easy if only 1:1 complex forms. In such a case one determines chemical shift of the ligand...

nuclei in the complexed molecule from the NMR spectrum taken at high M/L ratio, i.e., when all the ligand molecules are complexed. The observed average chemical shift is given by

$$\delta_{obs} = \delta_{free} \cdot f + \delta_{complexed} (1-f),$$

where f is the fraction of free ligand molecules. f can be calculated from this equation, all the δ's being known quantities. The same technique can be applied to determine free metal ion concentration, if metal NMR spectrum is being observed [9]. If complexes of higher stoichiometry form then one requires a more detailed computer analysis [83], where spectral parameters of complexes in addition to β_i's are variables to be determined. The present author has no direct experience of the analysis of spectral titration in a complex system, but it is possible that the results may some times be guess value dependent.

Weber [84] has pointed out that in spectral titration experiments using different forms of spectroscopy, one may not get the same equilibrium constant. He cites the example of the dissociation equilibrium between a nucleotide base pair studied by ultraviolet and NMR spectroscopy. The values obtained by the two methods are different. In his analysis, the 1:1 complex formed is a mixture of several structurally different complexes of the same stoichiometry. Thus the two

different forms of spectroscopy gives different weightage to the structurally different complexes. The equilibrium constant determined is the sum of the different equilibrium constants for the component 1:1 equilibria, which, in Weber's analysis are differently weighed before being combined, in UV and NMR spectroscopic analysis. In the analysis of the author of this thesis, however such discrepancies cannot occur if the stoichiometry is purely 1:1. The pK is equal to the value of p[C] ([C] is free concentration of ligand) at which half the maximum spectral charge is obtained, irrespective of whether there is more than one distinguishable species of 1:1 stoichiometry. Complications arise only when 1:2 species exist, without being taken into account. Even at low concentration they may affect spectral parameters substantially, and to different extents in different forms of spectroscopy.

In some other titration experiments, the free (or bound) metal concentration is determined. One can use radioactive nuclei (^{45}Ca and $^{120-124}Eu$) and carry out millipore filtration or equilibrium dialysis experiments [6]. These well established techniques are applicable only to macromolecules. For small ligands like amino acids, solvent extraction using radioactive nuclei has been used [82]. There is an alternative way of determining free metal concentration. If a small concentration of a metal ion sensitive reporter dye (e.g. murexide) with

absorption or fluorescence spectrum is added to the solution, the metal ligand equilibrium is coupled to metal dye equilibrium. Thus, as free metal concentration changes in the solution, with change in ligand concentration in a titration experiment, the metal-dye equilibrium is displaced. The displacement can be spectrophotometrically measured with high precision and accuracy. The technique has been used in kinetic experiments where metal concentration is measured as a function of time [6]. A range of dyes can cover a large concentration range. Metal ion sensitive electrodes are now commercially available and are very convenient devices [6]. But no electrode exists for any lanthanide ion. Ca^{2+} sensitive electrode can measure concentration upto 10^{-5} ML^{-1}. The reporter dyes, in contrast, can detect lanthanide ions as well as Ca^{2+} ion and are sensitive to lower concentration values (in the case of Ca^{2+}).

Eu^{3+} is the lanthanide ion of choice because (i) its size is very close to that of Ca^{2+} (ii) it has large hypersensitivity and (iii) of all the hypersensitive transitions of the different lanthanide ions it has the minimum number of component bands. Amino acids as ligands are interesting in their own right. They and the peptides are also useful model systems for the study of protein-metal ion interaction. There is a considerable amount of debate about the structure of metal amino acid complexes. For example, Sherry and co-workers [69] interpret their NMR results on the model that lighter

lanthanide ions co-ordinate carboxylate group of amino acids in a monodentate fashion, whereas heavier lanthanides co-ordinate in a bidentate fashion (both the oxygens co-ordinate). Williams and co-workers [70] reach exactly the opposite conclusion. Involvement of the amino group in chelation is also debated [76, 81]. The amino acids chosen by us (aspartic acid, glutamic acid, aspargine, glutamine) have the added complication of a possible co-ordination site in the side chain.

Analysis of the titration data can be best done by computer programmes [83]. In the work described in this thesis, we used a programme, written by Gans and co-workers [85] which can handle equilibria resulting in as many as twenty species simultaneously present in solution. The equilibria studied by us turned out to be stoichiometrically simple, but the titration and data analysis procedures remain valid for more complicated systems to be studied in our laboratory later.

The use of the reporter dye murexide for the measurement of free metal ion concentration in solution requires accurate values of metal-murexide equilibrium constants. Values of the accuracy desired by us were not available in literature. Thus we undertook the determination of these quantities.

In Chapter II of this thesis we describe the methods of determination of lanthanide-murexide equilibrium constants. In Chapter III the methods of determination of lanthanide-amino

acid equilibrium constants are described. Results on the oscillator strength and the line shape of the $^5D_2 \leftarrow {}^7F_0$ hypersensitive transition of Eu^{3+} ion is given in Chapter IV.

References

1. J. Axelson, Ann. Reviews of Physiology, 33, 1, 1971.

2. R.P. Rubin, Pharmacol. Reviews, 22(3), 389, 1970.

3. S. Ebashi and M. Endo, Progress in Biophysics and Molecular Biology, 18, 123, 1968.

4. F.N. Briggs and R.J. Solaro in Metal Ions in Biological Systems, Volume 6, Ed. Helmut Sigel, Marcel Dekker Inc., New York and Basel, 1976.

5. L.V. Heilbrunn and F.J. Wiercinski, J. Cell and Comp. Physiol, 29, 15, 1947.

6. R.H. Kretsinger and D.J. Nelson, Co-ordination Chemistry Reviews, 18, 29, 1976.

7. R.J.P. Williams, Quart. Revs., 24(3), 331, 1970.

8. C.K. Luk, Biochemistry, 10, 2838, 1971.

9. T. Andersson, E. Chiancone and S. Forsen, Eur. J. Biochem., 125, 103, 1982.

10. A. Levitzki and J. Reuben, Biochemistry, 12, 41, 1973.

11. D.W. Darnall and E.R. Birnbaum, Biochemistry, 12, 3489, 1973.

12. M. Epstein, K. Levitz and J. Reuben, Biochemistry, 13, 1777, 1974.

13. B.W. Mathews and L.H. Weaver, Biochemistry, 13, 1719, 1974.

14. M.S. Kayne and M. Cohn, Biochem. Biophys. Res. Commun. 46, 1285, 1972.

15. E. Nieboer, D. East, J.S. Cohen, B. Furier and A.N. Schechter, Proc. 10th Rare Earth Conference. May 1973, Carefree, Arizona, U.S. Department of Commerce, Springfield, Va, quoted in Ref. 6.

16. B. Furie, A. Eastlake, A.N. Schechter and C.B. Anfinsen, J. Biol. Chem., 248, 5821, 1973.

32. W.D. Horrocks, G.F. Schmidt, D.R. Sudnick, C. Kittrel and R.A. Bernheim, J. Am. Chem.Soc., 99, 2378, 1977.

33. C-L.A. Wang, R.R. Aquaron, P.C. Leavis and J. Gergely, Eur. J. Biochem., 124, 7, 1982.

34. C-L. A. Wang, P.C. Leavis, W.D. Horrocks and J. Gergely, Biochemistry, 20, 2439, 1981.

34(a) W.D. Horrocks and D.R. Sudnick, J. Amer. Chem. Soc., 101, 334, 1979.

35. J. Krebs and E. Carafoli, Eur. J. Biochem., 124, 619, 1982.

36. K.B. Yatsimirskii and N.K. Davidenko, Co-ordination Chemistry Reviews, 27, 223, 1979.

37. D.E. Henrie, R.L. Fellows and G.R. Choppin, Co-ordination Chemistry Reviews, 18, 199, 1976.

38. B.R. Judd, Phys. Rev., 127, 750, 1962.

39. G.S. Ofelt, J. Chem. Phys., 37, 511, 1962.

40. C.K. Jorgensen and B.R. Judd, Mol. Phys., 8, 281, 1964.

41. S.F. Mason, R.D. Peacock and B. Stewert, Mol. Phys., 30, 1829, 1975.

42. W.T. Carnall, P.R. Fields and K. Rajnak, J. Chem. Phys., 49, 4412, 1968; W.T. Carnall, P.R. Fields and B.G. Wybourne, J. Chem. Phys., 42, 3797, 1965.

43. R.D. Peacock, Chem. Phys. Letters, 16, 590, 1972.

44. B.R. Judd, J. Chem. Phys., 44, 839, 1966.

45. K. Bukietynska and G.R. Choppin, J. Chem. Phys., 52, 2875, 1970.

46. G. Blasse, A. Brit and W.C. Nieuwpoort, J. Chem. Phys. Solids, 27, 1587, 1966.

47. H.C. Bolton, W. Fawcett and I.D.C. Gurneis, Proc. Phys. Soc., London, 80, 199, 1962.

48. P. Kislink, W.F. Krupke and J.B. Gruber, J. Chem. Phys., 40, 3606, 1964.

49. J.W. Rakestraw and G.H. Dieke, J. Chem. Phys., 42, 873, 1965.

50. J.L. Ryan and C.K. Jorgensen, J. Phys. Chem., 70, 2845, 1966.

51. J.L. Ryan, Inorg. Chem., 8, 2053, 1969.

52. D.E. Henrie and B.K. Henrie, J. Inorg. Nucl. Chem., 36, 2125, 1974.

53. J.B. Gruber, E.R. Menzel and J. Ryan, J. Chem. Phys., 51, 3816, 1969.

54. D.E. Henrie and G.R. Choppin, J. Chem. Phys., 49, 477, 1968.

55. R.D. Peacock, Structure and Bonding, Springer-Verlag, 22, 84, 1975.

56. W.F. Krupke and J.B. Gruber, Phys. Rev. A, 139, 2008, 1965.

57. W.F. Krupke, Phys. Rev. A, 145, 325, 1966.

58. R.D. Peacock, J. Chem. Soc. A, 2028, 1971.

59. D.M. Gruen and C.W. DeKock, J. Chem. Phys., 45, 4551, 1966.

60. J. Blanc and D.L. Ross, J. Chem. Phys., 43, 1286, 1965.

61. R.D. Peacock, (a) Chem. Phys. Letters, 10, 134, 1971; (b) J. Chem. Soc., Faraday II, 68, 169, 1972.

6 . R. Pappalardo, J. Chem. Phys., 49, 1545, 1968.

63. J.T. Bell, C.C. Thompson and D.M. Helton, J. Phys. Chem., 73, 3338, 1969.

64. R. Reisfeld, Structure and Bonding, Springer-Verlag, 13, 53, 1973.

65. J.D. Axe, J. Chem. Phys., 39, 1154, 1963.

66. B.G. Wybourne, Spectroscopic Properties of Rare Earths, Interscience, New York, 1965.

67. C.K. Jorgensen, Modern Aspects of Ligand Field Theory, North Holland Publishing Co., p. 293, 1971.

68. G. Blasse, Structure and Bonding, Springer-Verlag, 26, 43, 1976.

69. A.D. Sherry and E. Pascual, J. Amer. Chem. Soc., 99, 5871, 1977.

70. B.A. Levine and R.J.P. Williams, Proc. Roy.Soc., A345, 5, 1975; B.A. Levine, J.M. Thorton and R.J.P. Williams, J. Chem. Soc. Chem. Commun., 669, 1974.

71. E.V. Sayre, D.S. Miller and S. Freed, J. Chem. Phys., 26, 109, 1957.

72. D.E. Karakker, Inorg. Chem., 6, 1863, 1967.

73. C. Brecher, H. Samelson and A. Lempicki, J. Chem. Phys., 42, 1081, 1965.

74. H. Samelson, C. Brecher and A. Lempicki, J. Mol. Spectroscopy, 19, 349, 1966.

75. G.R. Choppin, D.E. Henrie and K. Buijs, Inorg. Chem., 5, 1743, 1966.

76. R. Prados, L.G. Stradtherr, H. Donats Jr. and R.B. Martin, J. Inorg. Nucl. Chem., 36, 689, 1974.

77. N.K. Davidenko, A.G. Goryushko and K.B. Yatsimirskii, J. Inorg. Chem. (Russ.), 18, 1785, 1973, quoted by Ref. 36, but could not be located even after a thorough search of literature.

78. E.R. Birnbaum, J.E. Gomez, and D.W. Darnall, J. Amer. Chem. Soc., 92, 5287, 1970.

79. M. Cefola, A.S. Tompa, A.V. Celiano and P.S. Gentile, Inorg. Chem. 1, 290, 1962; other references on potentiometric results are given in Chapter III.

80. S. Lal, Aust. J. Chem., 23, 1571, 1972.

81. A.D. Sherry, E.R. Birnbaum and D.W. Darnall, J. Biol. Chem., 247, 3489, 1972, other references on NMR determination of equilibrium constant are given in Chapter III.

82. S.P. Tanner and G.R. Choppin, Inorg. Chem., 7, 2046, 1968; A. Aziz and S.J. Lyle, J. Inorg. Nucl. Chem., 33, 3407, 1971.

83. F. Gaizer, Co-ordination Chemistry Review, 27, 195, 1979; P. Gans, Co-ordination Chemistry Reviews, 19, 99, 1976.

84. G. Weber, in Advances in Protein Chemistry (C.B. Anfinsen, J.T. Edsall and F.M. Richards Ed) Vol. 29, p. 76, 1975.

85. A. Sabatini, A. Vacca and P. Gans, Talanta, 21, 53, 1974; P. Gans, A. Sabatini and A. Vacca, Inorg. Chem. Acta., 18, 237, 1976.

CHAPTER 2

Metal-Murexide Equilibrium

In an experiment aimed at the quantitative study of metal-ligand equilibrium in solution, one measures the concentration of free metal ion as a function of its total concentration and that of the ligand molecule. This is called a titration experiment. The data at each titration point are then fed as input to a computer programme designed to choose the most reliable model for the complex species in solution and their respective equilibrium constant. The free metal ion concentration is determined spectrophotometrically. One measures ΔA, the difference in absorption between a sample cell containing a definite concentration of metal ion, ligand and a metal ion sensitive ''reporter'' dye murexide, and a reference cell containing an identical concentration of murexide and ligand (its presence makes no difference), but not metal ion. It can be shown (see later), that $\Delta A = \Delta\varepsilon[MMu]$, where $\Delta\varepsilon$ is the difference in molar absorptivity of MMu (the metal-murexide complex) and Mu (murexide). [MMu] refers to the molar concentration of metal-murexide complex. The formula assumes an 1:1 metal-murexide complex. In the concentration ranges studied, this assumption is valid [1]. The total concentration of murexide ($[Mu]_T$) is known. The concentration of free murexide $[Mu]_f$ is obtained by difference. One can choose conditions (see later in this chapter) such that $[Mu]_f$ and [MMu] are measured

very accurately (error less than 1%). The concentration of free metal $[M]_f$ is given by the formula $[M]_f = \frac{[MMu]}{K_{MMu}[Mu]_f}$. Thus any systematic and random error in the value of K_{MMu} is carried over to an error in $[M]_f$. If incorrect values of $[M]_f$ are given as inputs to the programme that analyses the titration data, one may get an incorrect model as the "best fit model". Thus even if the solution contains only an 1:1 complex, the programme may claim to detect 1:2 and 1:3 species (ML_2, ML_3). Since the programme used is a versatile one, one tends to believe such a result. If the error is large, the programme may fail to reach convergence. Even if the error in M_f is not large, and somehow, the correct model is chosen, one will obtain incorrect values of stability constants. Thus the accuracy and precision of the values of K_{MMu} are crucial in the study of metal-ligand equilibrium.

There are four earlier reports on equilibrium constants of metal-murexide equilibrium [1-4]. Three of them [1-3] ignore metal-buffer binding. Geier's [3] report is the only one that includes lanthanide-murexide equilibrium. His primary interest was in the kinetics of the reaction. He determined the values of equilibrium constant to check that the ratio of the rate constants equal the value of equilibrium constant. The accuracy of the rate constants being 10-20%, a value of K of comparable accuracy was enough for his purpose. He does not discuss the degree of precision

of his measurement, but quotes the value of $K^{association}_{Eu-Mu}$ to be 1.5×10^4 at 12°C and pH 4.0. He does not discuss the problem of buffer binding to metal. The buffer used and its concentration are not even mentioned. [MMu] is directly determined experimentally from the ratio of $\triangle A$ and $\triangle \varepsilon$. $[Mu]_f$ is determined by subtracting [MMu] from $[Mu]_T$, the total concentration of murexide. The concentration of free metal ions $[M]_f$ is determined by subtracting [MMu] from $[M]_T$. The ratio of [MMu] to the product of $[M]_f$ and $[Mu]_f$ is calculated to give K_{MMu}. The values so obtained show very high precision. But these highly precise values lack accuracy, because metal-buffer binding has been ignored. It turns out that ignoring the latter introduces a systematic error in these values. Balaji et al. [4] from our laboratory pointed this out. Almost simultaneously several other groups [5,6] stressed the obvious importance of recognizing that buffer binds metal, in addition to keeping the pH constant.

The analysis of Balaji et al. [4] proceeds as follows: The mass balance equation for the metal ion is

$$[M]_T = [M]_f + [MMu] + [MB] + [MB_2]$$

assuming that the metal ion forms only a 1:1 and 1:2 complex with the ion of the buffer solution. This leads to the equation

$$[M]_T - [MMu] = [M]_f (1 + K_{MB} \cdot B_f + K_{MB_2} \cdot B_f^2)$$

where B_f is the concentration of free buffer ions. One calls $[M]_T - [MMu] = [M]_f^{apparent}$, because this is what one would have calculated for $[M]_f$ if one naively ignored buffer binding to metal. Further $[B]_f \simeq [B]_T$ since $[B]_T \gg [M]_T$. Thus

$$[M]_f^{apparent} = [M]_f^{actual} (1+K_{MB} \cdot B_T + K_{MB_2} \cdot B_T^2)$$

At a given temperature and total buffer concentration the term within the bracket is a constant (called γ). Thus $K_{MMu}^{apparent}$ determined by ignoring metal-buffer binding is related to K_{MMu}^{actual} by the relation

$$K^{actual} = K^{apparent} \cdot \gamma$$

The two other concentrations that enter the calculation of K_{MMu} are not affected by the presence of buffer. [MMu] is directly calculated by dividing the observed $\triangle A$ by $\triangle \varepsilon$. $[Mu]_f$ is obtained by subtracting [MMu] from $[Mu]_T$. Since γ is a constant in a given experiment, $K^{apparent}$ is highly precise, but is clearly inaccurate.

Balaji et al. [4] had correctly pointed out the effect of buffer, but did not evaluate the correction factor accurately. Firstly they used modified literature values [4] for metal buffer binding constant. These values obtained from pH titration experiments have good precision but are inaccurate due to large systematic error [7]. Secondly, they used too high a concentration ($\sim$100 mM) of a buffer (acetate and phosphate)

that binds metal ions very strongly. Thus metal bound to buffer is substantial i.e., the sum of $K_{MB} \cdot B_T$ and $K_{MB_2} \cdot B_T^2$ in the correction factor derived above is orders of magnitude greater than 1. Thus error in K_{MB} and K_{MB_2} makes γ, the correction factor, significantly inaccurate. This would not be so if the buffer chosen bound metal ions weakly. Then $(K_{MB} \cdot B_T + K_{MB_2} \cdot B_T^2)$ would have been much less than 1. Any error in K_{MB} and K_{MB_2} would introduce a negligible percentage error in γ. Stated differently, $[M]_f$ actual is obtained by subtracting the sum of $[MB]$, $[MB_2]$, $[MMu]$ from $[M]_T$. Thus if the sum of $[MB]$ and $[MB_2]$ is as large as it is in the experiments of Balaji et al. [4], a systematic error of 10% in K_{MB} and K_{MB_2} [7] introduces in $([MB] + [MB_2])$ an error, whose absolute magnitude is of the same order as $[M]_f$. Thus it can make $[M]_f$ go wrong by a few hundred percent. Thirdly these authors used acetate buffer prepared from dried sodium acetate. In this method it is difficult to prevent moisture absorption completely. Thus the acetate concentration used by them in their calculation of γ is incorrect. The same applies to the concentration of the phosphate buffer used by them.

The ideal choice of a buffer would be one with a small but accurately and precisely known equilibrium constant for the association equilibrium with the metal ion. The pK of the acid or base used in the buffer should be close to the desired pH so that the buffer concentration can be low. Good

buffers [8] bind metal ions weakly, but their binding constants to Eu^{3+} are not known. In spite of small binding constants, binding of Eu^{3+} to Good buffers cannot be ignored because of high buffer concentration. If the buffer concentration is $\sim 10^{-2}$ M and $K_{MB} \sim 10$, metal bound to buffer (calculated by assuming Buffer (free) = Buffer (total) is not at all negligible ($\sim$ 7%) compared to metal bound to murexide (typical concentration : $Mu_f \sim 5 \times 10^{-5}$ M, $K_{Eu-Mu} \sim 3 \times 10^4$ at pH 6.5). The problem is aggravated by the fact that several Good buffers react with murexide (see chapter III) leaving TES as the only choice at pH $\sim$ 6.5. The pK of TES is 7.5 which is different from the desired pH by 1.0 unit. This rules out the possibility of using very low concentration of buffer. At pH 5.0, Good buffers are not available, leaving, acetate buffer as the only choice. Acetate binds Eu^{3+} more strongly (K = 134 at 15°C).

Eu^{3+} - Acetate equilibrium constants available in literature [7] had high precision and low accuracy. The authors estimate an error of 10%. Thus, a knowledge of accurate values of metal-buffer equilibrium constants are necessary, but are not available. However, an accurate determination of these constants is possible if an accurate value of K_{MMu} is available. Thus one concludes that the stability constants of Eu^{3+} - murexide equilibrium are best determined in the absence of a buffer.

This would however make the experiment considerably more complicated. The experiment for determining metal-murexide equilibrium constant in the presence of a buffer, would have to be carried out as follows : In a matched pair of cuvettes one adds identical volumes of the same buffered murexide solution. Then one adds definite volumes of buffered metal ion solution in one of them and an identical volume of buffer solution in the other. The difference in absorption (Δ A) is measured at a particular wavelength. The ratio of Δ A and the difference in molar absorptivity $\Delta\varepsilon$ at the same wavelength gives the concentration of [MMu] at a particular titration point. $[Mu]_f$ is calculated by subtracting [MMu] from $[Mu]_T$. $[M]_f$ is calculated by subtracting [MMu] and metal bound to buffer from $[M]_T$. K_{MMu} is then calculated. Any proton released on the formation of the complex MMu from the association of metal and murexide is ''swalloed'' by the buffer. One can get a large number of titration points easily, because addition of identical volumes of solution to both the cuvettes is mechanically done by a microliter pipette with admirable accuracy. If one were not to use a buffer solution, the pH would change on addition of metal ions. The extinction coefficient is dependent on pH. The measured Δ A gives the correct value of [MMu] only if the two cuvettes are at identical pH, in addition to having identical concentration of a murexide. Thus, if one does not use buffer solution, one cannot do titration by repeated addition of metal solution in order to get a

large number of points in one single experiment. The following method was adopted for the measurement of the concentration of metal-murexide complex formed on mixing definite concentration of metal and murexide

(i) Method for measurement of [MMu]:

The accuracy and the precision of this experiment depends critically on having exactly the same concentration of murexide in both the cuvettes. This is accomplished by weighing an identical volume in the two cuvettes in a semi-microbalance. The adjustment to identical volume is made by adjustable microliter pipettes. Then a cocktail of water and KCl (of appropriate concentration to make ionic strength 0.100) is added to the reference cuvette and an identical volume of metal solution (in water, with identical concentration of KCl) to the sample cuvette. The additions are made with the same microliter pipette. Even then the cuvettes are weighed in a semi-microbalance after the addition to check that the additions have been identical.

But the solutions are not buffered. This leads to a change in pH on metal addition, which has to be adjusted. This is done by addition of a dilute NaOH solution ($\sim$ pH 8). The approximate volume of the base solution needed can be estimated by a separate experiment carried out earlier. After addition of base, the solution in the cuvette is mixed and the final pH is checked by inserting a microelectrode into the

cuvette. The pH is almost always within 0.05 pH units of the pH of the murexide solution in the reference cuvette. If it is slightly outside the range, a known small volume of 1-2 μl of base or acid is added by an adjustable microliter pipette to bring the pH to the desired value.

To the murexide solution, in the reference cuvette one adds a volume of the solvent (an aqueous solution of KCl; $\mu = 0.100$; pH equal to that of the solution in the reference cuvette) identical in volume to that of the base added to the sample cuvette. This makes the total concentration of murexide equal in the two cuvettes. When the microelectrode is removed after the measurement of pH in the sample cuvette, a little liquid is lost. This does not affect the accuracy of the measurement because once the base is added and the solution is mixed in the cuvette, the concentration is fixed. The reason we worry about the volume of liquid is that it affects concentration. Since concentration is not affected by the loss of liquid at the time of removal of the microelectrode; this loss is unimportant. The 1-2 μl of liquid added for the final pH adjustment to the sample cuvette after the liquid in the cuvette has been mixed, makes no detectable difference to concentration since it is added to a volume of about 2 ml (a factor of 10^3).

After a little practice, the volume manipulation is no longer a serious source of error. The small difference

($\sim$ 0.05 pH unit) in the final pH between the two cells contributes to the error. Inspite of this, the standard deviation is 1-3%. Detailed error analysis given later shows that only a small part of this error comes from the inability to adjust pH exactly.

The difference in the absorption of the two cuvettes kept in thermostated cell compartments at the desired temperature is directly measured in a Cary 17 D spectrophotometer. The reading is taken from the digital panel meter. This reading fluctuates in the third decimal place. The mean is easily obtained by taking an average by visual observation. The typical error is $\pm$ 0.002. Thus if values of concentration are so choosen that the reading is sufficiently high (i.e. $\sim$ 0.100), the error is negligible. The error is, for example, 0.4% if the reading is 0.500, a typical value. Δ A is measured at 480 nm, the maximum of the difference spectra between the spectra of MMu and Mu. The value of Δ A measured as above gives the concentration of metal-murexide complex through the relation $\Delta A = \Delta \varepsilon$ [MMu]. The proof of this relation is given below :

(ii) <u>The relation $\Delta A = \Delta \varepsilon$ [MMu]:</u>

If the experiment is carried out as described above, then, remembering that the complex is 1:1, one gets

$$A_{sample} = C_1 \varepsilon_{Mu} \cdot L + C_2 \varepsilon_{MMu} \cdot L \quad (L \text{ is path length})$$

$$A_{reference} = (C_1 + C_2)\ \varepsilon_{Mu} \cdot L$$

Taking the **difference**,

$$\triangle A = C_2\ (\varepsilon_{MMu} - \varepsilon_{Mu}) \cdot L$$

$$= C_{MMu} \cdot \triangle \varepsilon \quad (\text{setting } L = 1 \text{ cm})$$

ε will have the units of $M^{-1}\ Cm^2$ if C_{MMu} is expressed in $M\ Cm^{-3}$ and L in cm.

(iii) Determination of $\triangle \varepsilon$:

Murexide in a suitable buffer (ionic strength 0.100 adjusted by adding KCl) is taken in the reference cuvette. An identical volume of the same solution of murexide is taken in the sample cuvette and is then saturated by a concentrated solution of Eu^{3+} ion. The volume of Eu^{3+} solution to be added is predetermined by an approximate experiment performed separately. The actual volume of Eu^{3+} solution added is determined by weighing in a semi-microbalance. An identical volume of the buffer-KCl cocktail is added to the reference cuvette by a microliter pipette. The same microliter pipette (100 µl) is used in both the additions. The difference in the two additions is thus always less than 1 µl. This is why a 100 µl pipette is preferred over, say, a 25 µl pipette. The equality of the volumes in the two additions is checked by weighing the reference cuvette after addition of the buffer-KCl cocktail. The difference in absorption of the two cuvettes

kept in thermostated cell compartment at the desired temperature is measured on the digital panel meter of the spectrometer. The wavelength of measurement is 480 nm, the maximum of the difference spectrum.

The concentration of murexide after taking the dilution by Eu^{3+} solution into account is equal to the concentration of Eu-murexide. There are enough Eu^{3+} ions to saturate both buffer and murexide. At pH 5.0, higher Eu^{3+} concentration is needed to saturate buffer, because acetate binds Eu^{3+} more strongly than does TES. The measured Δ A divided by the concentration of Eu-murexide (expressed in moles cm^{-3}) gives $\Delta \varepsilon$ (in M^{-1} Cm^{2}) per mole.

In the preliminary experiment that determines the concentration of Eu^{3+} ion to be added in order to saturate murexide, one adds Eu^{3+} ion solution in instalments of 100 µl by a microliter pipette till addition of one more instalment of 100 µl does not increase Δ A (after correcting for dilution). One then adds two or three more 100 µl volumes and confirms that Δ A after three or four successive additions remains unaltered. Sometimes, one may find that small changes of Δ A are occurring and one is not satisfied about saturation in the way described above, but the cuvette is overflowing. Then one has an idea about the order of magnitude of concentration needed to saturate the murexide solution, but does not know the exact concentration. In the final experiment one prepares

a more concentrated Eu^{3+} solution and adds a volume calculated on the basis of the experiment done earlier. More metal solution has to be added in instalments till Δ A does not change any more for three times in a row, thus confirming that saturation has been reached. The total volume of Eu^{3+} solution added is determined by weighing at the end. However if in the preliminary experiment, saturation is reached, one can add in a single instalment all the volume needed to saturate and the volume can be measured by weighing. This is more accurate than the experiment in which, in order to confirm saturation, one has to make three additions and mix after each addition by tilting the stoppered cuvette. From time to time, a little liquid may ooze out through the stopper. The error is small and avoidable if the stopper snugly fits. Even then, we have always carried out the preliminary titration to a satisfactory completion so that the final experiment is done by an one-shot addition. The data for the determination of $\Delta \varepsilon$ is presented in Table II. The first point in each separate experiment is, as discussed above, the most reliable, The other points are taken to confirm saturation. However the mean and standard deviation calculated from the two first points of the two separate experiments turn out to be virtually identical to those calculated from all the points reported in the table. The difference between the two first points is of the same order as that between the points in a single experiment. The reported mean and standard deviation are calculated by taking all the points into account.

(iv) Preparation of murexide solution :

Murexide used is of A.R. grade. It is confirmed to be pure by elemental analysis in our microanalytical laboratory. Solutions are made by pouring an approximately weighed amount of murexide in the solvent and filtering off the undissolved murexide. Measurements are made immediately because the solution deteriorates rapidly (stable for $\sim$ 1.5 hours at pH 5 and for $\sim$ 3.5 hours at pH 6.5, at 25°C).

(v) Determination of murexide concentration :

Murexide concentration is calculated from the formula $C_{Mu} = A/\varepsilon$ where A is the absorption of murexide measured against a blank of buffer and KCl and ε is the molar absorptivity, both at a given wavelength. Schwarzenbach and Gysling [1] reported the value of ε at 520 nm, pH 8.53, and an unspecified temperature. During our experiments, we noticed a dependence of ε on temperature. When a solution of murexide prepared at room temperature is allowed to equilibriate to a different temperature in the cell compartment of the spectrometer, the reading of optical density on the digital panel meter changes monotonically to a constant final value. This observation prompted us to determine the values of molar extinction coefficient under the exact experimental condition of pH, temperature and ionic strength, used by us.

The extinction coefficient of murexide is determined at the desired temperature ($15^{\circ}, 25^{\circ}, 35^{\circ}C$), pH (5.0, 6.5) and ionic strength ($\mu = 0.100$), by dissolving a definite quantity of murexide (weighed in a semi-microbalance) in a 1000 ml volume of solvent cocktail of water, KCl and buffer, in a volumetric flask. The experiment is repeated twice. The results are given in table III. Murexide was dissolved in deionised water, immediately filtered in a millipore filter and freeze dried. The thermogram of freeze dried murexide showed no water molecules present in murexide. Thus the molecular weight used is that of murexide without any water of crystallization (284.16).

The values of ε in Table III are determined at two wavelengths, 506 and 520 nm. The absorption maximum of murexide is at 520 nm. The choice of 506 nm is due to an error committed by a colleague who reported the maximum to be at 506 nm. Thus murexide concentration in all our experiments were determined at 506 nm. The value of ε at 520 nm determined by us is close to that reported by Schwarzenbach and Gysling [1]. They report a value of 1.355×10^{7} M^{-1} Cm^{2} at pH 8.53 in veronal buffer. This value lies in between our values at $15^{\circ}C$ and at $25^{\circ}C$. One pK of murexide is 9.2. Thus about 20% of the deprotonated form is present at pH 8.53. We found that the value of ε at pH 5.0 is identical to that at pH 6.5. This agrees with the expectation based on the values of pK. Schwarzenbach [12] has given the absorption

spectrum of murexide at neutral pH and that at pH 13. At the latter pH, two protons dissociate (pK = 9.2 and 10.5). Visual estimate on the plot given shows that the difference in the extinction coefficient is about 5%. One expects that the singly deprotonated species present at pH 8.53 will have an extinction coefficient in between the two i.e. will differ from that at neutral pH by less than 5%. Thus, on the basis of pH alone, a difference of $\sim$ 1 % is expected between our value and that determined by Schwarzenbach and Gysling [1]. One concludes, that the value of ε determined by these authors is consistent with that reported in our work.

(vi) Preparation of the metal solution :

Eu_2O_3 (solid) obtained from Sigma Chemical Company (purity 99.9% claimed by Sigma) was converted to $EuCl_3$ (solid) by repeatedly (3-4 times) evaporating to dryness with analar HCl. $EuCl_3$ is then dissolved in the desired buffer.

(vii) Determination of Eu^{3+} concentration :

The method used is that of titration with a standard solution of EDTA [9,10] in a buffer of pH 5.0 with Xylenol Orange as indicator. The titration is carried out in a quartz cell used usually in absorption spectroscopy. Acetate buffer at pH 5.0 and a drop of Xylenol Orange is added to the quartz cell. The weight of the liquid is determined by weighing the quartz cell in a semimicrobalance before and after the addition

of liquid. This weight gives the volume of the liquid. 100 µl of $EuCl_3$ is now added from a microliter pipette to the buffer. The exact volume is determined by weighing, eventhough the error incurred in assuming it to be 100 µl is $\sim$ 0.5%. A standard solution of EDTA is now added from an adjustable microliter pipette. An initial experiment fixes approximately the volume needed for reaching the end point. In the final titration, one adds a volume slightly less than the required volume and then cautiously adds microliter by microliter. Concentration of EDTA is kept at such a value that $\sim$ 300-400 µl of EDTA has to be added. Thus if the determination of end point is incorrect by 1-2 µl, the error introduced is only $\sim$ 0.5%. After the end point is reached, the quartz cell is weighed again to get the exact volume of EDTA added. The precision of this experiment is about 0.5%.

(viii) All optical density measurements were made on the Cary 17 D spectrophotometer, equipped with thermostated cell compartments. Microliter pipettes of Oxford Laboratories Ireland or of Sigma Chemical Company, U.S.A. were used. Not all the Sigma pipettes were of very good quality. The ones used were tested for their reproducibility by weighing out the liquid delivered. The 100 µl pipettes were good ($\lesssim$ 0.5% error). Pipettes of Oxford Laboratories were clearly better and more suited for our work. Pipettes need maintenance for satisfactory performance over a long period. They were

calibrated from time to time. This is essential for precise work. Matched cuvettes of 1 cm path length, from M/s Hellma, England, were used for spectral measurement. Doubly distilled, deionized water was used in all the experiments. The specific resistance of the deionised water used was 1-2 Megohm-Cm.

(ix) The data on the metal-murexide equilibrium constants at pH 5.0 and 6.5 and at three values of temperature (15°, 25°, 35°C) are summarized in Table I.

(x) K^+ binding to murexide :

KCl is present in very high concentration in the solution in order to maintain ionic strength. Thus eventhough K^+ is expected to bind murexide more weakly than does Ca^{2+}, one cannot ignore K^+ binding to murexide. We have used the following relation

$$[Mu]_f = [Mu]_T - [MMu].$$

But this is only the apparent value of free murexide. Now,

$$[Mu]_f^{actual} = [Mu]_f^{apparent} - [KMu]$$

$$= [Mu]_f^{apparent} - K_{KMu}[K^+]_{free}\,[Mu]_f^{actual}$$

or, $$[Mu]_f^{actual}\,(1 + K_{KMu}[K^+]_{free}) = [Mu]_f^{apparent}$$

As in the case of buffer anions $[K^+]_{free} = [K^+]_{total}$ because the concentration of KCl is much greater than murexide concentration (a ratio of 10^4).

Thus

$$[Mu]_f^{actual} = \frac{[Mu]_f^{apparent}}{1 + K_{KMu}\,[K^+]_{Total}}$$

Since K_{KMu} and K^+_{Total} are constant quantities, we get

$$[Mu]_f^{actual} = \gamma\,[Mu]_f^{apparent}$$

where γ is a constant in a particular experiment. Thus the quantity K_{KMu} determined by us differs from the actual equilibrium constant by this factor γ. The $[M]_f$ calculated using our values of K_{MMu} however is still correct. $[M]_f = K_{diss} \times [MMu]/[Mu]_f$. The factor γ appears in K_{MMu} as well as in $[Mu]_f$ and therefore cancels out. In the metal-ligand titrations, K^+ has been replaced by Na^+ from buffer at least partially. This introduces some error. In retrospect, this could have been avoided. One expects this error to be small.

Determination of stability constants for metal-buffer systems:

Eventhough we did not require the knowledge of metal-buffer equilibrium constants for the determination of Eu-murexide equilibrium constants, we need these value for our studies on metal-ligand equilibrium in Chapter III. Determination of metal-amino acid equilibrium will require many titration points and one has to carry out additions of ligand to a buffered metal solution. The buffer concentration remains fixed in these experiments. In order to correct for metal bound to buffer,

we do not need to know the ''real'' equilibrium constant which would give correct values of bound metal ions at all metal/buffer concentration ratios. Over a limited concentration range, one may get an 1:1 binding model as the "best fit", whereas in solution both 1:1 and 1:2 complexes form. Sometimes one may get more than one binding models as equally satisfactory. We are, however, not worried about this problem. All we need is a number that correctly gives the concentration of metal ions bound to buffer in the concentration ranges encountered in the study of metal-ligand systems.

The experiment is done as follows :

(i)(a) Preparation of TES-HCl Buffer at pH 6.5 :

TES-HCl salt as obtained from Sigma Chemical Company is stored in a dessicator. A definite amount is weighed out in a semi-microbalance and is dissolved in water in a volumetric flask. The volume of NaOH of known concentration needed for making the buffer at a pH of 6.5 is calculated and is added to the TES-HCl salt solution. The pH is measured after mixing. The final pH adjustment is done by addition of HCl or NaOH from a microliter pipette. The total volume of liquid at this stage is very close to the mark on the volumetric flask. The volume is now made up to the mark. The error in the buffer concentration is $\sim$ 0.1%. The error in weighing is insignificant because a large amount ($\sim$ 1 gm) is weighed. An error in the fifth place makes no difference. The error arises from

the maximum error one commits in reading the mark on the volumetric flask.

(b) Preparation of Na Acetate-acetic acid buffer :

A.R. Grade Na_2CO_3 is heated in an oven at 240°C for 2 hours. It is then stored in a dessicator till it comes to room temperature. A definite pre-calculated quantity of Na_2CO_3 is then weighed out and dissolved in water in a volumetric flask. A precalculated volume of Acetic Acid of known concentration is then added. Final pH adjustment is made using a procedure identical to that adopted for making the TES buffer. The maximum error in the concentration is once again $\sim$ 0.1%.

(ii) Titration :

Murexide in a buffer solution of known concentration and volume (ionic strength 0.100 maintained by KCl) is taken in the sample cuvette. The volume is determined by weighing. To the reference cuvette is added an identical murexide solution. One then adds metal solution of known concentration in instalments of 100 µl to the sample cuvette. An identical volume of buffer solution is added in each step to the reference cuvette. The difference in absorption ΔA^{480} gives [MMu] at each titration point. The buffer concentration remains constant at the value used in metal-ligand titration experiments (Chapter III). The metal concentration varies over the range used

in these experiments. Since K_{MMu} is known, one can calculate $[M]_f$ from the value of [MMu].

For the Eu^{3+} - TES equilibrium, one calculates K assuming 1:1 binding and that $[TES]_{total} = [TES]_{free}$. One finds that the K_{Eu-TES} calculated at various points remains constant with a small standard deviation. The values of K and the values of concentration used are given in Table IV. For the Eu^{3+} - acetate equilibrium, the data are fed in the computer programme used to analyse metal-ligand titration data (Chapter III). The programme accepts two binding models (1:1, or 1:2, metal-acetate) as almost equally satisfactory. The standard deviation is very small in either case. Thus metal bound to buffer calculated by either 1:1 or 1:2 model gives identical result. We used the 1:1 model. The results are given in Table V. If M_T/AC_T was varied over a much wider range, one of the two models might turn out to be valid or a more complicated model, say one which includes 1:1, 1:2 and 1:3 equilibrium, would emerge as the unique model. The parameters of this model would be the ''real'' equilibrium constants. We are however not interested in these real constants in these cases, but are content with the effective constants valid over a restricted range of concentration.

Estimate of precision :

In this section, we have used the following approximate rule. If $C = A \pm B$, then absolute error of C, $\eta_C \simeq (\eta_A^2+\eta_B^2)^{\frac{1}{2}}$,

if the errors in A and B are uncorrelated. If C = A/B or if C = AB, the relative error in C, $\varepsilon_C \simeq (\varepsilon_A^2 + \varepsilon_B^2)^{\frac{1}{2}}$, if errors in A and B are uncorrelated [11].

(1) The concentration of metal ion is determined from the formula

$$C_M = [M] = \frac{C_{EDTA} \times V_1(EDTA)}{V_2(\text{metal solution})}$$

V_1 and V_2 are determined by weighing. The maximum uncertainty in reading the weight in our semi-microbalance is $\sim$ 0.00005 g. Thus, measurement of volume by weighing is uncertain by 5×10^{-5} ml. The error is in the fifth place of decimal if the volume is expressed in milliliter. The ratio V_1/V_2 is correct to the fourth place of decimal. The concentration of EDTA solution has a maximum uncertainty of $\sim$ 0.5% , because of the uncertainty in reading the balance and the mark on the volumetric flask. An uncertainty of 0.00005 g in a typical weight of 0.01370 g is $\sim$ 0.5% . The maximum uncertainty in reading a volumetric flask is $\sim$0.2% in a 25 ml flask and is $\sim$0.1% for the large flasks. The EDTA solution is made only once. So, the uncertainty in its concentration shifts the mean value of the concentration of metal solution, but does not introduce any random error. The error in reading the end point introduces a standard deviation of $\sim$ 0.5% in the concentration of metal solution. The stock metal solution is then diluted in the cuvette. Since

the dilution is done by weighing, the dilution factor is correct to the fourth place of decimal. Thus error in the final metal concentration in the cuvette is also $\sim$ 0.5%. This means a typical value of 6.731×10^{-5} ML^{-1} has a standard deviation of $\pm 0.034 \times 10^{-5}$ ML^{-1}. We still quote the metal concentration to the third decimal place (in units of 10^{-5} ML^{-1}) in Table I, to avoid truncation error. Taking 6.731 as 6.73 in the case cited above is biased because, a re-determination could lead to a mean value to be 6.737 and then one would truncate it to 6.74.

(2) The error in ε arises from (i) the error in reading the value of absorbance on the digital panel meter of the spectrometer, (ii) error in reading the weight on the balance and (iii) error in reading the mark on the volumetric flask. The values of O.D. used in determination of ε are in the range of 1. The maximum error is $\sim$ 0.3%. The maximum error in weight is $\sim$ 0.02%. The maximum error in reading the mark on the 1000 ml volumetric flask is $\sim$ 400 µl i.e. $\sim$ 0.04%. Thus the maximum error in ε is $\sim$ 0.4%. The standard deviation of the two measurements made is $\sim$ 0.1%. In these two separate experiments, the different steps (i.e. absorbance measurement, weighing and filling in the volumetric flask) were carried out separately. Standard deviation is about one-third of the maximum error. Thus the standard deviation of 0.1% is close to (perhaps slightly less than) the

standard deviation one would get from, say five measurements.

(3) $\Delta \varepsilon = \frac{\Delta A}{C_{MMu}}$. The maximum error in ΔA is $\sim 0.3\%$ (0.002 in 0.600, a typical value). C_{MMu} at saturation is equal to the C_{Mu}. Now $C_{Mu} = \frac{A}{\varepsilon}$. Taking the standard deviation [6] to be one-third the maximum error (e_{max}), one gets the standard deviation in A to be 0.001 ($\sim 0.2\%$). σ for ε is $\sim 0.1\%$. Thus σ for C_{Mu} and C_{MMu} is $\sim 0.25\%$. σ for $\Delta \varepsilon$, then becomes $\sim 0.4\%$. The measured standard deviation is $\sim 0.5\%$.

(4) As discussed above σ for [Mu] is $\sim 0.25\%$.

(5) $[MMu] = \Delta A / \Delta \varepsilon$. σ for [MMu] is calculated to be $\sim 0.6\%$.

(6) $[Mu]_f$ is in all cases $\sim 50\%$ of $[Mu]_T$. Thus $[MMu] \simeq [Mu]_f$. Thus the relative error of 0.6% in [MMu] corresponds to an absolute error which is $\sim 0.6\%$ of $[Mu]_f$. The relative error of $\sim 0.25\%$ [Mu] corresponds to an absolute error which is about $\sim 0.5\%$ of $[Mu]_f$. Thus if $[Mu]_f = C$, then $\eta_C \simeq [(0.6 \times 10^{-2})^2 C^2 + (0.50 \times 10^{-2})^2 C^2]^{\frac{1}{2}} \simeq (0.8 \times 10^{-2})$. This means a relative error of 0.8% in $[Mu]_f$. The error would have been larger if [Mu] is almost saturated i.e. if $[MMu] \simeq 0.8$ or 0.9 of $[Mu]_T$.

(7) $[M]_f = [M]_T - [MMu]$. In all cases, we have chosen the values of concentration such that $[M]_f \simeq 0.5\ [M]_T$. Thus

the relative error in $[M]_f$ is $\sim$ 0.8% , equal to that for $[Mu]_f$.

(8) The relative error in K_{diss} calculated to be ratio $\frac{[M]_f[Mu]_f}{[MMu]}$ is $\sim$ 1.3% . The precision calculated from the several measurements of $K_{dissociation}$ is of this order. Thus the complication of pH adjustment in the cuvette does not lead to any substantial additional error.

(9) Three concentrations are directly determined, $[M]_T$, $[Mu]_T$ and [MMu]; two are calculated by difference. The values of concentration in Table I are quoted to third place of decimal (in units of 10^{-5} ML^{-1}), eventhough the error is in the second place. This is done to avoid truncation error. The philosophy is to keep each quantity to one place of decimal beyond the place where error has its first significant digit. The truncation is to be done at the last stage. K_{diss} has been quoted to third decimal place (in units of 10^{-5}) eventhough it has an error in the second place (sometimes barely in the first place). This is so, because $K_{dissociation}$ is not the final quantity of interest to us. For us, the final quantity is $[M]_f$. It is calculated from the formula $[M]_f = K_{diss} \times [MMu]/[Mu]_f$ and has a calculated relative error of $\sim$ 1.6% . This introduces a maximum error of 1 in the second decimal place of p[concentration]. The format of the computer programme used takes input as p[concentration]

to third decimal place. For example 6.500×10^{-5} ML^{-1} has an error of $\pm 0.104 \times 10^{-5}$. In the p[concentration] scale, the mean becomes 4.187. In the p-scale 6.60×10^{-5} is 4.181 and 6.40×10^{-5} is 4.194. Thus in the p-scale one writes 4.187 ± 0.007. So the input free concentration in the p-scale has an error in the third decimal place.

(10) The total concentration is fed as input to the programme to second decimal place (in units of 10^{-5} ML^{-1}). The error is also in the second decimal place.

(11) Our balance was calibrated with a standard weight supplied by the manufacturer.

(12) In retrospect, we could have removed the small uncertainty in the concentration of metal solution if EDTA solutions were always made in 100 ml volumetric flask. The weight of EDTA would have been larger, so as to make the error in reading the balance an insignificant error.

(13) In (6) and (7) above, we have pointed out that the error in $[M]_f$ and $[Mu]_f$ is kept low choosing $[MMu] \sim 50\%$ $[M]_T$ and $[Mu]_T$. Since $[M]_f$ and $[Mu]_f$ are determined by subtracting two quantities, one has to follow the Golden rule that one should never determine a quantity by subtracting two almost equal numbers. A look at the Eu-Murexide stability constant at pH 6.5 and 15°C show that points where $[M]_f$ and

$[Mu]_f$ approach 30% of $[M]_T$ and $[Mu]_T$ (points 1,5,6) increase the standard deviation. Thus saturation must be avoided.

(14) Eu-TES equilibrium constant has an error in first decimal place. The equilibrium constants are therefore quoted to two decimal places (e.g. 5.65 ± 0.36). The error may have arisen because the 1:1 binding model is an approximation. But the accuracy was sufficient for our purposes (Chapter III).

(15) A typical value of acetate equilibrium constant is 148.22. The standard deviation is 1.64% $\simeq \pm 2.36$. Thus the mean values used are quoted to first decimal place.

(16) The precision of the pH measurement : The Phillips pH meter used has a graduation at intervals of 0.1 pH unit. If the needle is half way through between two successive graduation, visual observation can roughly detect this. This does not mean that one puts the needle in the midpoint between two marks, say 6.4 and 6.5 and takes it as 6.45. But this still means that the maximum error is of the order of 0.05 pH units. Since pH measurement is made only once, one should quote the values as 5.00 ± 0.05 and 6.50 ± 0.05, where 0.05 indicates the maximum error.

Table I(i) : Dissociation constant of Eu-murexide complex at pH 5.0, 15°C

$[M]_T x10^5$ (ML^{-1})	$[Mu]_T x10^5$ (ML^{-1})	ΔA^{480}	$[MMu] x10^5$ (ML^{-1})	$[M]_f x10^5$ (ML^{-1})	$[Mu]_f x10^5$ (ML^{-1})	$K_{diss} x10^5$	Mean $K_{diss} x10^5$
6.731	5.819	0.355	2.563	4.168	3.256	5.295	
8.198	5.795	0.403	2.909	5.289	2.886	5.247	
8.622	7.673	0.513	3.704	4.918	3.969	5.270	5.267 (±0.076)
10.722	5.739	0.468	3.379	7.343	2.359	5.126	
9.985	7.632	0.558	4.029	5.956	3.603	5.326	
11.404	7.588	0.599	4.325	7.079	3.263	5.340	

Table I(ii) : Dissociation constant of Eu-murexide complex at pH 5.0, 25°C

$[M]_T \times 10^5$ (ML^{-1})	$[Mu]_T \times 10^5$ (ML^{-1})	ΔA^{480}	$[MMu] \times 10^5$ (ML^{-1})	$[M]_f \times 10^5$ (ML^{-1})	$[Mu]_f \times 10^5$ (ML^{-1})	$K_{diss} \times 10^5$	Mean $K_{diss} \times 10^5$
8.103	7.563	0.451	3.338	4.765	4.225	6.031	
9.610	7.534	0.496	3.671	5.939	3.863	6.244	
11.710	7.475	0.553	4.093	7.617	3.382	6.294	
8.004	6.392	0.388	2.872	5.132	3.520	6.290	6.237 (±0.010)
9.122	6.364	0.422	3.124	5.998	3.240	6.221	
10.541	6.329	0.454	3.360	7.181	2.969	6.345	

Table I(iii) : Dissociation constant fof Eu-murexide complex at pH 5.0, 35 °C

$[M]_T x10^5$ (ML^{-1})	$[Mu]_T x10^5$ (ML^{-1})	$\triangle A^{480}$	$[MMu] x10^5$ (ML^{-1})	$[M]_f x10^5$ (ML^{-1})	$[Mu]_f x10^5$ (ML^{-1})	$K_{diss} x10^5$	Mean $K_{diss} x10^5$
6.741	6.008	0.304	2.294	4.447	3.714	7.200	
8.435	5.968	0.350	2.641	5.794	3.327	7.299	
10.098	5.924	0.392	2.958	7.140	2.966	7.159	
8.634	7.286	0.416	3.140	5.494	4.146	7.254	7.184(±0.071)
12.750	7.159	0.524	3.955	8.795	3.204	7.125	
9.468	8.231	0.490	3.698	5.770	4.533	7.073	
11.692	8.176	0.554	4.181	7.511	3.995	7.177	

Table I(iv) : Dissociation constant of Eu-murexide complex at pH 6.5, 15°C

$[M]_T x10^5$ (ML^{-1})	$[Mu]_T x10^5$ (ML^{-1})	ΔA^{480}	$[MMu] x10^5$ (ML^{-1})	$[M]_f x10^5$ (ML^{-1})	$[Mu]_f x10^5$ (ML^{-1})	$K_{diss} x10^5$	Mean $K_{diss} x10^5$
6.118	7.669	0.470	3.582	2.536	4.087	2.893	2.986(±0.091)
7.129	7.626	0.512	3.902	3.227	3.724	3.080	
8.284	7.536	0.569	4.337	3.947	3.199	2.911	
7.149	8.026	0.536	4.085	3.064	3.941	2.956	
9.213	7.976	0.618	4.710	4.503	3.266	3.122	
10.441	7.934	0.670	5.107	5.334	2.827	2.953	

Table I(v) : Dissociation constant of Eu-murexide complex at pH 6.5, 25°C

$[M]_T x10^5$ (ML^{-1})	$[Mu]_T x10^5$ (ML^{-1})	ΔA^{480}	$[MMu] x10^5$ (ML^{-1})	$[M]_f x10^5$ (ML^{-1})	$[Mu]_f x10^5$ (ML^{-1})	$K_{diss} x10^5$	Mean $K_{diss} x10^5$
6.228	8.489	0.454	3.522	2.706	4.967	3.816	
7.360	8.447	0.520	4.034	3.326	4.413	3.638	
9.349	8.378	0.606	4.701	4.648	3.677	3.635	
6.481	6.172	0.383	2.971	3.510	3.201	3.782	
8.978	6.109	0.466	3.615	5.363	2.494	3.700	3.672 (±0.091)
8.161	7.484	0.512	3.972	4.189	3.512	3.704	
9.206	7.448	0.556	4.313	4.893	3.135	3.556	
6.983	7.524	0.470	3.646	3.337	3.878	3.549	

Table I(vi) : Dissociation constant of Eu-murexide complex at pH 6.5, 35°C

$[M]_T x10^5$ (ML^{-1})	$[Mu]_T x10^5$ (ML^{-1})	$\triangle A^{480}$	$[MMu] x10^5$ (ML^{-1})	$[M]_f x10^5$ (ML^{-1})	$[Mu]_f x10^5$ (ML^{-1})	$K_{diss} x10^5$	Mean $K_{diss} x10^5$
8.421	8.020	0.516	4.082	4.339	3.938	4.186	
10.690	7.939	0.590	4.668	6.022	3.271	4.220	
12.980	7.868	0.648	5.126	7.854	5.126	4.200	
6.670	6.829	0.387	3.062	3.608	3.767	4.439	4.313(±0.122)
8.922	6.762	0.462	3.655	5.267	3.107	4.477	
10.941	6.707	0.518	4.098	6.843	2.609	4.352	

Table II: Measurement of $\Delta\varepsilon$ at different pH and temperature
Wavelength: 480 nm

(i) pH 6.5, 15°C

$C_{Mu} \times 10^5$ (ML^{-1})	ΔA	$\Delta\varepsilon_{480} \times 10^7$ ($M^{-1}Cm^2$)	Mean $\Delta\varepsilon_{480} \times 10^7$ ($M^{-1}Cm^2$)
	(a) Experiment 1		
5.178	0.678	1.309	
4.936	0.646	1.309	
4.716	0.618	1.311	$1.312(\pm 0.003) \times 10^7$
	(b) Experiment 2		
5.036	0.663	1.316	
4.820	0.634	1.315	
4.620	0.608	1.316	

(ii) pH 6.5, 25°C

$C_{Mu} \times 10^5$ (ML^{-1})	ΔA	$\Delta\varepsilon_{480} \times 10^7$ ($M^{-1}Cm^2$)	Mean $\Delta\varepsilon_{480} \times 10^7$ ($M^{-1}Cm^2$)
	(a) Experiment 1		
5.371	0.690	1.285	
5.136	0.659	1.283	
4.920	0.631	1.282	$1.289(\pm 0.005) \times 10^7$
	(b) Experiment 2		
6.104	0.790	1.294	
5.831	0.755	1.295	
5.582	0.721	1.292	

(iii) pH 6.5, 35°C

$C_{Mu} \times 10^5$ (ML^{-1})	ΔA	$\Delta \varepsilon_{480} \times 10^7$ ($M^{-1}Cm^2$)	Mean $\Delta \varepsilon_{480} \times 10^7$ ($M^{-1}Cm^2$)
	(a) Experiment 1		
5.695	0.722	1.268	
5.438	0.691	1.271	
5.204	0.660	1.268	$1.264(\pm 0.005) \times 10^7$
	(b) Experiment 2		
5.879	0.742	1.260	
5.614	0.707	1.259	
5.374	0.675	1.256	

(iv) pH 5.0, 15°C

$C_{Mu} \times 10^5$ (ML^{-1})	ΔA	$\Delta \varepsilon_{480} \times 10^7$ ($M^{-1}Cm^2$)	Mean $\Delta \varepsilon_{480} \times 10^7$ ($M^{-1}Cm^2$)
	(a) Experiment 1		
6.735	0.929	1.379	
6.479	0.895	1.381	
6.242	0.862	1.381	
6.021	0.830	1.378	$1.385(\pm 0.006) \times 10^7$
	(b) Experiment 2		
6.273	0.870	1.388	
6.040	0.842	1.394	
5.830	0.812	1.393	

(v) pH 5.0, 25°C

$C_{Mu} \times 10^5$ (ML^{-1})	ΔA	$\Delta \varepsilon_{480} \times 10^7$ ($M^{-1}L^{-1}Cm^2$)	Mean $\Delta \varepsilon_{480} \times 10^7$ ($M^{-1}L^{-1}Cm^2$)
	(a) Experiment 1		
3.753	0.506	1.348	
3.623	0.486	1.341	
3.503	0.474	1.353	
3.390	0.456	1.345	$1.351(\pm 0.006) \times 10^7$
	(b) Experiment 2		
6.509	0.885	1.360	
6.226	0.845	1.357	
5.966	0.806	1.351	

(vi) pH 5.0, 35°C

$C_{Mu} \times 10^5$ (ML^{-1})	ΔA	$\Delta \varepsilon_{480} \times 10^7$ ($M^{-1}Cm^2$)	Mean $\Delta \varepsilon_{480} \times 10^7$ ($M^{-1}Cm^2$)
	(a) Experiment 1		
6.009	0.797	1.326	
5.750	0.760	1.325	
5.512	0.734	1.332	
5.293	0.705	1.331	$1.325(\pm 0.004) \times 10^7$
	(b) Experiment 2		
4.913	0.648	1.319	
4.709	0.623	1.323	
4.521	0.598	1.323	
4.348	0.575	1.320	

Table III : Extinction Coefficient of Murexide.

Experiment 1:

Weight of murexide = 0.02180 gms/1000 ml

Concentration of murexide= 7.672×10^{-5} ML^{-1}

Temperature	O.D. at 506 nm	O.D. at 520 nm	$\varepsilon^{506} \times 10^7$ $M^{-1}Cm^2$	$\varepsilon^{520} \times 10^7 M^{-1}Cm^2$
35°C	0.946	1.015	1.233	1.323
25°C	0.956	1.027	1.246	1.339
15°C	0.967	1.045	1.260	1.362

Experiment 2:

Weight of murexide = 0.02272 gms/1000 ml

Concentration of murexide= 7.995×10^{-5} ML^{-1}

Temperature	O.D. at 506 nm	O.D. at 520 nm	$\varepsilon^{506} \times 10^7$ $M^{-1}Cm^2$	$\varepsilon^{520} \times 10^7$ $M^{-1}Cm^2$
35°C	0.986	-	1.233	-
25°C	0.998	1.074	1.248	1.343
15°C	1.008	1.094	1.261	1.368

MEAN VALUES

$\varepsilon^{506}_{35^\circ C} = 1.233(\pm 0.000) \times 10^7$ $M^{-1}Cm^2$; $\varepsilon^{520}_{35^\circ C} = 1.323 \times 10^7$ $M^{-1}Cm^2$

$\varepsilon^{506}_{25^\circ C} = 1.247(\pm 0.001) \times 10^7$ $M^{-1}Cm^2$; $\varepsilon^{520}_{25^\circ C} = 1.341(\pm 0.002) \times 10^7$ $M^{-1}Cm^2$

$\varepsilon^{506}_{15^\circ C} = 1.260(\pm 0.0005) \times 10^7$ $M^{-1}Cm^2$; $\varepsilon^{520}_{15^\circ C} = 1.365(\pm 0.003) \times 10^7$ $M^{-1}Cm^2$

The measurements reported are at pH 6.5. Identical values are obtained at pH 5.0.

Table IV : Effective stability constants for Eu-TES Equilibrium

(i) pH 6.5, 35°C

$B_T = B_f = 0.100$ M					
$[M]_T x10^5$ (ML^{-1})	$[Mu]_T x10^5$ (ML^{-1})	$[MMu] x10^5$ (ML^{-1})	$[M]_f x10^5$ (ML^{-1})	$[MB] x10^5$ (ML^{-1})	$K_{association}$
13.800	7.292	4.296	6.184	3.320	5.37
17.781	7.238	4.755	8.259	4.767	5.77
17.105	7.577	4.921	7.991	4.193	5.25
20.189	7.534	5.221	9.735	5.233	5.38
22.370	7.503	5.356	10.76	6.254	5.81
10.170	6.688	3.346	4.318	2.506	5.80
12.275	6.660	3.655	5.246	3.374	6.43
16.426	6.855	4.414	7.799	4.213	5.40

Mean K = 5.65 ($\pm$0.36)

(ii) pH 6.5, 25°C

$B_T = B_f = 0.100$ M					
$[M]_T x10^5$ (ML^{-1})	$[Mu]_T x10^5$ (ML^{-1})	$[MMu] x10^5$ (ML^{-1})	$[M]_f x10^5$ (ML^{-1})	$[MB] x10^5$ (ML^{-1})	$K_{association}$
11.148	6.601	3.654	4.55	2.944	6.47
13.536	6.572	3.995	5.689	3.852	6.77
16.165	6.540	4.305	7.069	4.791	6.78
14.09	5.885	3.700	6.203	4.187	6.75
17.469	5.848	4.003	7.945	5.521	6.95
17.078	7.868	5.237	7.305	4.536	6.21
19.544	7.830	5.423	8.268	5.853	7.08

Mean K = 6.72 (±0.20)

(iii) pH 6.5, 15°C

$B_T = B_f = 0.100$ M					
$[M]_T \times 10^5$ (ML^{-1})	$[Mu]_T \times 10^5$ (ML^{-1})	$[MMu] \times 10^5$ (ML^{-1})	$[M]_f \times 10^5$ (ML^{-1})	$[MB] \times 10^5$ (ML^{-1})	$K_{association}$
14.091	5.889	3.879	5.763	4.449	7.72
17.47	5.852	4.169	7.397	5.904	7.98
22.114	7.495	5.724	9.651	6.739	6.98
27.684	7.406	5.945	12.150	9.589	7.81
9.813	6.559	3.582	3.593	2.638	7.34
14.328	6.505	4.245	5.609	4.474	7.97
14.354	5.330	3.597	6.198	4.559	7.36
10.882	5.367	3.262	4.627	2.993	6.47
24.914	7.317	5.739	10.859	8.316	7.66

Mean K = 7.61 ($\pm$0.33)

Table V(i): Effective stability constant for Eu-acetate equilibrium at pH 5.0, 15°C.

B_T = 0.0150 M

$[M]_T x10^4$ (ML^{-1})	$[Mu]_T x10^5$ (ML^{-1})	$[B]_f x10^2$ (ML^{-1})	$[M]_f x10^4$ (ML^{-1})	$[Mu]_f x10^5$ (ML^{-1})	$[MMu] x10^5$ (ML^{-1})	$[MB] x10^4$ (ML^{-1})	Mean $K_{association}$
1.61	5.06	1.49	0.47	2.68	2.38	0.94	
3.07	4.83	1.48	0.94	1.75	3.09	1.86	
4.40	4.62	1.47	1.35	1.31	3.33	2.67	
5.63	4.43	1.47	0.69	1.06	3.37	3.33	
0.82	5.97	1.50	0.23	4.17	1.81	0.46	
1.61	5.83	1.49	0.47	3.09	2.74	0.94	
3.07	5.56	1.48	0.92	2.03	3.53	1.83	
4.40	5.32	1.47	1.34	1.51	3.81	2.64	
5.63	5.10	1.47	1.69	1.22	3.89	3.34	134.27(±1.12)
6.75	4.90	1.46	2.07	1.00	3.90	4.06	
0.82	7.56	1.50	0.22	5.33	2.23	0.44	
1.61	7.38	1.49	0.46	3.96	3.42	0.91	
2.36	7.20	1.49	0.69	3.13	4.07	1.37	
3.07	7.04	1.48	0.90	2.61	4.43	1.79	
3.75	6.88	1.48	1.13	2.20	4.69	2.24	
5.03	6.59	1.47	1.55	1.68	4.91	3.05	
6.20	6.32	1.46	1.95	1.35	4.97	3.84	
7.28	6.07	1.45	2.42	1.09	4.98	4.71	
0.82	5.11	1.50	0.22	3.60	1.52	0.45	
1.61	4.99	1.49	0.46	2.67	2.34	0.93	
2.36	4.07	1.49	0.68	2.13	2.74	1.36	
3.07	4.76	1.48	0.92	1.75	3.02	1.82	
3.75	4.66	1.48	1.14	1.48	3.18	2.27	

Table V(ii): Effective stability constant for Eu-acetate equilibrium at pH 5.0; 25°C.

B_T = 0.0150 M							
$[M]_T x10^4$ (ML^{-1})	$[Mu]_T x10^5$ (ML^{-1})	$[B]_f x10^2$ (ML^{-1})	$[M]_f x10^4$ (ML^{-1})	$[Mu]_f x10^5$ (ML^{-1})	$[MMu] x10^5$ (ML^{-1})	$[MB] x10^4$ (ML^{-1})	Mean $K_{association}$
0.82	5.68	1.49	0.23	4.17	1.51	0.50	
1.60	5.54	1.49	0.45	3.22	2.32	0.99	
2.34	5.41	1.49	0.66	2.64	2.79	1.45	
3.05	5.29	1.48	0.84	2.26	3.04	1.84	
3.73	5.17	1.48	1.04	1.94	3.24	2.28	148.22(±2.37)
0.82	5.95	1.50	0.22	4.40	1.56	0.49	
2.34	5.67	1.48	0.70	2.67	3.00	1.54	
3.73	5.42	1.48	1.12	1.94	3.48	2.45	
5.00	5.19	1.47	1.53	1.50	3.68	3.33	
6.16	4.98	1.46	1.91	1.22	3.75	4.14	
7.24	4.78	1.45	2.25	1.04	3.76	4.84	
1.60	6.54	1.49	0.38	4.04	2.43	0.83	
3.05	6.24	1.48	0.83	2.65	3.52	1.82	
4.38	5.97	1.47	1.24	2.00	3.98	2.72	
5.59	5.72	1.46	1.64	1.57	4.15	3.57	
6.71	5.49	1.46	1.70	1.54	4.19	3.68	
7.74	5.28	1.45	2.32	1.12	4.16	4.98	

Table V(iii): Effective stability constant for Eu-acetate equilibrium at pH 5.0; 35°C.

B_T = 0.0150 M

$[M]_T x10^4$ (ML^{-1})	$[Mu]_T x10^5$ (ML^{-1})	$[B]_f x10^2$ (ML^{-1})	$[M]_f x10^4$ (ML^{-1})	$[Mu]_f x10^5$ (ML^{-1})	$[MMu] x10^5$ (ML^{-1})	$[MB] x10^4$ (ML^{-1})	Mean $K_{association}$
1.61	5.25	1.49	0.42	3.32	1.93	1.00	
2.36	5.13	1.49	0.62	2.75	2.39	1.49	
3.08	5.01	1.48	0.82	2.35	2.66	1.94	
3.76	4.90	1.48	0.97	2.13	2.87	2.29	
4.42	4.80	1.47	1.19	1.81	2.99	2.81	160.69(±0.80)
5.04	4.69	1.47	1.37	1.61	3.08	3.23	
0.83	8.83	1.50	0.19	6.95	1.89	0.47	
1.61	8.62	1.49	0.40	5.52	3.10	0.97	
3.08	8.23	1.48	0.76	3.99	4.24	1.82	
5.64	7.54	1.46	1.56	2.38	5.17	3.67	
6.77	7.24	1.46	1.90	1.99	5.26	4.44	
7.82	6.96	1.45	2.21	1.71	5.26	5.14	
0.83	6.40	1.49	0.22	4.93	1.48	0.52	
1.61	6.25	1.49	0.40	3.91	2.14	0.94	
3.08	5.97	1.48	0.85	2.74	3.24	2.02	
4.42	5.71	1.47	1.23	2.10	3.60	2.91	
5.64	5.47	1.46	1.59	1.70	3.76	3.74	
6.77	5.25	1.46	1.91	1.44	3.82	4.47	
7.82	5.05	1.45	2.22	1.23	3.82	5.17	

References

1. G. Schwarzenbach and H. Gysling (1949), Helv. Chim. Acta, 32, 1314.

2. L.B. Nanninga (1961), Biochim. Biophys. Acta, 54, 330.

3. V.G. Geier (1965), Berichte dier Bunsengessellschaft, 69, 617.

4. K.S. Balaji, S. Dinesh Kumar and P. Gupta-Bhaya (1978), Analytical Chemistry, 50, 1972.

5. Levine, M.C. Phillips and R.J.P. Williams (1977), Biochim, Biophys. Acta, 468, 364.

6. E.A. Noack and E.M. Heinen (1977), Eur. J. Biochem, 79, 245.

7. R.S. Kolat and J.E. Powell (1962), Inorganic Chemistry, 1, 293.

8. D.E. Gueffroy (Ed.) (1975), A Guide for the preparation and use of buffers in Biological Systems, Calbiochem, California.

9. A.I. Vogel (1968), A Text Book of Quantitative Inorganic Chemistry ELBS Edition, p. 436-441, Longmans Green and Co. Ltd., London.

10. I.M. Kolthoff and P.J. Elving (Eds) (1963), Treatise on Analytical Chemistry, Part II, Vol. 8, Interscience Publishers, New York.

11. John A. Ball (1978), Algorithms for RPN Calculators, Wiley Interscience.

12. G. Schwarzenbach (1960), Complexometric Titrations Methuen, London and Interscience, New York, p. 36.

CHAPTER 3

METAL LIGAND EQUILIBRIUM

Complex formation of the lanthanide ions with amino acids has been extensively studied. Techniques applied have been potentiometric titration [1-4], polarography [5], solvent extraction [6,7] and spectral titration using NMR spectroscopy [8-11, 13]. Cefola et al. [1] reported stability constants of Ce^{3+}, Pr^{3+}, La^{3+} and Nd^{3+} with glycine, β-alanine and aspartic acid. The values reported are large (e.g. $\log K_1 = 3.71$, $\log K_2 = 3.30$ in Nd^{3+}- Glycine equilibria, $\log K_1 = 5.40$, $\log K_2 = 4.08$, $\log K_3 = 3.06$ in Nd^{3+}- aspartic acid equilibria, $\log K_1 = 3.04$ in Nd^{3+}- β-alanine equilibrium, T = 30°C). The metal ligand ratio used is 1:12, 1:3, 1:1 i.e. ligand is in excess ($\sim 10^{-2}$ M). The authors consider data below pH $\sim$ 6 only, to avoid effect of hydrolysis of lanthanide ions. The data were analysed using Bierrum plots. Jones and Williams [2,3] studied the complex formation between histidine and a variety of lanthanide ions. They use a computer programme (called SCOGS, developed by Perrin and Sayce) to analyse the data. The programme rejects the formation of hydrolyzed species and polynuclear complexes. The model accepted by the computer programme assumes the simultaneous presence of two 1:1 equilibria and one 1:2 equilibrium leading to the formation of $[Ln(Hist)]^{2+}$, $[Ln(Hist)_2]^{+}$, $[Ln(HistH)]^{3+}$. The formation constants are high (e.g. in Nd^{3+}-histidine system $\log \beta$ (Nd-hist) = 4.40, $\log \beta$ $(Nd(Hist)_2) = 6.59$, $\log \beta (Nd(HistH)) = 11.77$ at 25°C, Ref. 2). Sekhon and Chopra [4] report values

of stability constant of the equilibria between the metal ion Ce^{3+} and amino acids leucine, valine, proline and hydroxy-proline. They analyse the data using Bierrum plot and do not take the effect of hydrolysis into account. They report a stoichiometry of 1:1 in the pH range 6-7.5 and the values of stability constants are large (e.g. log K_1 in Ce^{3+}-valine equilibrium is 5.02 at 25°C). Lal [5] has reported polarographic study of Eu^{3+}-proline and Eu^{3+}-tryptophan equilibrium. Eu^{3+} undergoes one electron reduction to Eu^{2+} in the first step and the polarographic wave associated with the reduction is shifted to more negative potentials with increased concentration of amino acid. The magnitude of the shift is a measure of complex formation. The pH alters from 2.3 to 5.1 during the titration. He concludes that Eu^{3+} forms both 1:1 and 1:2 complex with proline. The formation constants are $\beta_1 = 0.3$ and $\beta_2 = 1.78$. In sharp contrast the value of β_1 for Eu^{3+}-tryptophan association equilibrium is large - 6.25×10^6. The metal - amino acid concentration range covered in the experiment on metal-proline system is large and extends upto very large excess of ligand. Tanner and Choppin [6] used solvent extraction technique to study complex formation between Glycine and Ce^{3+}, Eu^{3+}, Pm^{3+}, Am^{3+}, Cm^{3+} at a fixed pH. The technique utilises the phenomenon that complex formation in the aqueous phase affects the extraction coefficient of the metal ion into the organic phase by dinonyl napthalene sulfonic acid. The extraction coefficient is measured by counting

radioactive metal nuclei in the two phases. The stability constants so determined are small in magnitude (e.g. Eu^{3+}-Glycine equilibrium constants at pH 3.64 are 4.1 at 0°C, 5.0 at 25°C, 6.0 at 40°C, 8.0 at 55°C) in sharp contrast to the results of Cefola et al. [1] on Nd^{3+}-Glycine system by potentiometric titration ($\log K_1 = 3.71$, $\log K_2 = 3.30$). Tanner and Choppin determine K as a function of temperature to determine $\triangle H^{\circ}$ and find that the complex formation is endothermic for all the systems studied by them (e.g. for Eu^{3+}-Glycine complex formation, $\triangle H^{\circ} = 2.3$ kCalmole^{-1}). The complexes are stablised by favourable values of $\triangle S^{\circ}$. The entropy change in the lanthanide-glycinate equilibrium is comparable to that in the lanthanide-acetate equilibrium. This result indicates that the effect of complex formation on hydration is comparable in the two cases. The lower stability of the glycinate complex compared to that of the acetate complex is probably due to the decreased ionic attraction in the Zwitterionic complex M^{3+}-O_2C-CH_2-NH_3^+ than in the acetate complex where the positive charge on the ligand is absent. To verify that the liganding species is the Zwitterion (and not the anion in a chelate), an experiment on Eu^{3+}-Glycine system was carried out at pH 5.82. A change of pH from 3.64 to 5.82, increases the Zwitterion concentration by 10%, whereas anion concentration is increased by a factor of about 100. At this pH assuming that complexing is due to the Zwitterion only a value of $K_1 = 6.2$ is obtained

at 40°C, which is equal to the value of K_1 determined at pH 3.64 at 40°C, assuming that the Zwitterion alone binds. Thus Tanner and Choppin [6] conclude that metal ion binds amino acid through the carboxylate alone and does not form a chelate involving NH_2 and $CO_2^{\ominus}$, accompanied by the release of the ammonium proton. These authors do not state the concentration of metal ion used, but ligand concentration was varied between 0.01 to 0.1 M. Aziz and Lyle [7] use the same technique to determine Eu^{3+}-alaninate stability constant. The value reported by them is 5.51 at 25°C. The pH of the experiment is not explicitly mentioned, but is presumably in the same range of Tanner and Choppin who determined the K for Eu^{3+} - ''Glycinate'', whereas Aziz and Lyle report data for Eu^{3+} - ''alaninate''. Sherry, Birnbaum and Darnall [9] studied the equilibrium between Nd^{3+} and histidine and alanine by spectral titration using NMR spectroscopy. The reported values of stability constant are 2.0 (Nd^{3+}-histidine, pH 4.0) and 6.5 (Nd^{3+}-alanine, pH 4.0). This work provides evidence for 1:1 monodentate complex below pH 5.0 and 1:1 bidentate complex above pH 6.0 in Nd^{3+}-histidine system. At high metal concentration two metal ions bind one histidine molecule. The binding sites are inferred from the data on contact shift. The monodentate complex co-ordinates through the carboxylate group. The bidentate co-ordination is through the carboxylate and the imidazole nitrogen (N_1). The hypothesis of co-ordination through imidazole nitrogen is tested by studies of Nd^{3+}

binding to 1-methyl and 3-methyl histidine. The latter follows the pattern of histidine, whereas the former shows only monodentate co-ordination. Sherry, Yoshida, Birnbaum and Darnall [10] determined stability constant of complex formation between Nd^{3+} and several amino acids and other carboxylate ligands by spectrophotometric titration using NMR and by potentiometric titration. Their data on potentiometric titration is analysed by the same programme SCOGS used by Jones and Williams [2]. The authors mention that the potentiometric data indicate substantial hydrolysis at pH 7.0. They observe that even though Jones and Williams [2] do not include any hydrolysed species in their calculation and presumably they do include them, their results agree. It remains unclear, however, how a value of 230 for K (data of Sherry et al. [10] for Nd^{3+}-histidine) can be thought to be in agreement with a value of $\log \beta = 4.40$ for $Nd(hist)^{2+}$ and $\log \beta = 11.77$ for $Nd(histH)^{2+}$ for the two 1:1 stability constants reported by Jones and Williams [2] not to mention the finding of the latter authors that 1:2 complex also forms. There is no discussion on the importance of hydrolysed species. If there are hydrolysed species in solution, the system requires more than one stability constant for its description. The value of 230 of K (Nd^{3+}-histidine) is perhaps a composite 1:1 stability constant.

In the NMR spectral titration, Sherry et al. [10] used $[Nd^{3+}]_{Total} = 0.05$ M and $[Ligand]_{Total} = 0.05 - 0.10$ M.

If K=10, the degree of saturation of metal ions vary between 0.28 to 0.54. If K=1, the variation is between 0.04 to 0.10. A linear Schatchard plot in this limited range of saturation, however, does not establish the stoichiometry to be 1:1. Deranleau in a very enlightening discussion on the theory of the determination of stability constants of weak complexes [14] has shown that the presence of multiple equilibria shows up as non-linearity (unless the sites are equivalent) in all the well-known graphical plots normally used for data analysis, such as Schatchard, Benesi-Hildebrand or Scott plot. Of these Schatchard is the most sensitive. The degree of saturation at which nonlinearity of a Scatchard plot is clearly detectable depends on the values of the stability constants. Deranleau's calculations show that for $K_1 = 10$ and $K_2 = 1$, the Schatchard plot is linear between $S = 0.2$ and $S = 0.5$, but any slope or intercept obtained by extrapolation of this limited data will be incorrect, because below $S = 0.2$, the slope is somewhat different. For $K_1 = 10$ and $K_2 = 0.1$, nonlinearity is visible even within the restricted range $S = 0.2$-0.5. Deranleau has shown that in the presence of multiple equilibria, the limiting slopes and intercepts are complicated functions of K_1 and K_2 and the corresponding spectral parameters ε_1, ε_2 or δ_1, δ_2 (depending on whether absorption spectroscopy or NMR spectroscopy is being used). However in order to obtain the limiting slope, and intercepts in the limit of $S \rightarrow 0$ and $S \rightarrow 1$, data over wider range is essential. Apart from the defect of

not having detected multiple equilibria because of observed linearity in a limited region of saturation, these experiments may have the shortcoming of having studied only very low saturation ($S < 0.1$), region, in those cases where K is closer to 1 than to 10. Deranleau [14] on the basis of a formula for the relative error derived by Weber [15] has pointed out that a satisfactory accuracy of the values of K is obtained only between the degree of saturation 0.2–0.8. This point has also been discussed in Chapter II. K_{MMu} is found to be in error at both low and high saturation limits. Thus the results of Sherry et al. [10] based on potentiometric and NMR titration experiments indicate that the values of equilibrium constants are small, but their quantitative accuracy is doubtful. Thus the agreement between two sets of data is also not very meaningful. The claim of agreement between their potentiometric data and those of Jones and Williams [9] is unfounded. Sherry and Pascual [11] determined the stability constant of alanine with several lanthanide ions at pH 3 at 24°C (μ = 2.2 M). They report a value of K of 0.7±0.1 and an 1:1 stoichiometry for all the lanthanide-alanine complexes. Their method (the same method is used in the earlier work of Sherry et al. [10]) is based on the equation

$$\frac{1}{\Delta_{obsd}} = \frac{1}{[M]_o K_1 \Delta_o} + \frac{1}{\Delta_o} \frac{[L]}{[M_o]} ,$$

where $[M]_o$ is the total concentration of metal, Δ_o is the chemical shift of the complex (observed on saturation) Δ_{obsd} is the measured chemical shift in a ''fast exchanging'' mixture containing free ligand of concentration [L]. The equation holds for a stoichiometry of 1:1. Thus a linear plot of $1/\Delta_{obsd}$ vs. $[L]/[M]_o$ gives $1/\Delta_o$ as slope and $1/[M_o]K_1\Delta_o$ as intercept. K_1 is then calculated. A knowledge of [L], however, presupposes a knowledge of K. Thus, a plot of $1/\Delta_{obsd}$ vs. $[L]_o/[M_o]$ gives a best fit for K, which is then used to calculate [L]. The new plot of $1/\Delta_{obsd}$ vs. $[L]/[M_o]$ gives a better value of K, which in turn gives a better value of [L]. The iteration is continued till $K_n - K_{n-1} < 0.1$. The concentration range used is $[M]_o = 0.2$ M and $[L]_o = 0.2$-0.8 M. A value of 0.7 M^{-1} of K gives the range of the degree of saturation of metal ions S to be 0.1-0.35. The range is limited. The highest saturation achieved is slightly above the minimum acceptable degree of saturation (0.2), according to Deranaleau-Weber criterion[14,15]. The range is insufficient for detecting multiple equilibria. The value of 0.7 M^{-1} at pH 3 is lower than the value of K of 6.5 for Nd^{3+} alanine at pH 4 [10]. This is explained by the incomplete ionisation of the carboxylate group at pH 3. Deranaleau [14] has strongly advocated the use of the entire saturation curve in the determination of thermodynamic (K) and spectral parameters (δ or ε) in a spectral titration rather than the limiting slopes and intercepts. This requires the use of a

computer programme for data analysis. Lenkinski, Elgavish and Reuben [12] have proposed an algorithm for the characterization of weak molecular complexes from NMR titration data and have discussed the criteria for the reliability of the results. The association equilibrium studied by them is that of DMSO with $Eu(fod)_3$, the well known shift reagent. The reliability criteria is a generalisation of Deranleau's criteria [14] for 1:1 complex. Deranleau points out that a reliable value of K demands S = 0.2-0.8. For $S < 0.2$ and $S > 0.8$, one of the three quantities that appear in the expression of equilibrium constant has large percentage error either because its small magnitude is not directly measured very accurately or if it is obtained by difference of two comparable quantities, the small difference is not much larger than the errors of the quantities being subtracted from each other. A reliable value of δ_o and ε_o demands a minimum value of S = 0.2. This has to do with the large error in measuring the small concentration of complex at $S < 0.2$. $S > 0.8$ is acceptable for this measurement, because the small value of the concentration of the molecule being saturated is unimportant in this case. The complex concentration is large and the percentage accuracy of this quantity determines the accuracy of ε_o or δ_o. The generalization of these criteria due to Lenkinski et al. [12] is stated as follows : The 1:1 complex is called RS, the 1:2 complex is RS_2. The contribution of RS and RS_2 to the

observed shift (due to both) at a given total concentration of R and S, depends on the stability constants of RS and RS_2 as well as their chemical shift values. Thus the pair K_1, δ_1 can be accurately determined if the conditions are such that the contribution of RS to the observed shift is large. One defines $P_1 = [RS]\delta_1/[S_t]\delta$ and $P_2 = 2[RS_2]\delta_2/[S_t]\delta$, which specify the fractional contribution of RS and RS_2 to overall shift. The accuracy of K_2, δ_2 pair is maximised when $P_2 \simeq 1$ and that of K_1, δ_1 pair is maximised when $P_1 \simeq 1$. To assess the accuracy of individual parameters, one defines the saturation factors (fractions) : $S_1 = [RS]/R_t$, $S_2 = [RS_2]/R_t$, $\sigma_1 = [RS]/S_t$ and $\sigma_2 = 2[RS_2]/S_t$. These quantities vary between 0 and 1. Generalized Deranleau criteria are (i) For accurate K_i, S_i should cover the range between 0.2 - 0.8, (ii) For accurate δ_i, $\sigma_i \gtrsim 0.2$, preferably $\sigma_i \simeq 1$. To meet these criteria, these authors carry out titrations at the following values of concentration (i) DMSO concentration is held constant at 20 mM and $Eu(fod)_3$ concentration is varied from 1.5 to 61.4 mM. The principle is to hold S_t (DMSO concentration) at the lowest possible value to permit easy observation of its resonances (Type I titration). (ii) $Eu(fod)_3$ concentration is held constant at 10 mM and DMSO concentration varies between 30 mM and 200 mM. The principle is to hold R_t (the total concentration of the species whose resonance is not being observed) at a value such that a measurable shift is observed even when $S_t = 20\ R_t$.

High S_t/R_t ratio favours formation of RS_2 complex ($[RS_2]/[RS] = (\beta_2/\beta_1)[S]_{free}$; $[S]_{free}$ is high when $S_t = 20\ R_t$). Calculation shows that if $4K_1 < K_2$ (i.e. if $\beta_2 > 4\beta_1^2$), Type II titration allows accurate determination of K_2 and δ_2 and Type I titration allows accurate determination of K_1 and δ_1. If $4K_1 > K_2$, K_2 and δ_2 can be accurately determined, but K_1 and δ_1 can not be determined with good accuracy. If $4K_1 = K_2$, conditions could be obtained for accurate values of all but K_1. A computer programme fits the data of Type I and Type II titration taken together to give best values of parameters. The saturation functions are then plotted and one checks that the reliability criteria have been met. The basic physical chemistry behind the approach is that concentration must be varied over a wide range to allow formation of both RS and RS_2. Since concentrations are measured by NMR contact shift values, the concentrations of RS and RS_2 must be such that the contribution of each species to the measured shift must be a substantial fraction of the observed shift i.e. the ratio of $[RS]/[RS_2]$ must be larger if the shift value of [RS] is smaller.

Using the method described above, Elgavish and Reuben [13] showed that Pr^{3+} and Yb^{3+} form 1:1 and 1:2 complexes with alanine. At 39°C and pH 4.5 ± 0.3, K_1 and K_2 of Pr^{3+}-alanine complex are 0.235 and 0.94 (in M^{-1}), and those of Yb^{3+}-alanine complex are 0.310 and 1.24 (in M^{-1}).

The relation $4K_1 = K_2$ shows that there are two equivalent binding sites for alanine on the lanthanide ion. A linear Schatchard plot establishes the equivalence of the sites and finds their number to be two. The chemical shift values of ML and ML_2 are equal. Thus the sites are equivalent magnetically as well as chemically. The concentration values used in Ln^{3+}-alanine titration are not quoted, but both Type I and Type II titrations are stated to have been carried out. In the study of sarcosine lanthanide ion interaction (for which K values are not given) ligand is 1 M and lanthanide ion concentration vary between 0.045 to 0.1 M. Ligand is in excess. The existence of 1:2 lanthanide - carboxylic acid complexes has also been reported by Inagaki, Takahashi, Tasumi and Miyazawa [8]. They study complex formation of Eu^{3+} ion with L - azetidine-2-carboxylic acid in D_2O solution by measurement of Eu^{3+} induced shift of the PMR spectrum. A least square curve fitting of the entire range of data using a computer programme was used for data analysis. An assumption of 1:1 stoichiometry is insufficient to fit the data. A good fit is obtained only if the presence of both 1:1 and 1:2 complex is included in the model. Deviation from 1:1 model becomes more evident as one increases $[S_o]$ (total concentration of carboxylate ligand) keeping $[L_o]/[S_o]$ ratio constant (L_o = total lanthanide ion concentration). This demonstrates that the relative as well as absolute values of concentration are important in determining relative proportion of complexes. The values of K_1 and K_2 are 3.6 and 0.6 (in M^{-1}).

There has been some difference of opinion amongst workers about the model of co-ordination of the amino acid with the metal ion. It has been stated earlier that Tanner and Choppin [6] conclude that co-ordination takes place through the carboxylate group in glycine. Sherry, Birnbaum and Darnall [9] conclude that carboxylate co-ordinates alone at low pH and in addition histidine N-1 co-ordinates above pH 6. Cefola et al. [1] on the basis of stability constant data obtained by them (these data are now in question; as discussed later) conclude that aspartic acid forms a tridentate complex (liganding through two carboxylates and one amino group). The difference of values log K between aspartate complex and glycinate complex is 0.2 for alkaline earth ions [16] but assumes the value of 1.8 for lanthanide ions [1]. These authors implicitly assume that glycinate is bidentate (perhaps on the basis of high values of K). Thus a high value of K of aspartate complex is thought to indicate tridentate co-ordination. Chaberek and Martell [17] had earlier concluded tridentate co-ordination for the aspartate complex of first flow transition metal ions.

Katzin [18] reports a study of absorption and circular dichroism spectra of complexes of Eu(III) ion with amino acids and sugar acids. In an earlier study Katzin [19] observed that the sign of the C.D. spectra of Pr(III) complexes of sugar acids is defined by the hydroxyl configuration

at the α-carbon when the pH is acidic. In neutral and alkaline pH, sign of the C.D. spectra is correlated with the sign of the hydroxyl configuration at the γ-carbon, where this is an asymmetric center. Thus two hydroxy acids, which have the same α-carbon configuration (d) and different configurations at the γ-carbons (an example is gluconic acid and galactonic acid pair) will have the same sign of C.D. spectrum at acid pH, but different signs at alkaline pH. This is thought to indicate γ-coordination at higher pH. The results are different for Eu(III) ion [18] in that the reverse sign of C.D. spectra is observed even at acidic pH, indicating chelation at acidic pH. The sign inversion is maintained at neutral pH. Complex formation of Zwitterionic amino acid to to Eu(III) through the carboxylate alone at low pH suffices to give a C.D., which is strongest in the $^5D_1 \leftarrow {}^7F_0$ band. The complex of gluconic acid at acidic pH has its strongest dichroism in this band. When pH is raised, the C.D. increases in intensity and the sign inverts for both the amino acid and the sugar acid. The $^5D_1 \leftarrow {}^7F_0$ absorption intensity however remains insensitive. The author is puzzled by the fact that sign inversion with increase in pH occurs for the deprotonation of the protonated amino group in the case of the amino acid and for the deprotonation of the hydroxyl group for the sugar acid. The resulting amino acid is singly charged and the resulting sugar acid is doubly charged. They reject the alternative possibility that hydrolysis at high

pH is responsible for the change in the sign of C.D. rather than chelation. The reason cited is that the change-over takes place at pH 5 in the sugar acid and at pH 7 in the amino acid. The author points out that the change in C.D. may require two negative charges. For the sugar acid it comes from carboxylate and the ionized hydroxyl group. For the amino acid, it comes from the carboxylate and a hydroxyl ion derived from solution. This may explain the higher pH necessary for the amino acid complex. Katzin observed a buffer resistance in the region of pH 6-7, when ammonia is added to raise the pH of the solution containing Eu(III) and alanine or serine. Aspargine containing solution leads to precipitation of Eu(III) ion. The buffer resistance is observed in the region 5-6 for the sugar acid gluconic acid. There is no attempt in Katzin's work to give a quantitative or semiquantitative theoretical basis for his interpretation. The chelation in the amino acid complex is based merely on the similarity of the sign inversion of C.D. with the sugar acids. Prados, Stradtherr, Donato and Martin [20] report careful pH titration studies on mixtures of lanthanide ions and a variety of ligands including several amino acids. They find that the solutions of lanthanide ions can be titrated to reproducible end points after addition of $\sim$ 2.5 equivalents of base. Eu(III) precipitates before the end point is reached. The titration curve shows less than one unit of pH rise during the titration. Thus lanthanide ion solution show buffer action.

The mid point of the buffer region varies across the lanthanide series from 9.3 to 7.6. The narrow pH range of the buffer region and the non-integral base equivalent needed suggest formation of polymers involving hydroxycomplexes. A large number of ligands, including alanine, aspargine, serine, histidine methylester and N-acetylhistidine, show a pH titration behaviour which is a superposition of those of the metal and the ligand. At pH values where carboxyl is unionized no complex formation takes place. Thus carboxyl groups ionize with their characteristic pK before any complex formation occurs. This is followed by titration of lanthanide ions which titrate in a manner identical to that of an uncomplexed ion. Thus the liganded H_2O molecules which get converted into hydroxide ions as a result of hydrolysis do so in a manner independent of the co-ordination of the carboxylate group. The amino group titrates next with a pK identical to that of uncomplexed amino acid. The equivalents of base consumed correspond to the total concentration of amino acid - complexed and uncomplexed. Thus the complexed amino acid titrates as though the NH_3^+ group is free. This establishes beyond doubt that NH_3^+ group does not co-ordinate. The co-ordination of NH_3^+ is to be accompanied by the release of a proton. Thus high pH can only enhance the formation of the complex with co-ordination through the amino group. The amino group of the complexed amino acid is found to be protonated at a high pH around the pK of NH_3^+ group. This means

that it was protonated at a lower pH also. We point out that CO_2H group of the amino acid behave in a similar manner, i.e. they do not co-ordinate at a pH where they are protonated. No spectral change is observed in NMR and C.D. at a pH where CO_2H is unionized [13,18]. L-aspartic acid exhibits a different titration behaviour. The aspartic acid carboxylates titrate first consuming base equivalents of the total concentration of aspartic acid. Metal hydrolysis consumes 2.0 equivalents of base to an inflection near pH 8 with a mid point near pH 7, irrespective of the molar ratio of aspartic acid and Ln(III) ion. This hydrolysis portion is more spread out on the pH axis and exhibits a mid point at a pH lower than that shown by aqueous lanthanide ions. Ammonium deprotonation occurs as usual.

Glutamic acid yields precipitates in the lanthanide ion hydrolysis region. Almost the full number of hydrolysis equivalents appear as with aqueous metal ions. These results are interpreted by a model which assumes that α-carboxylate co-ordinates the metal ion first. As the pH is raised the γ-carboxylate instead of chelating helps in the formation of polynuclear complexes, which assist precipitation.

Thus hydrolysis of lanthanide ions definitely occurs in spite of complex formation with amino acids. If a sufficient number of strongly bound lanthanide ions co-ordinate a lanthanide ion, no hydrolysis occurs as is the case with 2,6,dipicolinic acid [21]. Prados et al. [20] have clearly

shown that in the case of histidine an integral 2.0 equivalent per mole of Dy(III) or Ho(III) are titrated in the region of pH $\gtrsim$ 7. Thus the metal ion hydrolyses even though it is complexed to histidine. This is in contrast to the result that the computer programme SCOGS used by Jones and Williams [2,3] rejected the existence of hydrolysed species. Prados et al. [20] point out that the extensive hydrolysis of the lanthanide ions in lanthanide-amino acid complexes is an indication of weak binding. They propose that for alanine, serine or aspargine the hydrolysed species has a structure $[Ln_2^{3+}(OH)_5^- ala_2]_n^+$ where n is unknown. This is consistent with (a) the consumption of 2.5 equivalents of base per mole of lanthanide ions, and (b) the chemical composition (established by chemical analysis) of the precipitate from basic chloride solution of Pr(III) and Tm(III) being $Ln_2(OH^-)_5Cl$. An odd number of hydroxide ions evidently bridges two lanthanide ions. These workers propose that aspartic acid coordinates through the two carboxylate groups. The ammonium group remains protonated. Equimolar ratio of aspartic acid and Ln(III) yield titration curves of the same character as those with additional ligand. The simplest structure at the terminus of the hydrolysis region near pH 8 may be $[Ln^{3+}(OH)_2^- asp^-]^o$ which might be mononuclear [21]. The differences in behaviour with other ligands like alanine that make these authors to propose a mononuclear complex are (a) the hydrolysis part of the titration is more spread out on the pH axis

and (b) 2.0, not 2.5, equivalents of base are consumed. These authors find that the changes in the C.D. spectrum plotted as a function of pH shows a mid-point identical to that of the titration curve. The C.D. changes are therefore assigned to hydrolysis rather than to chelation, as proposed by Katzin [18].

There has been some attempt to work out the details of the location of the lanthanide ion on the carboxylate binding site of an amino acid. These attempts use NMR spectroscopy. The pH values of these experiments are kept low. This avoids complication due to hydrolysis. At low pH, it is also not necessary to consider NH_3^+ binding to the metal ion (accompanied by deprotonation). It will necessitate high pH, if at all it is operative (the evidence of Prados et al. [21] is enough to exclude it at all pH values).

Levine and Williams [22] on the basis of contact shift data and a detailed computer search for the structure that fits the data best, conclude that the lighter lanthanides (Pr^{3+} ---- Tb^{3+}) bind to both the oxygen atoms of the carboxylate i.e. carboxylate is bidentate, whereas the carboxylate is monodentate towards the heavier lanthanide ions (Dy^{3+} ---- Yb^{3+}). Sherry and Pascual [11] using a similar approach find that in alanine, the trend is just the reverse, i.e. carboxylate is bidentate towards the heavier lanthanides and monodentate towards the lighter ones. The cause for the discrepancy

according to Sherry and Pascual [11] is the incorrect separation of the observed shift into contact and pseudo contact contributions in the work of Levine and Williams [22]. Even a small error leads to large discrepancy in structural parameters. Elgavish and Reuben [23] conclude on the basis of relaxation enhancement data that lanthanide-amino acid complexes are isostructural through the lanthanide series and the carboxylate acts as a bidentate ligand. They point out possible reasons for the difference of their conclusion with those of Levine and Williams [22] and Sherry and Pascual [11] to be (a) complication due to formation of higher than 1:1 complex (b) inadequate separation of dipolar and contact contribution to shift and (c) inadequacy of axial model of dipolar shift. In a later more detailed work, Elgavish and Reuben [13] conclude on the basis of shift and relaxation data that a unique position for the lanthanide ion could not be determined with certainty. The lanthanide complexes of sarcosine are found to be isostructural through the lanthanide series. However, if the Ln^{3+} ion is placed on the plane of the carboxylate, it gets located at an impossibly short distance from one oxygen atom. With the assumption that the ion is in a plane perpendicular to that of the carboxyl group and bisecting the O-C-O angle, a Ln-O distance of 2.57 A^{o} is obtained which is in good agreement with crystal structure of lanthanide complexes of carboxylates. An alternate description

in terms of a mixture of bidentate and monodentate (2.57% only) structure is found to be consistent with shift and relaxation data. Deviation from bidentate co-ordination of carboxylate binding sites of rigid (and therefore simpler to analyze unambiguously) ligands like O-toluate has been suggested from the shift and relaxation enhancement data of Pennington and Cavanaugh [25]. The relaxation time for the ortho proton relative to the orthomethyl proton of O-toluate is found to be shorter than expected. The authors suggest that either Gd^{3+} preferentially binds to the carboxylate oxygen nearer the ortho proton or the internal rotation of the methyl group is affecting the correlation time for the O-methyl protons. Thus the details of the co-ordination of the lanthanide ion to the carboxylate moiety is very much a matter of contemporary research and debate. The situation is obviously more complicated than straight forward chemical intuition would like to conclude.

Thus there exists considerable need for further investigation in the field of determination of structure of lanthanide-amino acid complexes in solution as well as in the field of determination of stability constant of lanthanide-amino acid equilibria in solution.

Choice of metal ion :

We decided to choose hypersensitive transitions intensity as the spectral technique for structural investigation.

Obviously Eu^{3+} ion was our choice. Eu^{3+} occupies a position in the field of lanthanide spectroscopy similar to the position of hydrogen atom in quantum mechanics. The nondegenerate ground state ($^7F_0$) makes detailed analysis easier. For example there are only a maximum of five component transitions in the $^5D_2 \leftarrow {}^7F_0$ transition band. Thus a meaningful lineshape analysis is possible, whereas if both the ground and excited state had degeneracy, this would be considerably more difficult. Eu^{3+} also has the advantage of having a hypersensitive fluorescence emission ($^5D_0 \longrightarrow {}^7F_2$), which originates from a non-degenerate excited state. This emission line also is amenable to detailed analysis.

Choice of ligand :

Of the amino acids, we have chosen Aspartic acid, Glutamic acid, Aspargine and Glutamine as our ligands. Uptil now, as is evident in the discussion presented above, Alanine and Sarcosine have been studied as ligands co-ordinating lanthanide ions. They are simple because the side chains do not provide binding sites. Histidine has been studied in lesser detail. The ligands chosen by us have just these features. It is these features that make them more complicated and therefore more interesting. There is a possibility of chelation. More than one carboxylate moiety of aspartate and glutamate are almost always used to hold a Ca^{2+} ion in the Ca^{2+} binding proteins [25]. There is also evidence of a

peptide group binding Ca^{2+} ion in a protein [25]. Thus the carboxylate and carboxamide side chains of the ligands studied by us make them more useful model systems for the study of protein binding site. In the case of glutamine and aspargine, even if the side chain carboxamide group does not bind the metal ion, its presence in the vicinity mimicks a metal binding site of a protein more closely.

Choice of technique for stability constant determination:

The experimental technique used by us uses a metallochromic indicator murexide as a monitor of Eu^{3+} concentration. In sharp contrast to the spectral titration using e.g. NMR spectroscopy, this technique measures free Eu^{3+} concentration directly. It is close to the solvent extraction technique [6,7] in this respect. It is experimentally simpler to perform particulately if one requires a large number of titration points. The pH titration technique was of less interest to us because we, in our laboratory, are interested in making measurements of stability constant on proteins with Ca^{2+} and Eu^{3+} ions being simultaneously present in solution.with an eye to measurement of co-operativity in metal binding in these systems. pH variation is essential in the pH titration technique. A macromolecule changes its structure, sometimes drastically, sometimes in a subtle way on pH variation. Thus measurement at a fixed pH is easier to interpret. Over and

of murexide solution is then taken in a quartz cuvette (purchased from Hellma, England) with a path length of 1 cm and a volume of about 3 ml. The exact volume is determined by weighing in a semimicrobalance. In a matched cuvette one then takes an identical volume of the same murexide solution. The volume is adjusted to be equal to that in the first cuvette by an adjustable microliter pipette. The adjustment is easily made to better than 0.5 µl.

$EuCl_3$ (made from Eu_2O_3 by repeated evaporation to dryness with Analar HCl; Eu_2O_3 was purchased from Sigma Chemical Company, U.S.A., certified purity $\rangle$ 99.9%) of known concentration (details of determination is in Chapter II) is added in known volume by a high precision microliter pipette (purchased from Oxford Laboratories, Ireland) to the murexide solution in one of the cuvettes. The volume of Eu^{3+} ion solution added is again determined by weighing the cuvette. The volume determined by weighing agreed in almost all cases with the volume supposed to have been delivered by the pipette. An identical volume of buffer is added to the second cuvette by the same microliter pipette. Weighing is once again carried out to establish that volume of the buffer is equal to that of the metal solution. The maximum difference is 0.5 µl.

The difference in absorption (ΔA) between the cuvette containing metal ion and the one without it is given by the

relation $\triangle A = \triangle\varepsilon[MMu]$, assuming only 1:1 complex is present. The determination of $\triangle\varepsilon$, the difference in the molar absorptivities of MMu and Mu is given in Chapter II. Thus [MMu] is experimentally measured. The total concentration of murexide $[Mu_T]$ obeys the relationship $[Mu]_T = [Mu]_f + [MMu]$. The values of equilibrium constant K_{MMu} are given in Chapter II. Thus known values of [MMu], $[Mu]_T$ and K_{M-Mu} gives $[M]_f$ ($[M]_f = [MMu]/K_{MMu}$ ($[Mu]_T - [MMu]$)).

Ligand solution is prepared by dissolving known weight of amino acids in buffer (ionic strength adjusted to 0.100 by addition of KCl) in a volumetric flask. The amino acids (purchased from Sigma Chemical Company and E. Merck) are stored in dessicators. The concentration is calculated from the known weight of amino acid and the known volume of the volumetric flask. Ligand solution is added to the cuvette containing metal solution (sample cuvette) in instalments of 100 µl. The pipettes of smaller volume increase the possibility of error in volume delivery. In one out of 20 deliveries, a deviation of 1 µl occurs. But the error it introduces is smaller if the 100 µl pipette is used. For each delivery of ligand solution to the sample cuvette, one adds an identical volume (using the same pipette) of buffer to the reference cuvette. $\triangle A$ keeps on decreasing as ligand solution is added, i.e. as the titration progresses. Thus one is able to measure the concentration of free metal in mixtures of different concentrations of metal and amino acids.

The titration experiment is carried out in a stoppered cell obtained from M/s Hellma, England. A small volume of liquid may sometime leak onto the stopper, but this is negligible to the total volume. A thermostated water bath circulates water around the sample compartment to maintain the temperature at the desired value.

The raw data i.e. $[M]_f$ at definite values of $[M]_T$ and $[L]_T$ are then parametrized in terms of overall stability constants β_i's, which appear as coefficients in the mass-balance equations for total metal and total ligand concentration, $[M]_T$ and $[L]_T$.

$$[M]_T = [M]_f + \sum_i \beta_i [M]_f [L]_f^i$$

$$[L]_T = [L]_f + \sum_i i\beta_i [M]_f [L]_f^i$$

$[M]_f$, the free metal concentration is experimentally determined but $[L]_f$ is not determined at all.

Choice of Concentration :

In a titration experiment, one would ideally like to determine $[M]_f$ and $[L]_f$ at all possible values of $[M]_T$ and $[L]_T$. In a particular experimental approach, only certain concentration ranges can be investigated. In the experiments done by us, restrictions arise from the spectral characteristics of metal-dye system (K, $\Delta\varepsilon$), the magnitude of metal

ligand stability constant and the solubility of the ligand. The range of optical density that can be measured accurately by the spectrometer being used also sets a limitation. Cary 17-D spectrometer of course provides a very wide range. So this is not really a limitation for us, An O.D. below 0.100 is however not measured because the percentage error of reading the digital panel meter increases rapidly below this range (the magnitude of the reading error remains constant ± 0.002). Thus a lower limit to the measurement of [MMu] and therefore $[M]_f$ is set by consideration of spectrometer accuracy.

Murexide concentration has to be high enough to be accurately measurable in a spectrometer. An O.D. between 0.6 and 1.1 has been used. At a certain murexide concentration the initial Eu^{3+} ion concentration can neither be too high nor too low. If it is too high, murexide is almost saturated. $[Mu]_f$ determined by subtracting [MMu] from [Mu], two comparable concentration values, will have large percentage error. The inaccuracy of $[Mu]_f$ is carried over to the value of $[M]_f$, which is calculated from the formula $[M]_f = [MMu]/K_{MMu}\,[Mu]_f$. If it is too low, initial ΔA (α [MMu]) is too small. If we further restrict ourselves to titration points with $\Delta A > 0.100$, very few titration points are obtained in a single titration. In addition, a small value of $[M]_T$ means a small value of $[M]_f$. Thus the response of the metal-dye equilibrium (i.e. the magnitude of its displacement) is small on increasing the ligand concentration by a certain amount. Thus successive

titration points separated by more than the experimental error are harder to obtain. The problem of having low $[M]_T$ is less if the solubility of ligand is higher or if the values of metal-ligand stability constant were higher.

Increase of $[Mu]_T$ can give a high value of initial $\triangle A$ for a given value of $[M]_T$, thus removing one difficulty of using low $[M]_T$. But a high value of $[Mu]_T$ leads to formation of 1:2 metal murexide complex. The spectral and thermodynamic properties of 1:2 metal-murexide equilibrium are not known. We became conscious of this complication near the end of our work and discarded all data that are suspect because of this complication.

Another experimental approach to achieving titration of low values of $[M]_T$ is to use a different dye e.g. Arsenazo (III) which binds Eu^{3+} with a larger K and a larger $\triangle \varepsilon$. A larger $\triangle \varepsilon$ is useful in measuring small changes in [MD]. $\triangle \varepsilon$ is very much like an amplifier gain where input signal is [MD] and output is $\triangle$ A. Thus the resolution of the titration increases. One can get intermediate points in the titration i.e. measure M_f at M_T/L_T ratios which were earlier skipped because of the inability of the experimental set-up to distinguish between the values of M_f at two successive titration points i.e. because of lack of resolution. Because of higher $\triangle \varepsilon$, one gets a larger $\triangle$ A for the same concentration of [MD]. Taking advantage of a large value of K, one can use a comparatively smaller concentration of M_T to obtain the same [MD].

The difficulty of getting small changes in the displacement of metal-dye equilibrium because of only small increase in [ML] complexes at small $[M]_T$ concentration will remain. The problem however is less, because small changes in [MD] are detectable because of high value of $\Delta\varepsilon$.

At a high $[Mu]_T$ (O.D. $>$ 1.1), one can use a high value of $[M]_T$, without saturating murexide and without introducing the complication of 1:2 complex. The range of $[L]_T$ covered would still remain the same. Thus the range of M_L/L_T concentration that would be accessible in these experiments with high $[Mu]_T$ is unlikely to give any additional information, particularly about the presence of metal-ligand complexes of higher stoichiometry (since lower M_T/L_T ratio already covered is more favourable for formation of 1:2 complex). More data would have been obtained at lower saturation ranges, which would not improve the accuracy of the values of β calculated on the basis of the data already accumulated.

Choice of buffer to maintain fixed pH :

The titration experiments are carried out at a fixed value of pH, maintained by a buffer solution. As discussed in Chapter II, the metal-buffer interaction, if ignored, substantially modifies the equilibrium constant being determined. The buffer solution may interact with the dye also. Thus the choice of buffer needs careful analysis.

Firstly, the pK_a of the buffer system must be as close to the desired pH as is possible. The minimum concentration necessary to maintain the value of pH within desired limits is thus reduced.

Secondly, $K_{metal\text{-}buffer}$ (later called K_{MB}) should be small and be known accurately and precisely. If K_{MB} is small, the percentrge of metal bound to buffer is small. For a given precision of K_{MB}, the error introduced in the calculation of metal bound to ligand is smaller if K_{MB} is smaller. As an example, if 40% of metal is bound as MB, and 10% of metal is bound as ML, a 5% error in K_{MB} introduces a 20% error in metal bound to ligand, whereas if 10% of metal is bound as MB, the same precision of 5%, introduces an error of 5% in calculation of ML. The magnitude of this error is dependent on the relative value of K_{MB} and K_{ML}. Obviously the error is half of what we stated above, if 20% (and not 10%) of metal is bound as ML.

Thirdly, the dye should not react with the buffer solution. Good buffers are, in general, weak binders of metal ions. However Pipes was found to interact chemically with murexide. This is presumably due to the nitrogen lone pair of the heterocyclic ring in Pipes. Histidine also reacts with murexide. This factor renders a large number of Good buffers with nitrogen containing heterocyclic rings unusable for titration with murexide as metal-indicator.

Since Eu^{3+} precipitates above pH 6.5, the highest pH at which titration could be carried out is 6.5. TES with a pK of 7.5 is still useful at this pH. It does not react with murexide. Its binding constant with Eu^{3+} is small. The determination of Eu^{3+}-TES equilibrium constant K is found to be high. Thus TES-HCl was chosen as the buffer at pH 6.5.

The choice was more difficult at pH 5.0 when one excludes the buffers that react with murexide, one is left with Bis-Tris and Bis-Tris propane. Preliminary experiments show that the association constant of the Eu^{3+}-Bis Tris equilibrium is $\sim 10^5$. A literature report which appeared simultaneously agrees with this finding [29]. Bis-Tris propane was not readily available. Thus we decided to use acetate buffer, instead of having to wait for the arrival of Bis-Tris propane from abroad and then discover that, like its parent buffer Bis-Tris, it binds Eu^{3+} with a high value of K_{ass}.

Acetate buffer was prepared from Na_2CO_3 and acetic acid, as described in Chapter II. The acetate concentration is known precisely. It is exactly twice the concentration of Na_2CO_3, which is known precisely since the solution is made by weighing Na_2CO_3 in a semimicrobalance and dissolving it in water in a 1 liter volumetric flask.

The binding constant of Eu^{3+} with acetate is known with good precision, but poor accuracy [30]. It was redetermined in our laboratory, as described in Chapter II.

Choice of buffer concentration :

In Eu^{3+}-aspartic acid and in Eu^{3+}-Glutamic acid titrations, we prepare $EuCl_3$ as well as ligand solution in the buffer (μ = 0.100 with KCl). A 15 mM acetate buffer however cannot withstand the protons liberated from the dissolution of 10^{-2} M aspartic and glutamic acid and the final pH is 3.5 - 4.0. The pH of the ligand solution is always adjusted to 5.0 by addition of KOH solution. Any pH change during the titration is due to the formation of any complex that releases protons or due to the displacement of metal-murexide equilibrium that accompanies complex formation. A small pH change of 0.1 pH unit is observed in Eu^{3+}-aspartic acid and in Eu^{3+}-Glutamic acid titration at pH 5.0. No significant pH change is observed in Eu^{3+}-aspargine and in Eu^{3+}-Glutamine titration. The buffer concentration used at pH 6.5 is 100 mM. The concentration is sufficiently high to resist any significant pH change for all the four ligands.

A small pH change from 4.95 to 5.05 introduces very little error as is evidenced by the high precision of the values of β determined at a pH 5.0. The buffer concentration would have to be considerably higher if the pH change were to be completely avoided. The error in the value of ML due to the error in K_{MB} would then be larger. The minimum value of buffer concentration would have to be such that during the titration, the pH changes from 0.05 units below to 0.05 units

above the desired pH of titration. One thus determines an average value of the binding constant, if it is pH dependent, over a range of pH values, which is not necessarily equal to the values at a precise pH of 5.0. The inaccuracy is however small.

In the experiments reported in this work, a buffer concentration of 15 mM at pH 5.0 is the minimum possible value in Eu^{3+}-Aspartic acid and in Eu^{3+}-Glutamic acid titration. In the Eu^{3+}-Aspargine and Eu^{3+}-Glutamine titration at pH 5.0 there is no observable pH change during a titration. Thus it is possible to reduce the buffer concentration. The reduction would in all probability improve the accuracy and precision of the determination of β. The effect of the error of K_{MB} on the values of K_{ML} is determined by changing the value of K_{MB} by $\pm\sigma$, 2σ, 3σ from the mean value in the input data of the programme that parametrizes the titration data. Such a determination shows that in Eu^{3+}-aspargine system at pH 5.0 and 15°C, K_{ML} changes by 8% if K_{MB} is changed by its standard deviation ($\sim$ 1%). At 25°C, the change is 10%. At 35°C, it is less, about 5%. For the maximum error (3σ) in K_{MB}, the change in K_{ML} is 25% at 15°C. The large sensitivity of K_{ML} to a small ($\sigma \simeq 1\%$) change in K_{MB} is understandable when one looks at the following data : At pH 5.0, in Eu^{3+}-aspargine and in Eu^{3+}-glutamine titrations [MB] is $\sim$ 50% of $[M]_T$, whereas [ML] is only 5-15% of $[M]_T$ and is only 5 to 15 times the error in [MB]. In retrospect one should have

used a lower buffer concentration. If pH changes during a titration, Eu^{3+}-murexide stability constant changes from one titration point to another. One, however uses K_{MMu} determined at a fixed pH value to calculate free concentration of Eu^{3+}. It is this quantity that becomes incorrect due to pH change during a titration. The change of 0.1 unit of pH does not change K_{MMu} significantly. The loss of accuracy and precision arising from the slight alteration of pH during a titration is however more than offset by the gain from the use of lower concentration of buffer. The choice of buffer concentration made in our experiments is just optimum in Eu^{3+}-aspartic acid and in Eu^{3+}-Glutamic acid systems. The concentration of 15 mM. Acetate at a pH 5.0 and 35°C in the Eu^{3+}-Aspartic acid system leads to the following results : [MB] is 60-37% of $[M]_T$, [ML] is 19-51% of $[M]_T$ and is 63-255 times the standard deviation in [MB]. The change in K_{ML} is $\sim$ 1% when K_{MB} is changed by an amount equal to its standard deviation (σ) of $\sim$ 1%. The change is $\sim$ 3% if K_{MB} is changed by 3σ ($\sim$ 3%). The pH change during a titration is 0.1. The larger values of metal-ligand binding constant makes the titration data more accurate.

The buffer concentration at pH 6.5 is 100 mM. It is sufficiently high to be able to resist any significant pH change in all titration experiments at this pH. The buffer concentration could perhaps have been lowered substantially. Even though Eu^{3+}-TES binding constant ($\sim$ 10) is considerably

smaller than Eu^{3+}-Acetate binding constant ($\sim$ 100), the considerably higher concentration of TES ($\sim$ 100 mM as compared to $\sim$ 15 mM of acetate) resulted in a comparable fraction of metal ion being bound as metal-buffer complex at the two pH values. In Eu^{3+}-Aspartic Acid titration at pH 6.5 and 35°C, [MB] is 22-11% of $[M]_T$, (cf 60-37% at pH 5.0) and 35°C [ML] is 23-46% of $[M]_T$ (cf 19-51% at pH 5.0, 35°C) and is 26-104 times the error in [MB]. In Eu^{3+}-Glutamine titration at pH 6.5, [MB] is 15-30% of $[M]_T$, [ML] is 12-40% of $[M]_T$ and is 11-46 times the error in [MB]. As one would expect when K_{MB} is altered by σ, K_{ML} of Eu^{3+}-Glutamine equilibrium is more sensitive than that of Eu^{3+}-Glutamic Acid equilibrium. The changes are 1.5% at 25°C and 35°C and 4% at 15°C in the latter case and are 10% at 15°C, 7% at 25°C and 6.5% at 35°C in the former case. In accordance with one's expectation, the sensitivity of K_{ML} to error in K_{MB} is less is Eu^{3+}-Glutamine/Aspargine system at pH 6.5 than in the same systems at pH 5.0. These data indicate that 100 mM TES concentration was too high. A lower value of concentration that allows a change of pH from 6.45 to 6.55 during the titration, is clearly a more appropriate choice.

The values of K_{ML} obtained when K_{MB} is altered by the $\pm\sigma$, 2σ and 3σ are given in Tables I-IV for all the systems studied.

Saturation factor :

The reliability of the stability constant data depends on the range of saturation covered in the titration experiment. In the presence of buffer and murexide, the saturation factor (S) is calculated from the formula

$$S = \frac{[ML]}{[M]_T-[MB]-[MMu]} = \frac{[ML]}{[ML]+[M]_f}$$

In the following, we indicate the range of the value of S studied in the experiments performed by us. In the Eu^{3+}-Aspartic acid titrations at pH 5 and 15°C, S varies between 0.44 - 0.76. The range is 0.44 - 0.77 at pH 6.5 and 35°C. The range is similar in the Eu^{3+}-Glutamic Acid system and in Eu^{3+}-Aspartic acid system at other temperature values. In the Eu^{3+}-Aspargine titration at pH 5 and 15°C, S varies between 0.11 - 0.35. The range is 0.26 - 0.61 at pH 6.5 and 35°C. The range is similar in the Eu^{3+}-Aspargine system at other temperature values and in the Eu^{3+}-Glutamine system.

The range covered is insufficient for detecting multiple equilibria in the Eu^{3+}-Aspargine and Eu^{3+}-Glutamine system at pH 5.0. In addition a significant portion of the range is below S = 0.2, the minimum limit allowed by Deranleau [14]. The error in these measurements is also large. The large standard deviation does not owe its origin to the small absolute magnitude of the stability constants. The

values are small in these systems even at pH of 6.5, but the standard deviations are also small. The standard deviations in Eu^{3+}-aspartic acid and in Eu^{3+}-Glutamic Acid systems are small. These ligands bind more strongly, compete more effectively with murexide and buffer and cover a wide range of saturation. Lowering the buffer concentration could help in increasing the range of saturation in aspargine and glutamine titration experiments.

In retrospect, a very useful approach in the choice of concentration is to carry out a calculation using a computer programme on the basis of the β values obtained to decide on the concentration values that will give wider ranges of concentration, use these to calculate a new value of β (which may or may not equal to the β obtained earlier) and repeat the process again to cover the whole range of saturation. The gap in the saturation region between S = 0.2 to 0.4 in the Eu^{3+}-Aspartic Acid and in the Eu^{3+}-Glutamic acid systems can be covered by titrating ligand (in the cuvette) with metal (added from the micropipette).

Error in $[M]_T$ and $[L]_T$:

The error in $[L]_T$ arises from the ligand and from the error in reading the mark on the 25 ml volumetric flask. The amount weighed is large ($\sim$ 100 mg), leading to a negligible percentage error ($\sim 10^{-4}$ %). The error in reading

the volume in a 25 ml flask, estimated as described in Chapter II, is $\sim$ 0.2%. Thus error in $[L]_T$ is 0.2%. The error in $[M]_T$ is estimated to be (see Chapter II) 0.5%.

Error in $[M]_f$ and $[L]_f$:

The smallest magnitude of $\triangle$ A (proportional to [MMu]) read from the Digital panel meter of the Cary 17D spectrometer is 0.100. The error in reading this O.D. is $\pm$0.002 ($<$ 2%). The error in $\triangle\varepsilon$ is $\sim$ 0.5%. Thus the largest error in [MMu] is $\sim$2%. The error in $[Mu]_f$ obtained by subtracting [MMu] from $[Mu]_T$ is $\sim$ 2%, because the error in $[Mu]_T$, as estimated in Chapter II, is 0.25%. At large values of [MMu], the error in $[Mu]_f$ increases, even though [MMu] is increasingly more accurately measurable. This is so because, as stated above, the small magnitude of $[Mu]_f$ has a much larger percentage error due to the small percentage error in accurately known $[Mu]_T$ and [MMu]. The maximum degree of saturation of $[Mu]_T$ achieved is 0.7. As discussed in Chapter II, [MMu] has a standard deviation of 0.6%. The σ of $[Mu]_T$ is $\sim$ 0.25%. If [MMu] = 0.7 $[Mu]_T$, [MMu] = (7/3) $[Mu]_f$, a relative error of 0.6% corresponds to an absolute error of 1.2% of $[Mu]_f$. The relative error of $\sim$ 0.25% of $[Mu]_T$ corresponds to an absolute error of 0.8% of $[Mu]_f$. The formula used in Chapter II, leads to a relative error of $\sim$ 1.5%. Thus at the two extreme points of a titration, the error in $[Mu]_f$ is of the order of 2%. The

error is less in the intermediate points. The error in $[M]_f$ calculated from the formula $[M]_f = [MMu]/K_{MMu} \cdot [Mu]_f$ is therefore $\sim$ 2.5% or less.

$[L]_f$ is not directly measured and is calculated in the data processing programme as equal to $[L]_T - \sum_i [ML_i]$. $[L]_T \gg [L]_b$ under the conditions of the experiment, but $[ML_i]$ is inferred from $[M]_T - [M]_f$ a quantity accurately known in the intermediate saturation region (0.2 - 0.8). Thus $[L]_f$ (= $[L]_T - [ML]$) derives its error primarily from $[M]_f$, the error in $[M]_T$ being $\sim$ 0.5% and that in $[L]_T$ being $\sim$ 0.2% . Thus inaccuracy of $[L]_f$ is of the order of $\sim$ 3% at the extreme points and less in the middle. K_{ML} [$[ML]/[M]_f[L]_f$ has a standard deviation of this order in all the experiments reported excepting the Eu^{3+}-Aspargine and Eu^{3+}-Glutamine titration at pH 5.0. The errors in these cases derive their origin from large percentage inaccuracy in the value of [ML] determined at low saturation [ML] = $[M]_T - [M]_f$. If $[M]_f = 0.9\ [M]_T$, then a 3% error in $[M]_f$ is carried over as a 27% error in [ML]. Comparatively smaller standard deviations observed in Eu^{3+}-Aspargine titration at pH 5.0 and 15°C and 25°C thus may not be a measure of the real error. The large percentage error in [ML] leads to only a small percentage error in $[L]_f$ because of the latter's large magnitude. For a typical value of $[M]_T$ of 5.2×10^{-4} M and of $[L]_T$ of 2.83×10^{-2} M, if $[M]_f$ is $2.6\ (\pm 1.3) \times 10^{-4}$ M ($\sim$ 50% error), error in $[L]_f$

$(= [M]_T - [M]_f)$ is $\sim 3\%$. In agreement with the above, we find that removal of first one or two and the last titration point in each set reduces the standard deviation. The error in [ML] due to the error in K_{MB} is a separate source of error and is evaluated separately as described earlier.

Total and relative values of $[M]_T$ and $[L]_T$:

The absolute and relative values of concentration of complexes of different soichiometry depends on the total concentration values of the metal and the ligand. In Table V we summarize the ranges of concentration of $[M]_T$ and $[L]_T$ used in the different experiments. The ligand has always been much in excess. $[L]_T$ is restricted by limited solubility. $[M]_T$ is restricted by consideration discussed earlier in detail.

Nature of the values determined :

The equilibrium constant (β_i) determined in the experiments reported in this chapter can be operationally defined as the coefficient of the term $[M]_f [L]_f^i$ in the mass-balance equation of $[M]_T$. The same coefficient appears as the coefficient of the term $i[M]_f[L]_f^i$ in the mass-balance equation of $[L]_T$. Thus if two different chemical species of the same stoichiometry (1:1) form with equilibrium constants K_1 and K_2, then $\beta_1 = K_1 + K_2$. The discussion given at the beginning of the chapter points out the possibility of a variety of

structural isomers of a 1:1 alanine-Ln^{3+} complex. The formation equilibrium for each isomer is described by one equilibrium constant. At pH 6.5, hydrolyzed metal-amino acid complex is a subclass of 1:1 complexes formed. The measured β_1 is sum of all the separate K's.

The controversy about large vs small values of β of lanthanide-amino acid equilibrium :

The early pH titration data [1-4] clearly stand in sharp contrast to the solvent extraction data [6,7], NMR data [9-11,13] and polarographic data [5] (for amino acids other than tryptophan), in that the values of β are large in the former, whereas they are small in the latter. The values determined by us are also small (Table I-IV). Thus we tend to agree with other workers [6,13,20] that the early pH titration work was incorrect. But we do not agree with the point made in literature [13] that this is due to neglect of lanthanide hydrolysis above a pH of 6. As discussed earlier Cefola et al. [1] ignored all data at pH $>$ 6 in their data analysis. Jones and Williams [2] considered data above pH $>$ 6 and their analysis showed hydrolysed species is absent. The source of error in Cefola et al.'s work is therefore not known and that in the work of Jones and Williams [2,3] may owe its origin to the failure of the computer analysis to recognise hydrolysed species. It is a pity that the paper of Sherry et al. [10] gives no details about how

their method could identify hydrolyzed species, even though from the description given, their method looks identical to that used by Jones and Williams [2,3].

The values of β of lanthanide-acetate equilibrium also show sim lar discrepancy. Kolat and Powell [30] found that $\beta_1 = 202$ and $\beta_2 = 8020$. They considered data below pH 5 only. The experimental data is obtained on a Sodium acetate-acetic acid buffer at pH 4.01 which changes its pH on addition of metal, when these values are used in the analysis of our data, the metal ion bound to ligand turns out to be negative, if one calculates $[ML] = [M]_T - [MMu] - [M]_f - [MB]$, where [MMu] is directly determined (from observed $\triangle A$), $[M]_f$ from the relation $[M]_f$ [= $[MMu]/K_{MMu}\ [Mu]_f$ and [MB] is calculated from the formula $K[M]_f[B]_f$ taking $[B]_f \simeq [B]_T$. The programme does not assume $[B]_f \simeq [B]_T$, but nonetheless, it fails to converge. The values obtained by Kolat and Powell [30] in the Nd^{3+}-acetate equilibrium are $\beta_1 = 166$ and $\beta_2 = 5780$. Sherry et al. [10] find by NMR spectroscopy K = 83, whereas potentiometric titration gives K = 93. The saturation range studied in the NMR experiment is 0.65 - 0.85. The range may not be wide enough for detection of multiple equilibria in the graphical analysis used. Thus the value of β determined may represent a composite equilibrium constant. The value of saturation studied is neither too small nor too large. Thus it should give an accurate value of the concentration of bound ligand in the range of concentration studied.

The same is true in the experiments on Eu^{3+}-acetate system reported in Chapter II ($S \simeq 0.5$ at 15°C $S \simeq 0.7$ at 35°C). The discrepancy between the results of Sherry et al. [10] and our results (Chapter II) on one hand and that of Kolat and Powell [30] on the other, is thus not explained.

pH and temperature dependence of β :

The following trends are observed in the data given in Table I-IV :

(1) Eu^{3+}-Aspargine : (i) At pH 5.0, the values of β show an increase with an increase of temperature from 15°C to 25°C. There is no difference between the value at 25°C and that at 35°C within experimental error. The difference is barely significant if β is calculated using $K_{MB} \pm 3\sigma$. (ii) At pH 6.5, the values of β show a decrease with increase of temperature from 15°C to 25°C. There is no difference between the value at 25°C and that at 35°C within experimental error. (iii) The values of β at pH 6.5 are greater than their counterparts at pH 5.0 much beyond the errors of measurement.

(2) Eu^{3+}-Glutamine : (i) At pH 5.0, the values of β show an increase with an increase of temperature from 15°C to 25°C. There is a very small decrease beyond experimental error in going from 25°C to 35°C if one uses K_{MB} (mean value) to calculate β_{ML}. This difference is insignificant if one uses $K_{MB} \pm 2\sigma$ or $K_{MB} \pm 3\sigma$ to calculate β_{ML}. This trend is

similar to those of Eu^{3+}-Aspargine system. (ii) At pH 6.5, the value of β_{ML} rises only slightly beyond experimental error if one uses K_{MB} (mean value) to calculate β_{ML}. The rise is not statistically significant when one uses $K_{MB} \pm \sigma$ to calculate β_{ML}. The value increases beyond experimental error in going to 35°C. (iii) The value of β at pH 6.5, is only slightly greater than its counterpart at pH 5.0. The difference is not statistically significant when one uses $K_{MB} \pm 2\sigma$ or $K_{MB} \pm 3\sigma$ to calculate β_{ML}. The value of β at pH 6.5 and 25°C is equal to its counterpart at pH 5.0 within the error of measurement. The value of β at pH 6.5 and 35°C is greater than its counterpart at pH 5.0 beyond experimental error.

(3) Eu^{3+}-Aspartic Acid System : (i) The values of β at pH 5.0 show an increase with increase of temperature in going from 15°C to 25°C. The increase of temperature from 25°C to 35°C leads to no increase of β within the error of measurement. This trend is similar to those of Eu^{3+}-Glutamine and Eu^{3+}-Aspargine systems at pH 5.0. (ii) The values of β show a decrease with increase of temperature. The decrease is more significant in going from 15°C to 25°C. This trend is similar to that observed in Eu^{3+}-Aspargine system, but not to that observed in Eu^{3+}-Glutamine system. (iii) The values of β at pH 6.5 and 15°C and 25°C are greater than their counterparts at pH 5.0. The valuesof β at pH 6.5 and 35°C is equal to that at pH 5.0 and 35°C. This trend is similar to that in

the Eu^{3+}-Aspargine system (15°C and 25°C) even though it is not as clear cut in the Eu^{3+}-Glutamine system.

(4) Eu^{3+}-Glutamine System : (i) At pH 5.0, the values of β show an increase with an increase of temperature. The trend is similar to that in the Eu^{3+}-Aspartic Acid system, excepting that in the latter system, the increase is not observable in going from 25°C to 35°C (ii) At pH 6.5, the value of β decreases with increase of temperature. The decrease is smaller in going from 25°C to 35°C (iii) The values of β at pH 6.5 and at 15°C and 25°C are larger than their counterparts at pH 5.0. At 35°C, the value of β at pH 5.0 is greater. The increasing and decreasing trends of β values with increase of temperature at the two different pH values cross and $\beta_{pH\ 5.0}$ is $>$ $\beta_{pH\ 6.5}$ at 35°C. In the Eu^{3+}-Aspartic Acid system, at pH 5.0, there is no increase on change of temperature from 25°C to 35°C. The β values are equal at the two pH values at 35°C.

Thus at pH 5.0 in Eu^{3+}-Aspargine, Eu^{3+}-Glutamine and Eu^{3+}-Aspartic Acid systems, β_{ML} value increases in going from 15°C to 25°C, but it either decreases or remains constant when temperature is increased from 25°C to 35°C. This is indicative of the presence of more than one equilibrium of the same (1:1) stoichiometry, some of which are endothermic and some are exothermic. The measured β is the sum of the equilibrium constants for the several different independent equilibria simultaneously present in solution. Tanner and

Choppin [6] find that Eu^{3+}-Glycine equilibrium is endothermic. Glycine has only one carboxylate group. Aspartic Acid has two (pK_{diss} = 1.94 at 25°C (μ = 0.1) for the α-carboxylic acid and pK_{diss} = 3.71 at 25°C (μ = 0.1) for the side chain carboxylic acid [31]). Thus Aspartic Acid can form a chelate. Co-ordination of only one carboxylate in Glycine cannot release enough energy to compensate for the dehydration energy, one pays for as a result of complex formation. Co-ordination of more than one carboxylate may lead to release of more energy resulting in an exothermic reaction. We suggest that in Eu^{3+}-Aspartic Acid system, one obtains a mixture of a chelate with both the carboxylates as co-ordinating groups (exothermic) and one or more complexes involving the co-ordination of only one carboxylate group (endothermic).

The stability constant β determined in this experiment is the ratio $([Eu(Asp)]^{3+} + [Eu\ Asp^{-}]^{2+})/[Eu]^{3+}([Asp]+[Asp]^{-})$, where [Asp] denotes the concentration of the zwitterionic form with the side-chain carboxyl group unionised and $[Asp]^{-}$ denotes the concentration of the form with side-chain carboxyl group in the ionised form. The concentration terms of [Asp] and $[Asp]^{-}$ in the denominator can be separately calculated from the known value of pK of proton dissociation equilibrium. The two terms in the numerator cannot be separated. In the complex Eu^{3+} (Asp), with the side-chain carboxylic acid group ptotonated, the binding is through the ionised α-carboxylate group. By analogy with the known values of stability constants

of lanthanide-glycinate or alaninate complexes [6,7,10,11], one expects the formation constant of this complex to be below 10. The $(Eu^{3+}(Asp^{-}))^{+2}$ complex may be of two kinds : (i) α-carboxylate or side-chain carboxylate alone binds (ii) a chelate forms involving binding by both the carboxylate groups. In a ligand with two ionised $CO_2^{(-)}$ groups, one expects a chelate to be more preferred than the complexes stated in (i). The pK_{diss} of Acetic acid is 4.76, whereas pK_{diss} of side-chain carboxylic acid 3.71. By analogy, one would expect association constant of Eu^{3+}-acetate equilibrium to be larger than that of Eu^{3+} complexes with only the side-chain carboxylate of aspartic acid. The former being $\sim$ 100 between 15°C and 35°C, the latter will be $\sim$ 100. One concludes that the largest contribution to the Eu^{3+}-aspartic acid stability constant comes from the chelate. The simultaneous presence of the complex in which only α-carboxylate co-ordinates and side-chain carboxylic acid is unionized is consistent with the observation made in the discussion given earlier that binding induced ionisation is not observed in α-carboxylic or α-amino group. The trend of temperature dependence is similar in Eu^{3+}-Aspargine and in Eu^{3+}-Glutamine systems, but the magnitude is much smaller.

The values of β are of the same order as that of Eu^{3+}-Glycine equilibrium, thus indicating co-ordination through α-carboxylate group. One need not postulate the existence of a chelate involving the α-carboxylate and the

side chain carboxamide group as contributing exothermicity to the mixture. The side-chain carboxamide may have a variety of orientations with respect to Eu^{3+} ion, which lead to energy changes of different magnitudes. The favourable orientations may release ion-dipole interaction energy to lead to overall exothermicity. If the carboxamide group is pointing away from Eu^{3+} ion the system is more like Eu^{3+}-glycine complex and is expected to be endothermic. The extreme case of a favourable orientation is co-ordination to the metal ion. The endothermic complex will be stabilised by entropy, as is the case with Eu^{3+}-Glycine complex. Eu^{3+}-Glutamic acid system shows endothermicity at pH 5.0. The pK_{diss} of side-chain carboxylic acid is larger (4.07 at 25°C $\mu = 0.1$) [31]. This means that the proportion of the complex in which only α - carboxylate co-ordinates to Eu^{3+} is more than it is in the Eu^{3+}-Aspartic Acid complex. The endothermic component being more predominant, one expects that the temperature dependence will show overall endothermicity, in contrast to the Eu^{3+}-Aspartic acid case, where the contribution of the exothermic chelates nullifies the contribution of the endothermic equilibrium and temperature independence is observed between 25°C and 35°C.

At pH 6.5, both the carboxylic acid groups are completely ionised. Thus very little of the endothermic complex forms at this pH. Thus the overall exothermicity is expected. The same is true of Glutamic acid.

At pH 6.5, according to Prados et al. [20] Aspartic acid-Eu^{3+} complex is substantially hydrolysed, Aspargine-Eu^{3+} complex is hydrolysed to a slight extent and Glutamic acid-Eu^{3+} complex is hydrolysed and polynuclear complexes form. Glutamine-Eu^{3+} complex has not been studied by Prados et al. [20].

The higher values of β of Eu^{3+}-Aspargine complex at pH 6.5 compared to those at pH 5.0 is consistent with the presence of hydrolysed complexes at pH 6.5. Sonesson [32] in his extensive pH titration studies on lanthanide-acetate equilibria (He also finds high values of β) find that hydrolysis is significant at higher pH values for heavier lanthanide ions and leads to higher values of β. At pH 6.5, hydrolysis begins to be significant [20]. Thus at this pH, unhydrolysed and hydrolysed Eu^{3+}-Aspargine complexes are both present. The quantity β is the ratio $[Eu\text{-}Aspgn]/[Eu]^{3+}[Aspgn]$ at pH 5.0. At pH 6.5 it is the ratio $([Eu\text{-}Aspgn]+[Eu(Aspgn)OH^{-}])/[Eu^{3+}][Aspgn]$. Eu^{3+}(aquo) ion does not hydrolyse at pH 6.5. Thus β (at pH 6.5) = β(at pH 5.0) + $[Eu(Aspgn)(OH^{-})]/[Eu^{3+}][Aspgn]$ i.e. β (at pH 6.5) = β(at pH 5.0) + β_h (h for hydrolytic equilibrium : the constant however does not include proton concentration and therefore is pH dependent). Thus β_h has the value of 23.5 at 15°C, 13.6 at 25°C and 13.84 at 35°C (using the mean value of K_{MB} in the calculation) at pH 6.5.

Eu^{3+}-Glutamine system at pH 6.5 contrasts the Eu^{3+}-Aspargine system in two respects (i) The difference of β value at pH 5.0 from that at pH 6.5 is zero or very small (ii) A weak endothermicity is observed rather than a weak exothermicity. Prados et al. [20] have not reported any data on lanthanide-Glutamine system, but in view of the similarity of results obtained by them in a large number of lanthanide-amino acid systems, one expects Glutamine complex to be similar to the Aspargine-complex in its hydrolytic behaviour. The difference (i) and (ii) mentioned above need not be interpreted as indicative of absence of hydrolysis. The value of ΔG° changes by as little as 650 calories per mole if K changes from 10 to 30 at around $300^{\circ}K$. Small differences in hydration, which affects both energy and entropy can account for a change of this magnitude. Thus if at pH 6.5, one expected by analogy with the Eu^{3+}-Aspargine system a value of K of $\sim$ 30, one need not be surprised to have obtained K $\sim$ 10. The same effect can explain a change from weak exothermicity in the Eu^{3+}-Aspargine system at pH 6.5 to weak endothermicity in the Eu^{3+}-Glutamine system at the same pH. Since energy released in Eu^{3+}-OH^{-} interaction is about the same in the two cases, weak endothermicity (change of β of 7 to 11 in response to change of temperature from $15^{\circ}C$ to $35^{\circ}C$ means ΔH° is +5 kcal/mole) may mean higher degree of dehydration of the metal ion. This effect will also be lower compared to that in the Eu^{3+}-Aspargine system in pH 6.5 (the degree of

exothermicity is $\sim$ 2 kcal/mole corresponding to a change of β from 33 to 28 in going from 15°C to 35°C). It is to be pointed out that the effects being interpreted are small in magnitude. In view of the small change in β with change in pH, a pH titration experiment on lanthanide-Glutamine system is perhaps worth performing in spite of any expectation based on analogy. It is possible that the pH at which hydrolysis sets in is slightly higher than in the Eu^{3+}-Aspargine case, resulting in smaller values of β_h at a pH of 6.5.

The relationship between β at pH 5.0 and β at pH 6.5 is not as simple in Eu^{3+}-Aspartic Acid and Eu^{3+}-Glutamic acid systems. In Eu^{3+}-Aspartic Acid equilibrium, measured β at pH 6.5 is the ratio $([Eu^{3+} Asp^-] + [Eu^{3+} Asp^- OH^-$ or/and $(OH)_2])/[Eu^{3+}][Asp^-]$, since Aspartic Acid exists only in the anionic form, whereas at pH 5.0 β is the ratio $([Eu^{3+} Asp] + [Eu^{3+} Asp^-])/[Eu^{3+}]([Asp^-]+[Asp])$. The relationship is more complex in Eu^{3+}-Glutamic acid system because of the presence of polynuclear complexes. Thus a simple analysis of their relative values is not possible.

We have discussed evidence existing in literature [13] for 1:2 lanthanide-alanine complexes. Titrations performed by us have been carried out with large excess of ligand concentration (compared to metal concentration) but the absolute magnitude of free ligand concentration is $10^{-3} - 10^{-2}$ M. If β_1 and β_2 values are comparable, as is the case with alanine, it is difficult to form a substantial concentration of $[ML_2]$

complex at this level of metal concentration. Elgavish and Reuben [13] could have absolute concentration of ligand ranging upto 1.5 M. It was possible to find a nonzero value β_2 comparable to that of β_1 only at such high concentration. This is a case where low solubility of ligand stands in the way of determining β values for complexes of higher stoichiometry. At the range of concentration accessible, β_2 would be detectable only if it is several order of magnitudes larger.

In analysing titration data, we have not considered the possibility of a mixed complex with ligand and buffer both simultaneously binding to the metal ion. Measurement of β at a different buffer concentration can decisively demonstrate the presence or the absence of such mixed complexes. The ratio of the concentration of mixed complex to that of metal-ligand complex is $\beta_{\text{mixed complex}} \cdot [\text{Buffer free}]/\beta_{\text{Metal-ligand complex}}$. Free concentration of buffer is in the range of $\sim 10^{-2}$ M. If the ratio of the β values is of the order of unity, the mixed complex will not be detectable in the presence of the metal-ligand complex.

The computer programme used for data analysis is an improved version of MINIQUAD written by Sabatini et al. [33]. The later modifications were obtained from Dr. P.Gans of Shelfield University. The programme in the form used in this work is given in Appendix **A**, with sufficient details to be useful to someone using it for the first time.

β (Eu^{3+}-Aspargine values)
Calculated

	Using mean value of K_{MB}	Using $K_{MB} \pm \sigma$	Using $K_{MB} \pm 2\sigma$	Using $K_{MB} \pm 3\sigma$
pH 5.0 15°C	9.5(±2.89%)	10.00(±2.72%)	10.44(±2.66%)	10.39(±2.55%)
		9.11(±2.99%)	8.67(±3.17%)	8.23(±3.40%)
25°C	14.8(±4.1%)	15.74(±4.04%)	16.7 (±3.96%)	12.0 (±3.9 %)
		13.86(±4.25%)	12.9(±4.4%)	12.0 (±4.53%)
35°C	14.6(±5.3%)	14.8(±5.2%)	15.19(±5.07%)	15.53(±4.47%)
		14.16(±5.42%)	13.81(±5.55%)	13.47(±5.7%)
pH 6.5 15°C	33.0(±1.72%)	32.0(±1.76%)	31.01(±1.8%)	30.04(±1.82%)
		3 .0(±1.7%)	35.02(±1.6%)	36.02(±1.62%)
25°C	28.4(±4.63%)	29.0(±4.5%)	29.6(±4.4%)	30.2(±4.3%)
		27.8(±4.75%)	27.2(±4.9%)	26.6(±5%)
35°C	28.0(±1.08%)	28.76(±1%)	29.24(±0.96%)	30.3(±0.9%)
		27.25(±1.2%)	26.50(±1.3%)	25.74(±1.4%)

Table I : The values of stability constant of Eu^{3+}-aspargine complex at different pH and temperature values. The standard deviations are quoted in bracket. The values of β_{ML} obtained by using values of metal-buffer stability constant different from the mean value of 1, 2 and 3 times the standard deviation show the effect of the error of K_{MB} measurement on values of β_{ML}.

	$\beta(Eu^{3+}$-Glutamine) Calculated			
	Using mean value of K_{MB}	Using $K_{MB} \pm \sigma$	Using $K_{MB} \pm 2\sigma$	Using $K_{MB} \pm 3\sigma$
pH 5.0 15°C	4.96(±24%)	5.36(±22%)	5.75(±21%)	6.14(±20%)
		4.57(±26%)	4.18(±28%)	3.78(±31%)
25°C	7.8(±9.6%)	8.6 (±9%)	9 35(±8.4%)	10.12(±7.9%)
		7.03(±10.5%)	6.26(±11.5%)	5.49(±13%)
35°C	6.1(±6.9%)	6.36(±6.75%)	6.61(±6.63%)	6.87(±6.52%)
		5.8 (±7.1%)	5.59(±7.2%)	5.33(±7.35%)
pH 6.5 15°C	7.4(±3.2%)	8.34(±3.05%)	9.23(±2.93%)	10.12(±2.9%)
		6.57(±3.64%)	5.7 (±4.09%)	4.8 (±4.9%)
25°C	8.0(±2.5%)	8.60(±2.17%)	8.98(±1.94%)	9.7 (±1.6%)
		7.52(±3%)	6.98(±3.5%)	6.4 (±4.12%)
35°C	11.84(±3.2%	12.61(±2.89%)	13.05(±2.84%)	14.1 (±2.7%)
		11.09(±3.2%)	10.35(±3.4%)	9.6 (±3.6%)

Table II : The values of stability constant of Eu^{3+}-Glutamine complex at different pH and temperature values. The standard deviations are quoted in bracket. The values of β_{ML} obtained by using values of metal-buffer stability constant different from the mean value of 1,2 and 3 times the standard deviation show the effect of the error of K_{MB} measurement on values of β_{ML}.

β (Eu^{3+}-Aspartic Acid)

Calculated

		Using mean value of K_{MB}	Using $K_{MB} \pm \sigma$	Using $K_{MB} \pm 2\sigma$	Using $K_{MB} \pm 3\sigma$
pH 5.0	15°C	216.9(±2.8%)	218.6(±2.85%)	220.3(±2.86%)	221.9(±2.86%)
			215.2(±2.8%)	213.5(±2.83%)	211.8(±2.84%)
	25°C	245.3(±2.9%)	249.0(±2.91%)	252.7(±2.9%)	256.5(±2.93%)
			241.5(±2.9%)	237.8(±2.89%)	234.1(±2.88%)
	35°C	244.9(±2.4%)	246.1(±3.6%)	247.3(±2.43%)	248.5(±2.43%)
			243.6(±2.42%)	242.4(±2.42%)	241.2(±2.42%)
pH 6.5	15°C	380(±3.4%)	384.0(±3.9%)	388.4(±3.9%)	392.8(±3.8%)
			375.2(±4.07%)	370.8(±4.14%)	366.4(±4.21%)
	25°C	293(±1.08%)	295.6(±1.07%)	297.7(±1.06%)	299.9(±1.05%)
			291.3(±1.09%)	289.2(±1.2%)	287.1(±1.11%)
	35°C	239(±2.2%)	236.4(±2.24%)	233.3(±2.3%)	230.0(±2.35%)
			243.7(±2.17%)	216.2(±2.14%)	249.4(±2.11%)

Table III : The values of stability constants of Eu^{3+}-Aspartic Acid at different pH and temperature values. The standard deviations are quoted in bracket. The values of β_{ML} obtained by using values of metal-buffer stability constant different from the mean value of 1,2 and 3 times the standard deviation show the effect of the error of K_{MB} measurement on values of β_{ML}.

β (Eu^{3+}-Glutamic Acid)
Calculated

		Using mean value of K_{MB}	Using $K_{MB} \pm \sigma$	Using $K_{MB} \pm 2\sigma$	Using $K_{MB} \pm 3\sigma$
pH 5.0	15°C	82.9(±3.0%)	84.5(±2.8%) 81.2(±3.0%)	87.1(±2.7%) 79.5(±2.8%)	89.5(±2.8%) 78.1(±3.0%)
	25°C	161.9(±2.9%)	166.1(±2.29%) 157.8(±2.94%)	170.2(±2.82%) 153.7(±2.99%)	174.4(±2.8%) 149.6(±3.05%)
	35°C	268.2(±2.17%)	269.6(±2.17%) 266.8(±2.12%)	271.0(±2.17%) 265.4(±2.17%)	272.4(±2.18%) 264.0(±2.19%)
pH 6.5	15°C	227 (±1.9%)	211.0(±2.43%) 218.5(±2.28%)	207.2(±2.51%) 222.1(±2.21%)	203.7(±2.59%) 226.0(±2.14%)
	25°C	188 (±1.72%)	186.5(±1.77%) 191.7(±1.68%)	184.1(±1.82%) 193.4(±1.63%)	181.8(±1.87%) 195.7(±1.6%)
	35°C	178 (±2.25%)	175.2(±2.36%) 181.7(±2.14%)	171.9(±2.5%) 185.1(±2%)	168.7(±2.6%) 188.2(±1.95%)

Table IV : The values of stability constants of Eu^{3+}-Glutamic acid at different pH and temperature values. The standard deviations are quoted in bracket. The values of β_{ML} obtained by using values of metal-buffer stability constant different from the mean value of 1, 2 and 3 times the standard deviation show the effect of the error of K_{MB} measurement on values of β_{ML}.

System	pH	Temp.	Total Concentration of $EuCl_3$ $[M]_T$(Moles per lit)	Total Concentration of Ligand $[L]_T$(Moles per lit)
Eu^{3+}-Aspargine	6.5	35°C	1.31×10^{-4} to 8.48×10^{-5}	1.34×10^{-2} to 5.5×10^{-2}
			1.51×10^{-4} to 1.05×10^{-4}	1.27×10^{-2} to 5.31×10^{-2}
			1.84×10^{-4} to 1.27×10^{-4}	1.32×10^{-2} to 5.45×10^{-2}
			2.07×10^{-4} to 1.77×10^{-4}	1.88×10^{-2} to 3.74×10^{-2}
	5.0	15°C	5.2×10^{-4} to 3.71×10^{-4}	1.31×10^{-2} to 5.14×10^{-2}
			8.00×10^{-4} to 5.72×10^{-4}	1.30×10^{-2} to 5.11×10^{-2}
			9.72×10^{-4} to 7.27×10^{-4}	2.36×10^{-2} to 5.06×10^{-2}
			1.07×10^{-3} to 8.34×10^{-4}	1.85×10^{-2} to 5.08×10^{-2}
Eu^{3+}-Aspartic Acid	6.5	35°C	1.78×10^{-4} to 1.24×10^{-4}	3.33×10^{-3} to 1.39×10^{-2}
			1.99×10^{-4} to 1.53×10^{-4}	3.31×10^{-3} to 1.14×10^{-2}
			2.25×10^{-4} to 1.55×10^{-4}	3.44×10^{-3} to 1.43×10^{-2}
			1.59×10^{-4} to 1.09×10^{-4}	3.50×10^{-3} to 1.44×10^{-2}
	5.0	15°C	4.29×10^{-4} to 3.10×10^{-4}	3.62×10^{-3} to 1.43×10^{-2}
			7.54×10^{-4} to 5.22×10^{-4}	3.74×10^{-3} to 1.55×10^{-2}
			1.23×10^{-3} to 8.80×10^{-4}	3.69×10^{-3} to 1.45×10^{-2}
			9.48×10^{-4} to 6.58×10^{-4}	3.72×10^{-3} to 1.55×10^{-2}
			1.55×10^{-4} to 1.11×10^{-3}	3.66×10^{-3} to 1.45×10^{-2}

Table V : Total concentration of $EuCl_3$ (M_T) and Amino Acid (L_T) used in titration experiments. The values of concentration remain approximately the same at other values of temperature. The range used in Eu^{3+}-Aspartic Acid titration is about the same as that used in Eu^{3+}-Glutamic Acid titration and that used in Eu^{3+}-Asparginе titration is about the samc as the used in Eu^{3+}-Glutamine titration.

References

1. M. Cefola, A. Tompa, A. Celiano and P. Gentle, Inorg. Chem., 1, 290, 1962.

2. A.D. Jones and D.R. Williams, J. Chem. Soc. A 3138, 1970.

3. A.D. Jones and D.R. Williams, J. Chem. Soc. A 3159, 1971.

4. B.S. Sekon and S.L. Chopra, Thermochim. Acta. 7, 151,1973.

5. S. Lal, Aust. J. Chem., 25, 1571, 1972.

6. S.P. Tanner and G.R. Choppin, Inorg. Chem. 7, 2046, 1968.

7. S. Aziz and S.J. Lyle, J. Inorg. Nucl. Chem., 33, 3407, 1971.

8. F. Inagaki, S. Takahashi, M. Tasumi and T. Miyazawa, Bull. Chem. Soc. Japan, 48, 853, 1975.

9. A.D. Sherry, E.R. Birnbaum and D.W. Darnall, J. Biol. Chem. 247, 3489, 1972.

10. A.D. Sherry, C. Yoshida, E.R. Birnbaum and D.W. Darnall, J. Am. Chem. Soc., 95, 3011, 1973.

11. A.D. Sherry and E. Pascual, J. Am. Chem. Soc., 99, 5871, 1977.

12. R.E. Lenkinski, G.A. Elgavisch and J. Reuben, J. Mag. Res., 32, 367, 1978.

13. G.A. Elgavisch and J. Reuben, J. Mag. Res., 42, 242, 1981.

14. D.A. Deranleau, J. Amer. Chem. Soc., 91, 4044, 4050, 1969.

15. G. Weber in Molecular Biophysics Ed. B. Pullman and M. Weissbluth, Academic Press, 1965, p. 377.

16. R.F. Lumb and A.E. Martell, J. Phys. Chem., 57, 690, 1953.

17. S. Chaback and A.E. Martell, J. Amer. Chem. Soc., 74, 5052, 1952.

18. L.I. Katzin, Inorganic Chemistry, 8, 1649, 1969.

19. L.I. Katzin, Inorganic Chemistry, 7, 1183, 1968.

20. R. Prados, L.G. Stadtherr, H. Donato and R.B. Martin, J. Inorg. Nucl. Chem., 36, 689, 1974.

21. H. Donato and R.B. Martin, J. Am. Chem. Soc., 94, 4129, 1972.

22. B.A. Levine and R.J.P. Williams, Proc. Roy. Soc. London, A, 345, 5, 1975.

23. G.A. Elgavisch and J. Reuben, J. Amer. Chem. Soc., 100, 3617, 1978.

24. B.T. Pennington and J.R. Cavanaugh, J. Mag. Res., 31, 11, 1978.

25. R.J. Kretsinger and B. Nelson, Co-ordination Chemistry Reviews.

26. P. Gans, Co-ordination Chemistry Reviews, 19, 99, 1976.

27. F. Gaizer, Co-ordination Chemistry Reviews, 27, 195, 1979.

28. Eur. Jour. Biochemistry, 107(2), 455, 1980.

29. R.S. Kolat and J.E. Powell, Inorganic Chemistry, 1, 293, 1962.

30. A.E. Martell and L.G. Sillen, Stability Constants of Metal-ion Complexes, Supplement No. 1, Special Publication No. 25, The Chemical Society, London, 1971, page 339, 343, 383, 387.

31. A. Sonesson, Acta. Chem. Scandinavia, 12, 1937, 1958.

32. A. Sabatini, A. Vacca and P. Gans, Talanta, 21, 53, 1974.

CHAPTER 4

Hypersensitive Transitions

In this chapter, we first describe the experimental methods used to measure the enhancement of oscillator strength of $^5D_2 \leftarrow\!\!- {}^7F_0$ hypersensitive transition of Eu^{3+} ion in its amino acid complexes, at different values of temperature. The absorption band is resolved into a sum of several Gaussians. The parameters of the Gaussian (i.e. position of center, height and width at half height) are the variables of the curve fitting programme. The results of the analysis of line-shape are summarized. The magnitude of the molar enhancement of oscillator strength as well as the results of line shape analysis are then discussed.

Experimental Method :

(i) Preparation of solutions : Eu_2O_3 (99.9% pure) purchased from Sigma Chemical Company, USA is converted to $EuCl_3$ (solid) by repeated evaporation with Analar HCl. $EuCl_3$ is dissolved in a 0.100 M KCl solution. The latter is prepared by dissolving Analytical Grade KCl in deionised water. The solution is filtered through Millipore Filter. Its concentration is then determined by the procedure described in Chapter II. Amino Acids are stored in a dessicator. The solution of amino acid ligand is prepared by weighing a definite amount and dissolving it in Deionised Millipore water (μ = 0.100 with KCl) kept in a volumetric flask (prewashed with Millipore water).

The quantity weighed is large. The error in ligand concentration is estimated to be entirely negligible (discussed in Chapter III). Millipore water is used to minimise contamination with dust. This is necessary in order to reduce any error introduced in the small absorption signal to be measured, arising from scattering of light by dust particles.

(ii) Both metal and ligand solution are unbuffered. This creates considerable problem in adjustment of pH of the mixture of the two solutions to the desired value after mixing them in the cuvette for absorption measurement. In spite of this difficulty, use of buffer is avoided. If buffer is used, Eu^{3+} ion binds to buffer and the complex absorbs light. The free concentration of Eu^{3+} ion in the reference and in the sample cell are different. Thus the concentration of Eu^{3+}-buffer complex is not going to be equal in the two cuvettes. Thus the difference in absorption that is experimentally measured will have to be corrected for absorption of Eu^{3+}-buffer complex. The error of measurement of K and $\triangle\varepsilon$ of Eu^{3+}-buffer complex will introduce additional error in the determination of the enhancement of oscillator strength of the hypersensitive band. This is particularly true because the difference of absorption being measured is small in absolute magnitude. A small error in K and $\triangle\ \varepsilon$ of Eu^{3+}-buffer complex is likely to introduce a large percentage error in the value of $\triangle A$ being measured.

(iii) Preparation of solutions for spectroscopic measurement : A mixture of ligand and metal solutions at a fixed pH is prepared in the cuvette for spectroscopic measurement in the following way : The ligand solution at a pH greater than the desired pH is weighed in a cuvette. Eu^{3+} solution is added to the ligand. The $EuCl_3$ solution is concentrated ($\sim$ 0.7-0.8 M). The pH has to be low ($\sim$ 4) in order to obtain a concentrated solution. The pH changes on addition of Eu^{3+} solution. Therefore, one has to adjust the pH by addition of NaOH solution after the liquids are mixed. The exact volume to be added is predetermined by one or more trial experiments carried out by immersing the cuvette in a water bath maintained at the desired temperature. In an actual experiment, one adds a weighed volume of ligand, metal and NaOH solution to the cuvette and mixes them. The cuvette is then immersed in a water bath fixed at the desired temperature. A microelectrode is then immersed in the cuvette and the resultant pH is measured. Its value is almost always equal to the desired pH within $\pm$0.05 units. Sometimes a minor adjustment of pH is necessary. This is carried out by addition of 1-2 µl of NaOH or HCl. 1 µl is 5×10^{-4} times of 2 ml, the total volume. Thus this addition does not alter the concentration values significantly. When the microelectrode is removed from the cuvette, a small volume of liquid is lost. This loss introduces no error. The various components of the

mixture are already mixed and equilibrium is attained. The concentration values are not altered when a small volume is lost. The 1 or 2 µl of NaOH or HCl that may then be necessary is, in any case, much smaller than the volume of the liquid in the cuvette.

The solution in the reference cell is prepared by addition of an identical volume of $EuCl_3$ to a 0.100 M KCl solution of a volume identical to the volume of the ligand solution taken in the sample cell.

The spectrum is then recorded with the mixture of metal and ligand solution in the sample compartment and the $EuCl_3$ solution in the reference cell.

Let the value of total concentration of metal and ligand in the sample cell be $C_T(M)$ and $C_T(L)$. The concentration of metal in the reference cell is $C_T(M)$. Of the quantity $C_T(M)$, a certain fraction $C_B(M)$ is bound. Thus the measured difference in absorption is the difference in absorption of $C_B(M)$ in bound form and $C_B(M)$ in free form.

(iv) Recording of the spectrum : The quartz cells used for hypersensitive absorption measurements are a matched pair of Hellma cells. They were being used for the first time and therefore were absolutely scratch free. The base line of the Cary 17 D spectrometer in the region of interest is straightened-air vs air and cell vs cell before every experiment. The straightening is done with 0.02 O.D. full scale

and 0.6 nm/inch settings. Once the base line is set, it is not necessary to set it for sometime. The chart-speed is kept at 0.01 nm/sec, sometimes at 0.005 nm/sec. Thus the pen stays at the same wavelength for long and gives a complete recording of the noise. The middle point of the recorded sum of signal and noise is taken to be the magnitude of the signal. At the settings of the spectrometer, the pen fidelity is much higher than 1, the desired number that makes the recorded signal a true copy of what is instantaneously sensed by the photomultiplier. The resolution can be improved by further adjustment of the slit control but it increases noise unduly. The optimum spectral band width is 0.05 nm. The spectrometer was calibrated before the experiments were performed and 485.99 nm line of the Deuterium lamp was found to appear at 485.85 nm. The room was not at a fixed temperature. The calibration shifts by 0.003 nm/^{o}C. Thus a maximum change in calibration is $\sim$ 0.02 nm. The temperature in the cuvette is kept constant within $\pm$0.1 ^{o}C by circulating water at a constant temperature around the cuvettes from a constant temperature bath. The temperature of the water bath is fixed at a value depending on the room temperature, such that temperature as measured in the cuvette has the desired value (15^{o}, 25^{o} or 35^{o}C). The measurement is performed immediately after preparation of solution. When this is not possible due to lack of availability of the spectrometer,

a shift of wavelength as well as change of intensity are noticed on storage for 24 hours. At pH 6.5, concentration of Eu^{3+} is kept at a significantly lower value than that at pH 5.0 to avoid precipitation. The pH 6.5 spectra are therefore more noisy. The problem is particularly acute in the case of Glutamine at 35°C, Glutamic Acid at 35°C and Aspartic Acid at 25°C and 35°C. There is a special experimental difficulty of working at 15°C during the humid summer months. In spite of a dehumidifier, dew formation is unavoidable on the cuvette. The flatness of the base line is affected by as much as 0.0003 O.D. units.

(v) Lineshape analysis of the absorption curve : The observed absorption spectrum is expressed as a sum of several Gaussians. The center, height and half-width of the Gaussians are varied over a wide range using a computer programme (Details given in Appendix **B**) until the best least square fit is obtained. The programme used can fit the observed curve with as many as fifteen variables. Since there are three variables per Gaussian, five Gaussians with variable center, height and half-width can be used in curve-fitting ($y(x) = \sum_{i=1}^{5} Cie^{-(x-x_i)^{(o)}/2\sigma_1^2}$ where C_i, x_i and σ_i are height, center and width at half height of the i^{th} curve. If Ci=0, a particular Gaussian is absent). The maximum number of separate transitions in the $^5D_2 \leftarrow {}^7F_o$ band is five. Thus the programme is just adequate for our purpose.

The shape of the curve is read from the chart paper. The value of O.D. at a certain wavelength is taken to be the middle point of the recorded sum of signal and noise. If signal averaging is done to obtain a virtually noise-free curve one would obtain this middle point as the average signal. The slow chart speed used (0.1 nm/sec or 0.005 nm/sec) is crucial in obtaining a reliable estimate of the middle point of the noisy curve. The pen runs up and down manytimes almost at the same wavelength to give a complete record of the noisy signal.

Twenty spectra are obtained for the same system. The values of curve-fitting parameters obtained from different curves, give a reliable mean and standard deviation. In a large number of systems, standard deviation is sufficiently small to make the mean value a physically meaningful parameter. The results of line-shape analysis for the different systems studied are summarized in Table I.

The oscillator strength of a spectral transition is given by the formula [1]

$$f = 4.32 \times 10^{-9} \; 9n/(n^2+2)^2 \int \varepsilon(\bar{\nu}) \, d\bar{\nu} \quad ,$$

where $\varepsilon(\bar{\nu})$ is the measured molar extinction coefficient as a function of the frequency measured in wave numbers centimeters^{-1}, n is the refractive index. The area under the experimental absorption curve is measured by a planimeter in square inches. The area is divided by the concentration of the complex (calculated from total concentration of metal, total concentration of ligand and the known value of metal-ligand stability constant) to get the area representing enhancement per mole. 1 inch along y-axis on 0.002 O.D. full scale represents 0.02 O.D (In 0.05 O.D. Full scale it is 0.005 O.D.). 1 inch along x-axis is 0.06 nm at the speed used. Now, 0.002 O.D. means a value of $\varepsilon = 2\text{x}10^{-3}$ moles^{-1} lit cm^{-1} with a path length of 1 cm. i.e. = 2 in mole^{-1}cm^{2} unit. On the x-axis 0.06 nm = $6\text{x}10^{-9}$ cm. Thus 1 sq.inch = $2\text{x}6\text{x}10^{-9}$ mole^{-1}cm^{3} (in 0.02 O.D. Full scale used for amino acid complexes; it is $5\text{x}6\text{x}10^{-9}$ mole^{-1}cm^{3} for 0.05 O.D. Full scale used for Eu^{3+} aquo ion). Now, comes the conversion to expressing frequency in wave numbers, $d\bar{\nu} = \frac{d\lambda}{\lambda^2}$, where $\bar{\nu}$ is wave number and λ is wave length. Value of λ taken is that of the middle point of the band, 464.30 nm (in cm) n=1.33 gives $9n/(n^2+2)^2=0.84$. Area in sq.inch is multiplied by $0.84 \times (12\text{x}10^{-9}) \times (1/(464.30\text{x}10^{-7})^2) \times (4.32\text{x}10^{-9})$ to give oscillator strength in mole^{-1}cm (in 0.02 O.D. Full Scale; $12\text{x}10^{-9}$ is to be replaced by $30\text{x}10^{-9}$ in 0.05 O.D. Full Scale). The data of the molar oscillator strength of Eu^{3+} aquo ion is given in Table II, that of the molar enhancement of the

oscillator strength of the complexes is given in Table III. In Table II error is calculated in two different methods. The error in K_{ML} (calculated using mean value of K_{MB}) and the error in the area measurement give rise to an error in the molar oscillator strength. The concentration of the metal-ligand complex is calculated by calculating it by using $K_{ML} + \sigma$ and $K_{ML} - \sigma$. Thus one obtains the two error limits of the concentration of the complex. The molar oscillator strength is the ratio of the observed oscillator strength to the concentration of the complex. The area measurement has an error due to noise. The error in the ratio is calculated from the standard formula given in Chapter I. K_{ML} calculated from $K_{MB} \pm 3\sigma$ is also used to calculate the concentration of the complex. These quantities are then used to calculate molar oscillator strength. These values give the maximum error of oscillator strength values. When K_{MB} is changed to $K_{MB} \pm 3\sigma$, all the oscillator strength values at the same pH are shifted in the same direction. Thus comparison of values of oscillator strength at the same pH yields the same trends irrespective of whether K_{ML} calculated from mean K_{MB} or $K_{MB} \pm 3\sigma$ is used. While comparing values of oscillator strength at different pH values, one needs to consider the maximum error associated with measurement at a certain pH.

In the following, we state and discuss the results of line shape analysis for each system separately.

Eu^{3+} (aquo) ion :

The experiments are done at pH 3.0. The spectrum is identical at pH 4.0. The value of 3.0 of pH is chosen in order to get a sufficiently concentrated solution such that a good signal to noise is obtained. The spectra are resolved into a sum of three Gaussians. The parameters of the component Gaussians give a standard deviation that is expected in view of the magnitude of the noise. At 15°C, dew is formed on cuvette surface. The area under the curve does not show abnormally large standard deviation. The line positions show larger standard deviation than is seen at other values of temperature. The intensities show significant variation from one curve to another. The sum C_1+C_2 shows much smaller ($\sim$ 4%) standard deviation, than does C_1 and C_2 separately. The more clearly separated largest wavelength Gaussian shows a larger, yet acceptable error. Thus we quote the values of (C_1+C_2) and C_3 only. Dew formation on the cuvette surface at the time of the spectral measuremont is suspected from the variation in the values of C_1 and C_2 in going from one curve to anther. Dew is visibly formed when one takes the cuvette out. The best estimate of the separate values of C_1 and C_2 is obtained from the first one of all the absorption spectra recorded at 15°C. Dew formation is minimum in the first spectrum. The cuvette has stayed longer in the cell compartment when

the latter spectra are recorded and dew formation will have larger effect on them.

The values of intensity parameters C_1 and C_2 show larger standard deviation than does the sum C_1+C_2 at 25°C and 35°C. This is a result of the fact that the separation between the centers of the Gaussians is comparable to the sum of the widths at half height. At 25°C, separation between the centers is $\sim$ 0.62 nm, sum of widths at half height $\sim$ 0.57 nm. Standard deviation of C_1 is $\sim$ 25%, that of C_2 is $\sim$ 10%, but that of C_1+C_2 is $\sim$ 3%.

The intensity parameters do not change significantly when temperature is changed. The mean value of $(C_1+C_2)/C_3$ is larger (7.8) at 15°C, but the error is also large ($\pm$ 1.9). However if one considers only the first curve, the ratio is 9.7. The difference from the corresponding quantity at 25°C (6.4 $\pm$ 0.4) is within experimental error. The centers of the Gaussians show a small temperature dependent shift slightly beyond experimental error. The shift is obvious on comparing data at 15°C with the data at 35°C.

Eu^{3+}-Glutamic Acid system at pH 5.0 :

The spectra are resolved into four Gaussians at all three values of temperature. In the discussion that is to follow, we call the Gaussian at the lowest λ as the first Gaussian and the one at the highest λ as the fourth Gaussian

and so on. The second and the third Gaussians are located very close together. Whereas the separation between the centers of the first and the second Gaussian is 0.66 nm and that between the third and the fourth is 0.49 nm, the second and the third are separated by 0.24 nm. However this small separation is significantly above the error of measurement. All the fifteen spectra analysed give the same result, i.e. a resolution into four Gaussians with good precision of the parameters. In contrast, Eu^{3+}(aquo) ion spectra gives three Gaussians consistently in all the twelve spectra, which have been analysed. The lines centered at 464.30 nm and 464.54 nm (mean values at 35°C) in the Eu^{3+}-Glutamic acid spectra are shifted and merged together in the Gaussian centered at 464.49 nm in the Eu^{3+}(aquo) ion spectrum at 35°C. The inner Gaussian at 464.30 is shifted significantly so as to be resolvable in the Eu^{3+}-Glutamic acid system.

Another clear shift is that of the fourth Gaussian (at the highest wave length). It is shifted by - 0.43 ($\pm$0.03) nm at 35°C, - 0.48 ($\pm$0.05) nm at 25°C and - 0.59 ($\pm$0.03) nm at 15°C.

The intensity parameters show that the ratio $(C_1+C_2+C_3)/C_4$ is 1.83 $\pm$ 0.18 at 35°C, 1.82 $\pm$ 0.13 at 25°C and 1.79 $\pm$ 0.15 at 15°C. The same ratio in Eu^{3+} (aquo) ion is 7.8 $\pm$ 1.9 at 15°C, 6.38 $\pm$ 0.49 at 25°C, 6.78$\pm$0.58 at 35°C. The preferential enhancement of the longest

wavelength Gaussian is clearly established. The ratio C_4/C_1 is 1.75 ± 0.73 at 35°C and 1.91 ± 0.46 at 25°C for the Eu^{3+}-Glutamic Acid complex, whereas the same ratio is 0.48 (±0.11) at 35°C and 0.50(±0.13) at 25°C for the Eu^{3+} (aquo) ion. The longest wavelength Gaussian (at 465.03 nm at 35°C) is preferentially enhanced compared to the shortest wavelength Gaussian (at 463.96 nm at 35°C). The magnitude of the preferential enhancement in both cases is not significantly temperature dependent.

The values of C_2 and C_3 show abrupt changes in going from one curve to another for the same system. The standard deviation of C_2+C_3 is, however not large. This arises from the very close proximity of the two inner Gaussians and the uncertainty due to noise. The ratio $(C_2+C_3)/C_4$ is 1.26(±0.20) at 35°C and 1.29(±0.07) at 25°C, 1.29(±0.18) at 15°C, whereas in the aquo ion it is 4.75(±0.5) at 35°C, 4.33(±0.54) at 25°C (at 15°C the ratio has high uncertainty due to dew formation). Thus the highest wavelength Gaussian is preferentially enhanced compared to sum of the two inner Gaussians.

The ratio $(C_2+C_3)/C_1$ is 2.2(±0.9) at 35°C, 2.5(±0.6) at 25°C and 2.6(±0.8) at 15°C in the Glutamic Acid complex. The same ratio in the aquo complex has the value 2.3(± 0.5) at 35°C, 2.17(±0.56) at 25°C and 3.0 (the value of the first curve) at 15°C. The change is insignificant on change of temperature as well as complex formation.

The values of the width at half height show that the width of the first and the fourth Gaussian do not change significantly on complex formation with Glutamic Acid. The inner Gaussian of Eu^{3+} (aquo) ion has a width which is approximately the sum of the widths of the two inner Gaussians of the Glutamic Acid complex. This observation is consistent with the hypothesis that the Gaussian centered at $\sim$463.3 nm in Eu^{3+}-Glutamic Acid complex shifts by $\sim$ 0.1 nm in the Eu^{3+} (aquo) ion to merge with the Gaussian centered at 464.54 nm (at 35°C) to give the unresolvable inner Gaussian of Eu^{3+} (aquo) ion. The large width of the latter indicates that the shift is more like $\sim$ 0.1 nm rather than 0.2 nm. If the latter is the case, the width is not expected to be the sum of the widths of the inner Gaussians of the Glutamic Acid Complex. Thus there are three important features that emerge out of the comparison of the spectrum of Eu^{3+} (aquo) ion complex with the spectrum of Eu^{3+}-Glutamic acid complex.

(1) The Gaussians in the Glutamic Acid complex shift from their respective positions in the aquo complex. (i) One of the two Gaussians which are overlapping and appear to be one Gaussian at 464.49 nm at 35°C in the Eu^{3+}(aquo) ion spectra shift to longer wavelength by $\sim$ 0.1 nm and (ii) the Gaussian at the longest wavelength in the spectrum of Eu^{3+} (aquo) complex shifts to lower wavelength in the Eu^{3+}-Glutamic Acid complex by $\sim$ 0.4 nm.

(2) The relative intensities alter : the longest wavelength Gaussian in Eu^{3+} (aquo) is enhanced more significantly than the others.

(3) Temperature dependence of spectral parameters is not significant.

Eu^{3+}-Aspartic Acid system at pH 5 :

(i) The change in the positions of the centers of Gaussians with temperature are not significant.

(ii) As is observed in the Glutamic Acid system there are four Gaussians at 15°C and 25°C. The difference between the mean values of the positions of the centers is much larger than the standard deviations. The positions of the center of the first three Gaussians are exactly the same as those in the Eu^{3+}-Glutamic Acid system. The longest wavelength peak in this complex is at a significantly lower wave length compared to that in the Eu^{3+} (aquo) ion ($\sim$465.1 nm compared to $\sim$ 465.5 nm), but compared to the Eu^{3+}-Glutamic Acid system, it is at a slightly higher wave length ($\Delta\lambda \approx 0.05$ nm). One of the two inner Gaussians ($\sim$ 464.35 nm) is shifted to longer wave length to be merged into one Gaussian at $\sim$ 464.5 nm in Eu^{3+} (aquo) ion.

(iii) The spectrum of this system at 35°C shows one Gaussian centered at an intermediate wavelength ($\sim$464.4 nm) compared to two Gaussians at 15°C and 25°C ($\sim$464.35 and $\sim$ 464.55 nm).

There is a shift of the peak at 464.55 to lower wavelength, but the shift need not be large to lead to a merger, because the Gaussian at ∿464.35 has smaller intensity ($C_2 \simeq$ 0.45 and 0.28) compared to C_3 = 1.16 and 2.5).

(iv) The ratio $(C_1+C_2+C_3)/C_4$ is 3.13±0.36 at 15°C, 3.28±0.58 at 35°C and 7.29±4.62 at 25°C. The enhancement of the longest wavelength Gaussian is clearly established at 15°C and 35°C (for immediate comparison, the values of this ratio in Eu^{3+} (aquo) ion are 7.8 ± 1.9 at 15°C (or 9.7 for the most reliable first curve), 6.38 ± 0.49 at 25°C, 6.78 ± 0.58 at 35°C). At 25°C, the error is too large. The preferential enhancement of the longest wavelength Gaussian is however less than that observed in Glutamic acid complex (values for immediate comparison in the latter complex are 1.83 ± 0.18 at 35°C, 1.82 ± 0.13 at 25°C and 1.79 ± 0.15 at 15°C).

(v) The two inner Gaussians are quite close and are merged at 35°C. Therefore, in the discussion on the relative intensity, we will discuss the ratios $(C_2+C_3)/C_4$ and C_1/C_4. At all values of temperature, C_4 is comparatively larger compared to that in Eu^{3+} (aquo). The ratio $(C_2+C_3)/C_4$ is 4.75 (±0.50) at 35°C and 4.33 (±0.54) at 25°C in Eu^{3+} (aquo) ion, whereas in the Eu^{3+}-Aspartic Acid complex it is 2.55 (±0.6) at 15°C, 3.07 (±0.56) at 35°C and 6.76 (±4.3) at 25°C. The mean value at 25°C is anomalous and may reflect an artifact of curve fitting of a noisy curve.

The large error of course makes it equal to the values at 15°C and 35°C within error limits. The enhancement of the highest wavelength Gaussian is again indicated.

(vi) C_4/C_1 is 0.50(±0.13) at 25°C and is 0.48(±0.11) at 35°C, in Eu^{3+} (aquo) ion. In Eu^{3+}-Aspartic Acid complex it is 1.69 (±0.80) at 15°C, 2.5(± 1.5) at 25°C and 4.93 (±1.93) at 35°C. The relative enhancement of the longest wavelength Gaussian compared to the shortest wavelength peak is indicated.

The conclusions are similar to those in the Eu^{3+}-Glutamic Acid system except for the anomaly regarding the relative enhancement of the longest wavelength Gaussian at 25°C.

Eu^{3+}-Aspargine at pH 5.0 :

(i) At 15°C and 25°C, there are four Gaussians, their centers being approximately at the same wavelengths as those of the Eu^{3+}-Glutamic Acid and Eu^{3+}-Aspartic Acid systems. At 35°C, the two lower wavelength Gaussians shift very little or not at all. The two higher wavelength Gaussians merge into one Gaussian at an intermediate value of wavelength ($\sim$464.80 nm instead of two Gaussians at $\sim$ 464.5 and $\sim$ 465.1 nm).

(ii) At 15°C, there is large standard deviation in values of C_1, C_2 and C_3. However the intensity parameters that can be reliably discussed are $(C_1+C_2+C_3)$ and C_4. The standard deviations in these quantities are small. At 25°C and 35°C, values of C_1 and of (C_2+C_3) are also quoted separately. Standard deviation of C_1 is large, but is less than that at 15°C. At 15°C the ratio $(C_1+C_2+C_3)/C_4$ is 3.68 ± 1.38. At 25°C, it is 4.0 ± 2.1. The same ratios in Eu^{3+}(aquo) ion are 7.8 ± 1.9 and 6.4 ± 0.75. At 15°C, the ratio is 9.7 if one uses the value for the most reliable first curve. The preferential enhancement of the longest wavelength Gaussian is beyond experimental uncertainty. This ratio at 35°C is 1.82 ± 0.8 i.e. the longest wavelength Gaussian is enhanced more significantly. We believe that the difference of this value from that at 15°C and 25°C is an artifact of curve analysis and is coupled to the acceptance of a model with only one Gaussian at $\sim$ 464.80 nm rather than two separate Gaussians.

The conclusions are as follows :

(i) The highest wavelength Gaussian is preferentially enhanced. The values are in the same range as those of Glutamic Acid and Aspartic Acid complex, but large errors for the Aspargine complex prevent a comparison of relative values.

(ii) The highest wavelength Gaussian is also shifted by $\sim$ 0.4 nm to lower wavelength compared to Eu^{3+} (aquo) ion. The shifted location of the peak is the same as those in the Glutamic Acid and the Aspartic Acid complexes.

(iii) Temperature dependence of the lineshape is insignificant.

Eu^{3+}-Glutamine pH 5.0 :

(i) At 25°C and 35°C, the spectrum is resolved into three Gaussians. The highest wavelength Gaussian has its large characteristic shift of $\sim$ 0.4 nm. The wavelength of the lowest wavelength Gaussian is about the same as that in other complexes; as well as in Eu^{3+} (aquo) ion. The two separate inner Gaussians observed in the other amino acid complexes are merged.

(ii) The ratio of the intensity parameters show a preferential enhancement of the longest wavelength Gaussian. The ratio C_3/C_1 is 3.26 ($\pm$1.38) at 25°C and 3.57 ($\pm$1.43) at 35°C. This is to be compared with the value of the same quantity in Eu^{3+}(aquo) ion, 0.50 ($\pm$0.13) at 25°C and 0.48 ($\pm$0.11) at 35°C. The values are comparable to those in the Aspartic Acid and Glutamic Acid complexes. The longest wavelength Gaussian is preferentially enhanced.

(iii) The ratio C_2/C_3 in the Eu^{3+}-Glutamine complex corresponds to the ratio $(C_2+C_3)/C_4$ in the other complexes. The values of the ratio are 2.79 ($\pm$0.62) at 25°C and 2.76 ($\pm$0.56) at 35°C. These values are comparable to those in Eu^{3+}-Aspartic Acid system (2.55 ($\pm$0.60) at 15°C and 3.07($\pm$0.56) at 35°C), larger than those in Eu^{3+}-Glutamic Acid system (1.26 $\pm$ 0.20 at 35°C, 1.29 $\pm$ 0.07 at 25°C, 1.29 $\pm$ 0.18 at 15°C), but smaller than those in Eu^{3+} (aquo) ion. The Gaussian at the longest wavelength is preferentially enhanced.

(iv) At 15°C, there are only two Gaussians. The ratio of intensities is 15.2 ($\pm$1.6), which is in total disagreement with those at 25°C and 35°C.

(v) The ratio $(C_1+C_2)/C_3$ in this system corresponds to the ratio $(C_1+C_2+C_3)/C_4$ in the Eu^{3+}-Aspargine system. Its value in Eu^{3+}-Glutamine complex is 3.09 ($\pm$0.67) at 25°C and 3.04 ($\pm$0.59) at 35°C. In the Eu^{3+}-Aspargine complex, it has the same value within error limits. This value is again much smaller than in Eu^{3+} (aquo) ion (6.38 $\pm$ 0.49 at 25°C and 6.78 $\pm$ 0.58 at 35°C). The preferential enhancement of the highest wavelength Gaussian is clearly beyond the error limits. The magnitude is comparable to that of Aspartic Acid complex, but is less than that of Glutamic Acid complex.

Eu^{3+}-Glutamic Acid at pH 6.5 :

(i) The spectrum is resolved into two Gaussians. One of them corresponds to the longest wavelength Gaussian of the spectra at pH 5.0, but are at somewhat higher wavelength. The other Gaussian corresponds to the two inner Gaussians of pH 5.0 spectra.

(ii) The ratio $\frac{C_1}{C_2} \simeq$ 2 at 15°C and $\simeq$ 3 at 25°C (lower wavelength Gaussian carries the label 1).

(iii) The Gaussian at the lowest wavelength in the pH 5.0 spectra is either enhanced insignificantly or shifted.

(iv) The preferential enhancement of the longest wavelength peak is established, irrespective of the alternative possibilities stated in (iii). The ratio $(C_1+C_2)/C_3$ in Eu^{3+} (aquo) ion is 7.8 ($\pm$1.9) at 15°C and 6.4 $\pm$ 0.45 at 25°C.

(v) The spectral parameters in this system are temperature independent.

We conclude (i) Hypersensitive absorption lineshape is significantly pH dependent, i.e. the species at pH 6.5 is different from that at pH 5.0. (ii) The shift of the longest wavelength Gaussian is smaller than that at pH 5.0. (iii) The preferential enhancement of this peak is again observed. (iv) Temperature dependence is not observed.

Eu^{3+}-Aspartic Acid at pH 6.5 :

(i) There are two Gaussians at 15°C. Both are shifted to slightly lower wavelength compared to the Glutamic acid complex.

(ii) The Gaussian at the higher wavelength is more intense (by a factor of 5.6). This effect is consistent with the general observation that higher wavelength Gaussian is more enhanced. But the order of absolute magnitude is reversed.

(iii) The difference of this system with Eu^{3+}-Glutamic acid complex at pH 6.5 and Eu^{3+}-Aspartic Acid complex at pH 5.0 is clear.

(iv) The lowest wavelength Gaussian ($\sim$ 463.9 nm) observed at pH 5.0 is again either very low in intensity or is significantly shifted.

Eu^{3+}-Asparginc at pH 6.5 :

(i) The spectrum is resolved into four Gaussians at 15°C, but the one at longest wavelength centered at 464.76 nm is considerably more intense compared to the other three at lower wavelengths. The ratio $C_4/(C_1+C_2+C_3)$ is $4.68(\pm 2.49)$.

(ii) At 25°C, there is only one Gaussian centered at 464.66 nm. In both cases the Gaussians are much wider than observed in the systems discussed earlier (width at half height being

0.37 and 0.45 nm respectively), indicating that the Gaussian is formed as a result of overlap of several absorption lines.

The conclusions are :

(i) the lowest wavelength Gaussian is not enhanced at all or shifted significantly ($\sim$ 0.7 - 0.8 nm),

(ii) the other peaks are shifted compared to the cases discussed earlier and overlap to give rise to a wide Gaussian,

(iii) The phenomenon of a significant preferential shift and enhancement of the Gaussian at the longest wavelength is consistent with the observed line-shape.

Eu^{3+}-Glutamine at pH 6.5 :

(i) The curve is resolved into two Gaussians at 15°C and at 25°C. The Gaussians are centered at $\sim$ 464.3 nm and $\sim$ 465.1 nm. The former has a counterpart in Eu^{3+}-Aspartic Acid complex at pH 6.5. The latter has a counterpart in Eu^{3+}-Glutamic acid complex. However the second Gaussians of Aspartic Acid and Glutamic acid complexes are at a slightly different wavelength compared to that in Eu^{3+} - Glutamine complex.

(ii) The difference spectra of Eu^{3+}-Glutamine system is however different from those of Eu^{3+}-Aspargine system in that the former has a resolvable longest wavelength Gaussian, which is perhaps shifted to a slightly lower wavelength in the latter, so as to merge with other peaks.

(iii) The ratio of C_1/C_2 is $\sim$ 3 at both temperature values, indicating a preferential enhancement of the longest wavelength Gaussian.

(iv) The large shift ($>$ 0.4 nm) of the longest wavelength Gaussian is also observed.

(v) The lowest wavelength Gaussian is either not enhanced or shifted by $\sim$ 0.4 nm.

The important highlights of the above discussions are :

(1) All the amino acid complexes show a preferential enhancement of the longest wavelength Gaussian.

(2) The longest wavelength Gaussian is also shifted significantly.

(3) This preferential enhancement is larger for the Glutamic acid complex compared to the others. The other three amino acid complexes are not different within the limits of error in this respect.

(4) At pH 6.5, there are very distinct changes in the characteristics of the spectra.

(5) The preferential enhancement of the longest wavelength Gaussian as well as its large shift is observed at pH 6.5.

(6) The higher wavelength Gaussian is larger in intensity than the lower wavelength Gaussian in Aspartic Acid and Asparagine complex. The reverse is true in Glutamic Acid and Glutamine complex. The latter trend is observed at pH 5.0 for all ligands.

(7) The lowest wavelength Gaussian ($\sim$463.9 nm) of all the spectra at pH 5.0 is either not enhanced or shifted to higher wavelengths at pH 6.5.

(8) At pH 6.5, Asparagine and Glutamine complex give qualitatively different spectra in that in the latter, a Gaussian at $\sim$ 465.1 nm is resolvable.

(i) Regarding the observation (8) above, we point out that Glutamine also shows difference from Asparagine in value of equilibrium constant. The values of β at pH 5.0 and 6.5 are about equal in Glutamine, whereas significant difference exists in Asparagine. Different degree of hydrolysis at pH 6.5 may be the cause.

(ii) The difference between Aspartic Acid and Glutamic Acid (observation (6)) at pH 6.5 is also consistent with the proposal of Pradös et al. (Ref. 20 of Chapter III) that Glutamic acid may form a polynuclear complex and Aspartic Acid forms a mononuclear hydrolysed complex at pH 6.5.

(iii) The greater relative enhancement of the highest wavelength peak of the Glutamic Acid complex compared to that of the Aspartic Acid complex at pH 5.0 shows that there is a difference in the preferential enhancement of the highest wavelength Gaussian in the chelate involving co-ordination of two carboxylates as compared to a complex with co-ordination of a single carboxylate. Their relative proportion alters in going from Aspartic Acid to Glutamic Acid. The chelate is expected to be more dominant in Aspartic Acid complex (lower pKa of side chain carboxylate) than in the Glutamic Acid complex. The chelate therefore does not enhance the highest wavelength Gaussian as much as the complex with co-ordination of one carboxylate. This statement assumes that an additional CH_2 group in Glutamic Acid does not alter the structure of the chelate.

(iv) On this model, preferential enhancement of the longest wavelength Gaussian of Aspargine and Glutamine complexes should be higher, if one assumes that at pH 5.0 they form a simple complex with co-ordination of a carboxylate group. It is perhaps indicated that the carboxamide group influences the relative enhancement, perhaps by co-ordinating the metal ion.

(v) It is clear that lineshape has information about the complex. Further investigation with better signal to noise in the spectra will resolve many ambiguities. Simulation of the observed spectra with spectra theoretically generated

for complexes of specific structure, using existing theoretical models will give more definitive information.

In the next few months, we plan to work on a project to build the accessory necessary for signal averaging.

In the following, we discuss the data on oscillator strength :

The oscillator strength of Eu^{3+}(aquo) ion shows (Table II) an increase with increase of temperature. Vibronic interactions are unlikely to result in any significant temperature dependence of oscillator strength for a change of temperature of 20°C (see discussions in Chapter I). A pH of 3.0 is too low for the hydrolytic equilibria to exist. The temperature dependence of oscillator strength is interpreted on the model that equilibria exist between more than one hydrated species (with different hydration number). The equilibria are shifted by a change of temperature.

Spedding and co-workers [2-4] find that the partial molar volumes, heats of dilution and relative viscosities of aqueous solutions of lanthanide chlorides are all consistent with the assumption that La^{3+} to Nd^{3+} have a co-ordination number of nine, Gd^{3+} to Lu^{3+} have a lower co-ordination number of eight and intermediate lanthanides are a mixture of both species.

Morgan [5] conclude on the basis nuclear magnetic proton relaxation enhancement data that both octa - and nona-hydrate are present in aqueous solution.

Nakamura and Kawamura [6] on the basis of concentration dependence of relaxation rates of ^{139}La ion in aqueous solutions of halides, nitrate, sulfate and perchlorate conclude that an equilibrium $La(H_2O)_9^{3+} \rightleftharpoons La(H_2O)_8^{3+} + H_2O$ exist. Reuben [7] has attributed this result to instrumental artifact and concludes that a definite co-ordination number of 9 exists for La^{3+} in agreement with X-ray evidence quoted by them.

Karraker [8] observes a change of shape of all Nd^{3+} absorption bands as electrolyte concentration (or temperature) is increased and an increase in the oscillator strengths for the hypersensitive bands of Nd^{3+}, Ho^{3+} and Er^{3+} as electrolyte concentration or temperature is increased. On the basis of the known spectral lineshapes of 9 co-ordinated and 8 co-ordinates Nd^{3+} in bromate and sulfate salts, Karraker finds that the change of lineshape is interpretable in terms of a nine co-ordinate structure in dilute solution, which gradually changes over to an eight co-ordinate structure. Over a wide range of electrolyte concentration, a mixture of the two are present in solution. The physical reason for the change of co-ordination is that at high electrolyte concentration, Nd^{3+} must compete with H^+ and Li^+ for water of hydration. It is therefore indicated that octa and nonahydrate are of comparable stability in Nd^{3+}. The enhancement of hypersentitive transition is interpreted by the action of an increased electric field produced by high electrolyte concentration.

The $^5L_6 \leftarrow {}^7F_0$ transition in dilute aqueous $Eu(ClO_4)_3$ solution is temperature independent in the range 25-91°C. This is interpreted as indicating only one aquated species [9]. The lineshape of $^5D_1 \leftarrow {}^7F_0$ transition band is temperature dependent. Outer sphere complexing by ions such as $Cl^{\ominus}$ is believed to displace an equilibrium between different aquo ions and affect the lineshape of the transition.

Hinchey and Cobble [10] find that the partial molal entropy of 13 trivalent lanthanide ions based on modern thermodynamic data and corrected for internal electronic entropy do not demonstrate the effect on the entropy of the postulated change in hydration number occurring near the middle of the 4f group.

Sayre, Miller and Freed [11] recorded spectra of Eu^{3+} in aqueous and mixed alcohol-water solvent (with a spectrograph of one meter focal length) and observed five distinct absorption lines in pure alcohol solution and when increasing amount of water is added. Intensity increases on addition of water upto a composition of 15% water - 85% alcohol, but does not change beyond that. On the basis of number of absorption and fluorescence lines, the authors infer a D_{2h} symmetry in aqueous solution and a C_{2v} symmetry in alcoholic solution. Temperature dependence of solution spectrum is not studied by these workers.

Thus the interpretation of temperature dependence of the oscillator strength of $^5D_2 \leftarrow {}^7F_0$ transition in terms of equilibria between more than one aquated species of different hydration number is consistent with some reported evidence in literature.

Complex formation of metal with amino acids may displace the equilibrium between aquated ions. A part of the temperature dependence of the enhancement of oscillator strength in these complexes may be derived from this source. The magnitude of the temperature dependence observed in Eu^{3+} (aquo) ion ($\sim$ 8% in going from 15°C to 35°C) is not sufficient to explain the changes observed in the complexes.

The large enhancement ($\sim$ 200-500%) of oscillator strength of lanthanide ions when some of the co-ordinated water molecules are replaced by amino acid ligands is understable on the basis of existing theoretical models (Chapter I for detailed discussion). The lowering of the symmetry of microenvironment on amino acid co-ordination enhances the oscillator strength.

At pH 5.0, in Eu^{3+}-Asparginc and in Eu^{3+}-Glutamine complex, there is a decrease of oscillator strength followed by an increase with increase of temperature. Eu^{3+}-Aspartic Acid and Eu^{3+}-Glutamic Acid complexes at pH 5.0 shows an increase followed by a decrease of oscillator strength with

increase of temperature. The equilibrium constant data indicated the presence of both exothermic and endothermic equilibrium. If there is only one exothermic and one endothermic species, increase of temperature alters their relative proportion in a monotonic fashion. This would lead to a monotonic increase or decrease of molar oscillator strength with increase of temperature. The fact that this is not so, indicates that the number of species is larger, e.g. carboxylate can be monodentate and bidentate, one or both carboxylates in Aspartic and Glutamic Acids can co-ordinate in both monodentate and bidentate fashion, carboxamide may co-ordinate in Asparginc and in Glutamine (Chapter III gives a summary of the NMR work on the structure of Amino Acid-Lanthanide complexes.The NMR data indicate the variety of possible structures.)

The oscillator strength of Glutamine complex at pH 5.0 is greater than that of Asparginc complex at pH 5.0. The mode of co-ordination of carboxylate group is unlikely to differ significantly in going from Asparginc to Glutamine. Thus carboxamide group has a significant role to play in co-ordination. The fraction of complexes in which carboxamide co-ordinates metal ion is different in going from Asparginc to Glutamine. It is not possible to say whether the species with carboxamide co-ordination, has higher or lower molar oscillator strength. An experiment with formamide as ligand could shed more light in this direction.

While comparing results on a Eu^{3+}-Glutamic Acid system with those on Eu^{3+}-Aspartic Acid system, one must remember two facts : (i) The pK_a of side chain carboxylate of Glutamic Acid being higher (4.7 compared to 3.71 of Aspartic Acid), the proportion of chelates involving co-ordination of two carboxylate groups is higher in Aspartic Acid compared to that in Glutamic Acid. (ii) The molar enhancement of the oscillator strength of hypersensitive transitions of Nd^{3+} and Ho^{3+} complexes of carboxylic acids increase with increasing pK_a [12]. A chelate in the Eu^{3+} Glutamic Acid complex is likely to give higher molar oscillator strength compared to its Aspartic Acid counterpart. One extra CH_2 group in the former is unlikely to alter the structure of carboxylate oxygen atoms around the metal ion significantly enough to alter the molar oscillator strength. The observation that Glutamic Acid complex at pH 5.0 has consistently higher molar oscillator strength than its Aspartic Acid counterpart, means that the higher molar oscillator strength of the chelate more than offsets the lower proportion of the chelate. A more detailed pH dependent study is necessary to quantitatively sort out this effect.

The fact that Glutamine and Asparagine complexes have molar oscillator strengths comparable to Glutamic Acid and Aspartic Acid complexes, strongly indicates the possibility of co-ordination by carboxamide group. Quantitative oscillator

strength data on acetate complex is necessary before a definitive statement is made. The effect of coordination by a simple carboxylate alone will then be singled out. The higher molar oscillator strength at pH 6.5 and its monotonic increase with temperature are consistent with the model that the hydrolysed species have higher extinction coefficient and their relative proportion increases with increase of temperature. An exception to this trend is the data on Eu^{3+}-Glutamine at pH 6.5 at 35°C. The pH 5.0 data on Aspartic and Glutamic Acid show that qualitatively lineshapes are similar even though relative proportion of complexes with co-ordination of one or two carboxylate groups vary. The disappearance of the shortest wavelength Gaussian at pH 6.5 is indicative of the dominance of the hydrolysed species at pH 6.5. This is consistent with the statement that the magnitude and temperature dependence of the total oscillator strength is determined by those of the hydrolysed species alone. The polarizability of OH group is larger than H_2O. This is consistent with the higher molar oscillator strength of the hydrolysed species. The alteration of the lineshape indicates that replacing H_2O by $OH^{\ominus}$ has more specific influence on the enhancement or position of individual transitions.

The concentration of metal ion is much higher in the spectral measurements than that in the titration experiments. Since only 1:1 complexes formed at the concentration values

used in the titration experiments, one expects 1:1 complex alone at similar ligand concentration and higher metal concentration of the spectroscopic experiments. In order to form 1:2 complexes, one would require much higher ligand concentration. Thus, use of the stability constants reported in Chapter III in calculating molar oscillator strength enhancement in the present chapter is justified.

Table I

System	pH	Temperature (°C)	Centre of Component Gaussians (nm) $X_1^{(o)}$	$X_2^{(o)}$	$X_3^{(o)}$	$X_4^{(o)}$	Intensities of Component Gaussians c_1	c_2	c_3	c_4	Width at Half Height (nm) σ_1	σ_2	σ_3	σ_4
$Eu(aquo)^{+3}$		35°C	463.85 ±0.05	464.49 ±0.04	465.47 ±0.05		0.83 ±0.18	1.90 ±0.18	0.40 ±0.02		0.26± 0.027	0.30± 0.02	0.21± 0.01	
							c_1+c_2 : 2.71±0.19							
		25°C	463.93 ±0.07	464.55 ±0.05	465.55 ±0.03		0.84 ±0.20	1.82 ±0.19	0.42 ±0.03		0.28± 0.02	0.29± 0.004	0.22± 0.004	
							c_1+c_2: 2.68±0.07							
		15°C	464.14 ±0.17	464.67 ±0.07	465.61 ±0.03		c_1+c_2: 2.74± 0.11		c_3: 0.35±0.08					
							For the first curve: c_1=0.71, c_2=2.10, c_3=0.29							
	5.0	35°C	463.96 ±0.04	464.30 ±0.04	464.54 ±0.07	465.03 ±0.024	0.63 ±0.26	0.50 ±0.30	0.69 ±0.33	1.10 ±0.08	0.20± 0.03	0.11± 0.024	0.17± 0.028	0.23± 0.00
							c_1+c_2=1.39±0.20							
							$c_1+c_2+c_3$=2.01±0.14							
Eu-Glutamic Acid	5.0	25°C	464.01 ±0.05	464.38 ±0.06	464.62 ±0.07	465.07 ±0.04	0.58 ±0.14	0.96 ±0.20	0.49 ±0.20	1.11 ±0.03	0.24± 0.03	0.14± 0.02	0.13± 0.03	0.21± 0.01
							c_1+c_2=1.44±0.07							
							$c_1+c_2+c_3$=2.02±0.14							

contd...

Table I (continued)...

System	pH	Temperature (°C)	Centre of component Gaussians (nm) $X_1^{(o)}$	$X_2^{(o)}$	$X_3^{(o)}$	$X_4^{(o)}$	Intensities of Component Gaussians c_1	c_2	c_3	c_4	Width at Half Height (nm) σ_1	σ_2	σ_3	σ_4
Eu-Glutamic Acid	5.0	15°C	463.95 ±0.026	464.27 ±0.02	464.53 ±0.04	465.01 ±0.02	0.54 ±0.15	0.54 ±0.20	0.86 ±0.23	1.08 ±0.08	0.21± 0.03	0.11± 0.014	0.16± 0.024	0.22± 0.017
							$c_1+c_2=1.39\pm0.17$							
							$c_1+c_2+c_3=1.93\pm0.08$							
Eu-Glutamic Acid	6.5	15°C	464.55 ±0.05	465.16 ±0.04			0.51 ±0.07	0.21 ±0.06			0.28± 0.04	0.20± 0.03		
	6.5	25°C	464.55 ±0.03	465.24 ±0.04			0.82 ±0.12	0.27 ±0.10			0.35± 0.04	0.23± 0.06		
Eu-Aspartic Acid	6.5	15°C	464.39 ±0.03	464.92 ±0.06			0.21 ±0.10	1.07 ±0.09			0.24± 0.06	0.45± 0.03		
Eu-Glutamine	6.5	15°C	464.39 ±0.03	465.12 ±0.05			0.87 ±0.05	0.28 ±0.04			0.32± 0.03	0.26± 0.02		
	6.5	25°C	464.30 ±0.03	465.08 ±0.03			1.04 ±0.23	0.32 ±0.13			0.30± 0.05	0.24± 0.02		
Eu-Aspartic Acid	5.0	15°C	463.95 ±0.06	464.33 ±0.02	464.58 ±0.06	465.10 ±0.03	0.36 ±0.16	0.45 ±0.29	1.16 ±0.42	0.61 ±0.10	0.15± 0.03	0.12± 0.03	0.28± 0.08	0.17± 0.01
								$c_2+c_3=1.56\pm0.28$						
							$c_1+c_2+c_3=1.91\pm0.22$							

contd...

Table I (continued)

System	pH	Temperature (°C)	Centre of component Gaussians (nm) $X_1^{(o)}$	$X_2^{(o)}$	$X_3^{(o)}$	$X_4^{(o)}$	Intensities of component Gaussians c_1	c_2	c_3	c_4	Width at Half Height (nm) σ_1	σ_2	σ_3	σ_4
Eu-Aspartic Acid	5.0	25°C	463.96 ±0.03	464.35 ±0.02	464.54 ±0.05	465.16 ±0.03	0.22 ±0.17	0.28 ±0.15	2.50 ±0.38	0.42 ±0.26	0.11± 0.03	0.10± 0.03	0.13± 0.03	0.4± 0.05
							c_1+c_2 : 2.84±0.52							
							$c_1+c_2+c_3$: 3.06±0.41							
	5.0	35°C	463.89 ±0.02	464.42 ±0.01	465.10 ±0.03		0.14 ±0.05	2.12 ±0.20	0.69 ±0.11		0.10± 0.02	0.33± 0.02	0.2± 0.02	
							c_1+c_2: 2.26±0.17							
Eu-Asparagine	5.0	15°C	463.96	464.31	464.62	465.06	$c_1+c_2+c_3$: 2.14±0.21			0.58 ±0.21	0.16± 0.03	0.16± 0.04	0.17± 0.05	0.21± 0.03
	5.0	25°C	463.97 ±0.04	464.29 ±0.04	464.50 ±0.08	465.14 ±0.03	0.27 ±0.20	c_2+c_3: 1.43 ±0.30		0.40 ±0.21	0.12± 0.13	0.31± 0.09	0.19± 0.04	
							$c_1+c_2+c_3$: 1.64 ±0.21							
	5.0	35°C	463.85 ±0.06	464.30 ±0.08	464.80 ±0.14		0.26 ±0.18	1.30 ±0.49	0.85 ±0.30		0.15± 0.04	0.28± 0.06	0.33± 0.07	
							c_1+c_2: 1.55±0.41 (Corresponds to $c_1+c_2+c_3$ above)							

CONTD...

System	pH	Temperature	Total concentration of metal $(m_T)^1$ (moles lit^{-1})	Molar oscillator strength[2] (mole^{-1}cm) (x 10^6)
$[Eu(aquo)]^{+3}$	3.0	15°C	0.296	0.858(±1.1%)
		25°C	0.296	0.894(±1.1%)
		35°C	0.296	0.926(±0.7%)

Table II : Molar oscillator strength of $[Eu(aquo)]^{+3}$ ion at different values of temperature.

[1] Standard deviation ~ 0.5%

[2] Standard deviation of measurement of area under absorption curve is ~ 1% at 15°C, 25°C and 0.6% at 35°C. The standard deviation in molar oscillator strength is calculated from the formula given on page 85.

Table III

System	pH	Temperature	Total concentration of metal (M_T) (Moles Lit^{-1})	Total concentration of ligand (L_T) (Moles Lit^{-1})	Concentration of complex ML (calculated using the value of K_{ML} using mean K_{MB})	Molar enhancement of oscillator strength ($Mole^{-1}cm$) (using concentration calculated in previous column) x10^6	Concentration of complex ML (calculated using the value of K_{ML} using $K_{MB} \pm 3\sigma$)	Molar enhancement of oscillator strength ($Mole^{-1}cm$) (Using concentration calculated in previous column) x10^6
$[Eu\text{-}Asparginc]^{+3}$	5.0	15°C	0.0684	0.0927	0.0264±0.0004	3.61(±2.3%)	0.0276,0.0246	3.45,3.87
		25°C	0.0517	0.0965	0.0263±0.0005	2.61(±3.0%)	0.0282,0.0284	2.44,2.86
		35°C	0.0434	0.0951	0.0223±0.0005	3.80(±3.3%)	0.0229,0.0216	3.70,3.92
	6.5	15°C	0.032	0.102	0.0231±0.0001	3.70(±3.4%)	0.0236,0.0225	3.62,3.80
		25°C	0.028	0.102	0.0196±0.0003	4.59(±2.4%)	0.0203,0.0192	4.43,4.68
		35°C	0.0195	0.0951	0.0135±0.0001	5.55(±3.1%)	0.0139,0.0132	5.39,5.68
$[Eu\text{-}Glutamine]^{+3}$	5.0	15°C	0.0513	0.1286	0.0181±0.0024	4.6(±13.5%)	0.0205,0.0154	4.05,5.39
		25°C	0.0525	0.1284	0.0236±0.0011	3.7(±6.6%)	0.0266,0.0196	3.31,4.49
		35°C	0.0364	0.1308	0.0151±0.0005	4.5(±5.1%)	0.0160,0.0140	4.24,4.85
	6.5	15°C	0.020	0.119	0.0090±0.0001	4.5(±4.7%)	0.0105,0.0070	3.86,5.86
		25°C	0.0214	0.117	0.0099±0.0001	5.0(±2.3%)	0.0109,0.0088	4.55,5.64
		35°C	0.017	0.1128	0.0093±0.00012	2.61(±8.4%)	0.0097,0.0085	2.51,2.86
$[Eu\text{-}Aspartic\ Acid]^{+3}$	5.0	15°C	0.0621	0.0347	0.0303±0.0001	2.82(±3.1%)	-	-
		25°C	0.0667	0.0345	0.0309±0.0001	3.75(±2.0%)	0.0311,0.0308	3.73,3.78
		35°C	0.0539	0.0337	0.0289±0.0001	3.59(±1.9%)	-	-
	6.5	15°C	0.0113	0.0284	0.0989±0.0004	4.42(±3.3%)	-	-

contd...

Table III (continued)...

System	pH	Temperature	Total concentration of metal (M_T) (Moles Lit^{-1})	Total concentration of ligand (L_T) (Moles Lit^{-1})	Concentration of complex ML (calculated) using the value of K_{ML} using mean K_{MB})	Molar enhancement of oscillator strength ($Mole^{-1}cm$) (using concentration calculated in previous column)x10^6	Concentration of complex ML (calculated using the value of K_{ML} using $K_{MB}\pm3\sigma$)	Molar enhancement of oscillator strength ($Mole^{-1}cm$) (using concentration calculated in previous column)x10^6
[Eu-Glutamic]$^{+3}$ acid	5.0	15°C	0.0371	0.0341	0.0200±0.0001	5.36(±2.0%)	0.0202,0.0197	5.31, 5.44
		25°C	0.0381	0.0341	0.0238±0.0001	4.49(±1.9%)	0.0242, 0.0234	4.41, 4.56
		35°C	0.0414	0.0339	0.0269±0.0001	4.08(±2.4%)	-	-
	6.5	15°C	0.0073	0.0253	0.0059±0.0000	4.34(±4.8%)	0.0059, 0.00583	4.33, 4.38
		25°C	0.0074	0.0251	0.0058±0.0000	6.67(±3.7%)	0.0058, 0.00576	6.67, 6.72

Table III : Molar Enhancement of Oscillator Strength of $^5D_2 \leftarrow {}^7F_0$ transition in Eu^{+3}-Amino Acid Complexes.

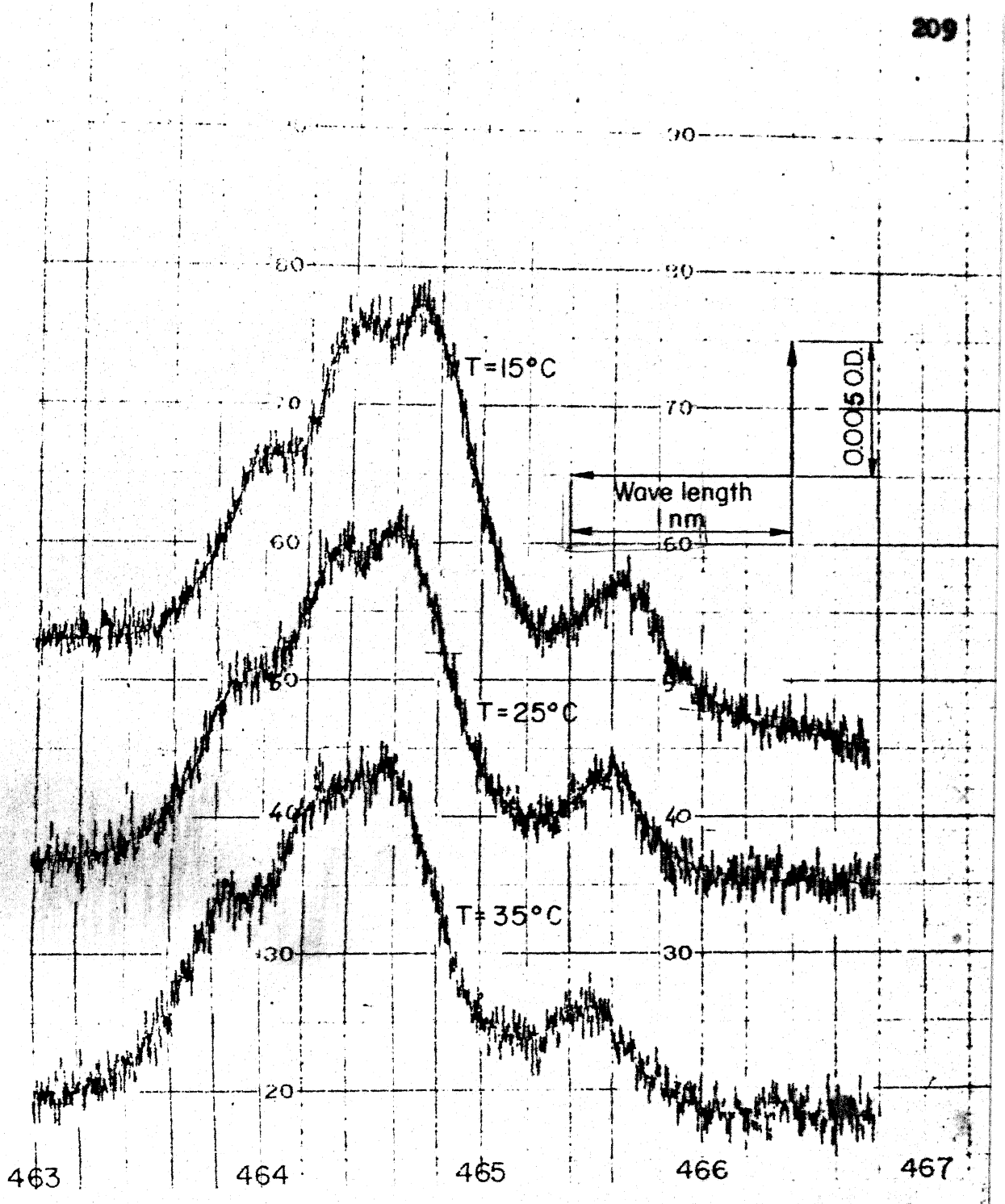

FIG.I: HYPERSENSITIVE ABSORPTION SPECTRA OF Eu^{3+}(aquo) ION IN .296M $EuCl_3$ SOLUTION (pH=3.00) AT THREE DIFFERENT TEMPERATURES. SHIFT OF THE PEAKS DEMONSTRATED.

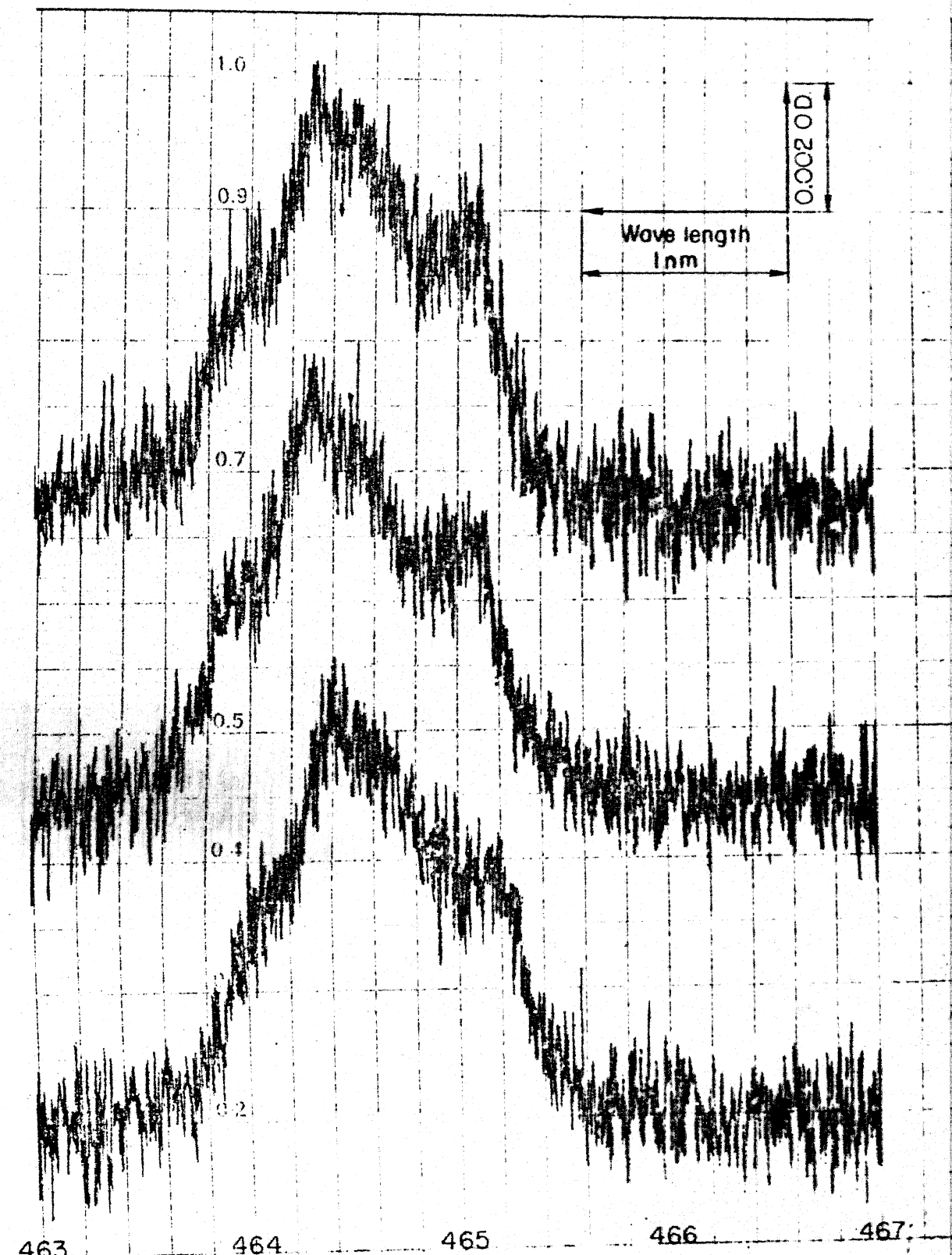

FIG.II: HYPERSENSITIVE ABSORPTION SPECTRA OF Eu^{3+} ION IN A Eu^{3+}-ASPARTIC ACID COMPLEX (Eu^{3+} CONCENTRATION=.0667M, ASPARTIC ACID CONCENTRATION=.0345M, pH=5.00, TEMPERATURE =25°C, IONIC STRENGTH=.100). DEMONSTRATION OF REPRODUCIBILITY FOR RELATIVELY MORE INTENSE ABSORPTION SPECTRA.

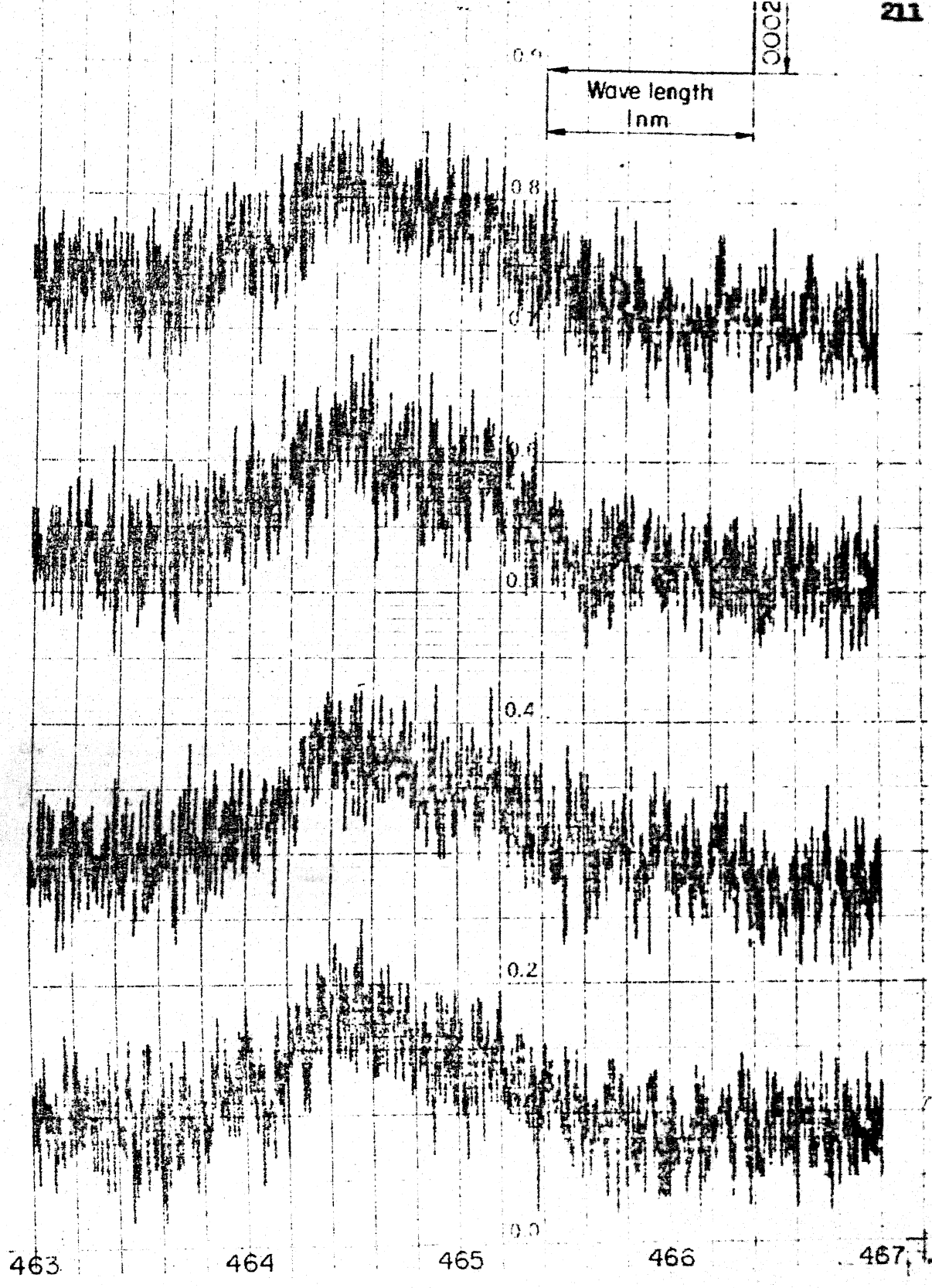

FIG. III: HYPERSENSITIVE ABSORPTION SPECTRA OF Eu^{3+} ION IN A Eu^{3+}-GLUTAMIC ACID COMPLEX (Eu^{3+} CONCENTRATION=.0074M, GLUTAMIC ACID CONCENTRATION=.025M, pH=6.50, TEMPERATURE =25°C, IONIC STRENGTH=.100). DEMONSTRATION OF REPRODUCIBILITY FOR RELATIVELY LESS INTENSE ABSORPTION SPECTRA.

References

1. W. Kauzmann, Quantum Chemistry, Academic Press, New York, 1957, p. 581.

2. F.H. Spedding, M.J. Pikal and B.O. Ayers, J. Phys. Chem., 70, 2440, 1966.

3. F.H. Spedding, S.A. Csejka and C.W. DeKock, J. Phys. Chem., 70, 2423, 1966.

4. F.H. Spedding and M.J. Pikal, J. Phys. Chem., 70, 2430, 1966.

5. L.O. Morgan, J. Chem. Phys., 38, 2788, 1963.

6. K. Nakamura and K. Kawamura, Bull. Chem. Soc., Japan, 44(2), 330, 1971.

7. J. Reuben, J. Phys. Chem., 79, 2154, 1975.

8. D.G. Karraker, Inorg. Chem., 7, 473, 1968.

9. K.B. Yatsimirskii and N.K. Davidenko, Co-ordination Chemistry Reviews, 27, 253, 1979.

10. R.J. Hinchey and J.W. Cobble, Inorg. Chem., 9, 917, 1970.

11. E.V. Sayre, D.G. Miller and S. Freed, J. Chem. Phys., 26, 109, 1957.

12. R.L. Fellows and G.R. Choppin, J. Cor-ordination Chem., 3, 209, 1973.

CHAPTER 5

Conclusions and Future Projections

In Chapter II, we have demonstrated that the stability constant of metal-murexide (or for that matter any metal-dye system) is best determined at a fixed pH in the absence of a buffer. The technique of adjusting pH in the cuvette by addition of acid or base works well. We propose to determine the stability constant at other values of pH and temperature.

In Chapter III, we have worked out the choice of experimental conditions for the determination of reliable values of stability constant of metal-ligand association reactions. To cover the whole range of saturation, one has to modify the conditions (e.g. concentration of buffer) in a few cases. It is also necessary to determine the stability constants of 1:2 metal-murexide complexes and of other metal-dye systems in order to cover the whole saturation range at different values of concentration. We propose to fill in these gaps. The temperature dependence of the values of stability constant shows the simultaneous presence of more than one equilibrium of the same stoichiometry, some endothermic and some exothermic. It is concluded that both the Aspartic acid and the Glutamic acid complexes at pH 5 are mixtures of a chelate with two carboxylates bound to metal and a simple α-carboxylate with only the α-carboxyl group coordinating the metal. The carboxamide group plays a significant role in stabilizing the Aspargine and Glutamine complexes

perhaps by coordination. The pH dependence clearly shows the presence of equilibria involving protons. In view of the evidence in literature, we conclude that at pH 6.5, we obtain hydrolyzed complexes.

In Chapter IV, we have demonstrated that the line-shape of the $^5D_2 \leftarrow {}^7F_0$ hypersensitive transition band of Eu^{3+} ion in complexes can be meaningfully analysed and that it has definite information. Clearly, these measurements require higher signal to noise ratio than we obtained. Cells with longer path length will make the study of metal-ligand system more precise. In addition, measurement at lower concentration of metal ions (at which stability constants are determined) will become possible. We are currently engaged in making a system for time averaging the spectrum, using the digital output of the Cary 17D spectrometer. With the data processing hook-up for signal averaging and long path length cells, it should be possible to enhance S/N by a factor of 100 easily (a factor 10, by using a cell of 10 cm path length, another factor of 10, by signal averaging 100 times; 100 runs means an overnight run). A good spectrum for one of the reasonably soluble ($\sim$0.2 mM) proteins (doped with Eu^{3+}) is thus a clear possibility. Simulation of the experimental spectrum with the spectra calculated on the basis of existing theories (we prefer the Mason-Peacock-Stewart theory) for specific structures is another project that we have undertaken. We propose to try

this technique on simulating the experimentally obtained Eu^{3+}(aquo) spectrum to a sum of the theoretical spectrum of $Eu(H_2O)_8^{+3}$ and that of $Eu(H_2O)_9^{+3}$. The relative proportion of the two will be determined. The equilibrium constant so determined will be calculated at each temperature to yield $\triangle H^{\circ}$. In the above, we will make definite assumption about the structure of the two aquo ions, on the basis of crystal structure. In amino acid complexes, the computer programme will generate various structures, calculate spectra for each and find the ''best fit'' structure. In our analysis in Chapter IV, we concluded that there are characteristic changes in band-shape - a preferential shift and enhancement for a specific component peak - on complex formation. The structural interpretation of this observation will be possible only after a detailed simulation of observed spectra with spectra calculated from theory for specific structures.

The important conclusions of lineshape analysis are summarized on p 191-193 and are not repeated here. The conclusions from oscillator strength data are : (i) There exists an equilibrium between more than one aquated species in Eu^{+3}(aquo) ion. The equilibrium is shifted by temperature (ii) The amino acid complexes are mixtures of isomers - a more complicated mixture than that of one endothermic and one exothermic complex (iii) The complexes are asymmetric

so as to give rise to substantial enhancement of oscillator strength (iv) Carboxamide plays a significant role in enhancement of oscillator strength. Exact nature of this aspect and some others can be clarified by more detailed pH dependent study and studies on Eu^{+3} complexes of ''fragments'' - acetate, formamide, glycine (v) Hydrolysed species at pH 6.5 absorb more intensely. Its proportion increases with increase of temperature.

Appendix A

```
C       PROGRAM MINIQUAD OFGANS ET. AL.
C       THIS PROGRAM EVALUATES THE BINDING CONSTANTS OF THE METAL-
C       LIGAND SYSTEMS USING THE NEWTON-GAUSS METHOD
        DIMENSION BABS(20),CI(20),KEY(20),BETA(20),JK(21),JOR(7,21)
        DIMENSION IVAR(20),SIGMA(20),A(7,23),BB(20,20),TITLE(20),LPR(5)
        DIMENSION X(420),S(420),U(420),V(420),W(420),B(23,420),ST(420,2
     1 ),T(7,200),CONC(7,200),STEPS(7,200),CB(20,200),CX(7),TT(7),
     2 HX(7),EPS(7),TOTC(7),ADDC(7),TITRE(7),JEL(4),EZERO(4),EMF(4),
     5 TOLC(5),DT(5),DDT(5,5)
        COMMON JINP,JOUT,AL10,LARS,TOL,TOLU,ACCM,NF,NRUN,TITLE,IFAIL
        OPEN(UNIT=1,FILE='INPUT.DAT')
        OPEN(UNIT=6,DEVICE='DSK',FILE='OUTPUT.DAT')
1       FORMAT(20A4)
2       FORMAT(////'TRIAL 1 - YOUR MODEL NO. ',I3,2X,20A4//)
3       FORMAT(16I5)
4       FORMAT('NO FREE CONCENTRATIONS TO CALCULATE, DATA REDUNDANT')
5       FORMAT(40I2)
6       FORMAT('SORRY, ALL BETAS WERE REJECTED DURING THE ITERATION')
        JINP=1;JOUT=6;TOL=1.E-03;TOLU=1.E-04;ACCM=1.
10      ACCM=ACCM/8.
        IF(ACCM/8.)20,20,10
20      NP=200
        AL10=ALOG(10.);LP=0;MODEL=1
30      READ(JINP,1)TITLE
        WRITE(JOUT,2)MODEL,TITLE
        READ(JINP,3)LARS,NK,N,MAXIT,IPRIN,NMBE,NC,JPR,KPR,(LPR(K),
     1 K=1,5);IF(NC)40,40,50
40      WRITE(JOUT,4);STOP
50      NEMF=NMBE-NC;IFAIL=0
        CALL DINP(NK,N,NMBE,NEMF,NP,NC,BETA,JOR,KEY,BABS,T,CONC,JEL,
     1 EZERO,EMF,TOTC,ADDC,TITRE,CX,TT,CI,HX,TOLC,DT,DDT,LP,MAXIT,
     2 IPRIN)
        IF(IFAIL)60,60,552
60      UU=1;M=0;DO 80 I=1,NK;IF(KEY(I))80,80,70
70      M=M+1;IVAR(M)=I
80      CONTINUE;NM=LP*NC;IF(MAXIT .GT. 0)GO TO 200
        CALL FUNCT (NK,NMBE,NC,LP,JOR,BABS,T,CONC,CX,CI,SS,KEY,CB,
     1 STEPS);GO TO 553
200     J=1;IVAR(M+1)=0;DO 250 I=1,NK;IF(KEY(I))210,250,210
210     IF(I-IVAR(J))240,220,240
220     KEY(I)=1;NMAJ=NM+J
        X(NMAJ)=BETA(I);J=J+1;GO TO 250
240     KEY(I)=-1;CI(I)=0.
250     CONTINUE;NF=0;NRUN=0;IFAIL=0;Q=0.;QC=1.
280     NMN=NM+M;NPNC=M+NC
        CALL MAMIN(NK,M,NMBE,NC,NPNC,NMN,LP,Q,QC,S,U,V,W,X,B,BT,
     1 CONC,T,IVAR,SIGMA,A,BB,BABS,CI,KEY,JOR,CX,TT,HX,EPS,SS,
     2 CB,MAXIT,IPRIN,STEPS);IF(IFAIL)300,400,400
300     M=M-1;IFAIL=0;IF(M)390,390,280
390     WRITE(JOUT,2)MODEL,TITLE
```

```
      WRITE(JOUT,6)GO TO 555
400   IF(SS .GT. UU) GO TO 552,UU=SS,DO 530 I=1,M
      IVENK=IVAR(I),NMAI=NM+I
530   BETA(IVENK)=X(NMAI)
552   CALL DOUT3(NK,M,NMBE,X,JQR,IVAR,SIGMA,SS,KEY,BB,BABS,
     1 MODEL,NM,NMN),K=IFAIL+1,GOTO(553,600,600,600,555,555,555,
     2 555,553),K
553   NK1=NK+1,IF(NMBE .GT. NK1)NK1=NMBE
      CALL STATS(NK,NMBE,LP,JQR,T,CONC,CB,SS,JPR,KPR,LPR,STEPS,
     1 JK,NK1)
555   READ(JINP,5)M,(IVAR(K),K=1,N),IF(N-M)555,560,560
560   IF(M)600,600,570
570   MODEL=MODEL+1,IF(IPRIN .NE. 0)WRITE(JOUT,2)MODEL,TITLE
      GO TO 200
600   STOP
      END
      SUBROUTINE DINP(NK,N,NMBE,NEMF,NP,NC,BETA,JQR,KEY,BABS,T,
     1  CONC,JEL,EZERO,EMF,TOTC,ADDC,TITRE,CX,TT,CI,HX,TOLC,DT,
     2  DDT,IP,MAXIT,IPRIN)
      DIMENSION BABS(NK),BETA(NK),KEY(NK),CI(NK),T(NMBE,NP),
     1  CONC(NMBE,NP),JQR(NMBE,NK),TITLE(20),CX(NMBE),TT(NMBE),
     2  HX(NMBE),TOTC(NMBE),ADDC(NMBE),JEL(NEMF),EZERO(NEMF),
     4  EMF(NEMF),TITRE(NMBE),TOLC(NC),DT(NC),DDT(NC,NC),A(7,4),
     5  V(5),U(5),S(5),D(5),CT(7),B(5,5),VOLM(6)
      COMMON JINP,JOUT,AL10,LARS,TOL,TOLU,ACCM,NF,NRUN,TITLE,
     1  IFAIL
1     FORMAT(2H (,I2,1H),F11.4,'E',I3,I8,7X,7I4)
2     FORMAT(//10X,'FORMATION    REFINEMENT    STOICHIOMETRIC'/
     1          10X,'CONSTANTS       KEYS        COEFFICIENTS  '/)
3     FORMAT(14I5)
4     FORMAT(F10.6,9I5)
5     FORMAT(8F10.7)
6     FORMAT(I5,11F8.3)
7     FORMAT(6E10.3)
9     FORMAT('0    LARS    MAXIT    IPRIN    TOL         TOLU
     1      ACCM'/3I8,3E15.3//'0    THERE ARE ',I3,'EQUILIBRIUM
     2  CONSTANTS',',I3,' OF WHICH ARE TO BE REFINED'//'
     3  THERE ARE',I3,'MASS-BALANCE EQUATIONS AND',I3,'UNKNOWN
     4  FREE CONCENTRATION(S) PER DATA POINT'//6X,'REACTION
     5  TEMPERATURE ',F6.2,' DEGREES CENTIGRADE'//' THE
     6  PROGRAM PROMISES TO TRY ITS BEST TO FIT YOUR DATA!!'//)
10    FORMAT(1HO,I5,' DATA POINTS HAVE BEEN READ IN AND',I5,
     1 'MAXIMUM WERE EXPECTED - REMEMBER,LARGER THE DATA SET
     2  EASIER AND BETTER WILL BE THE FIT!!'//)
9     FORMAT(1HO,'OBVIOUSLY,THE RUN HAD TO BE ABANDONED BEFORE
     1  REFINEMENT')
11    FORMAT('0    THE NUMBER N OF CONSTANTS TO BE REFINED DOES
     1  NOT AGREE WITH THE NUMBER OF NON-ZERO KEYS- PLEASE TAKE
     2  SOME CARE WHILE YOU PREPARE YOUR DATA SET,THANKS'//)
12    FORMAT(/8X,' CURVE ',I3,9E12.4/18X,9E12.4,F10.3)
```

```
      READ(JINP,5)TEMP,WRITE(JOUT,8)LARS,MAXIT,IPRIN,TOL,TOLU,
     1 ACCM,NK,N,NMBE,NC,TEMP,J=0,WRITE(JOUT,2),DO 105 I=1,NK
      READ(JINP,4)BETA(I),L,(JQR(K,I),K=1,NMBE),KEY(I)
      WRITE(JOUT,1)I,BETA(I),L,KEY(I),(JQR(K,I),K=1,NMBE)
      BETA(I)=BETA(I)*EXP(AL10*FLOAT(L)),IF(KEY(I))103,105,103
103   J=J+1
      CI(I)=0.
105   BABS(I)=BETA(I),IF(N-J)106,107,106
106   WRITE(JOUT,11)
      WRITE(JOUT,9)
      STOP
107   IP=0,NTC=1,DO 108 I=1,NC
108   CX(I)=1.E-10
110   READ(JINP,3)(JEL(L),L=1,NEMF)
111   READ(JINP,5)(TOTC(K),K=1,NMBE),(EZERO(L),L=1,NEMF),(ADDC(K),
     1 K=1,NMBE),VINIT
      WRITE(JOUT,12)NTC,(TOTC(K),K=1,NMBE),(EZERO(L),L=1,NEMF),
     1 (ADDC(K),K=1,NMBE),VINIT,NTC=NTC+1,IF(IP .EQ. 0) GOTO 1116
      DO 1113 I=1,NC
1113  CX(I)=CONC(I,ISTAR)
1116  ISTAR=IP+1
112   IS=LARS,IP=IP+1
113   READ(JINP,6)LUIGI,(TITRE(K),K=1,NMBE),(EMF(L),L=1,NEMF)
      IS=IS-1,IF(LUIGI)115,114,115
114   IF(IS)115,115,113
115   WRITE(JOUT,6)IP,(TITRE(K),K=1,NMBE),(EMF(L),L=1,NEMF)
      IF(IP-NP) 1115,1115,140
1115  DO 118 L=1,NEMF,NCPL=NC+L,IF(JEL(L))116,117,116
116   CX(NCPL)=EXP((EMF(L)-EZERO(L))*FLOAT(JEL(L))*11.6049/(TEMP+
     1 273.16))
      GO TO 118
117   CX(NCPL)=EXP(-EMF(L)*AL10)
118   CONTINUE,VOL=VINIT,DO 119K=1,NMBE
119   VOLM(K)=VOL+TITRE(K),DO 120 K=1,NMBE,TT(K)=(TOTC(K)+TITRE(K)
     1 *ADDC(K))/VOLM(K)
120   T(K,IP)=TT(K)
125   CALL MQ(NC,NK,NMBE,UO,KEY,CI,BABS,JQR,CX,TT,HX,A,V,U,S,D,CT,B)
      IF(IFAIL)129,129,300
129   DO 130 K=1,NMBE
130   CONC(K,IP)=CX(K)
140   IF(LUIGI)200,112,111
200   WRITE(JOUT,10)IP,NP,IF(IP-NP)300,300,250
250   WRITE(JOUT,9),STOP
300   RETURN,END
      SUBROUTINE MQ(NC,NK,NMBE,UO,KEY,CI,BABS,JQR,CX,TT,EPS,A,V,U,
     1 S,D,CT,B),DIMENSION KEY(NK),CI(NK),BABS(NK),JQR(NMBE,NK),
     2 CX(NMBE),TT(NMBE),EPS(NMBE),A(NMBE,NC),V(NC),U(NC),S(NC),D(NC),
     3 CT(NMBE),B(NC,NC),TITLE(20),COMMON JINP,JOUT,AL10,LARS,TOL,TOLU
     4 ACCM,NF,NRUN,TITLE,IFAIL,ITS=0,Y=1.,0=0.,QC=1.,NEG=1
5     DO 30 I=1,NK,IF(KEY(I))30,10,10
```

```
10      CI(I)=BABS(I)$DO 20 J=1,NMBE
20      CI(I)=CI(I)*CX(J)**JQR(J,I)
30      CONTINUE
        UO=0.$DO 50 I=1,NMBE$CT(I)=CX(I)$EPS(I)=CX(I)-TT(I)
        DO 40 J=1,NK
40      EPS(I)=EPS(I)+FLOAT(JQR(I,J))*CI(J)
50      UO=UO+EPS(I)*EPS(I)
60      IEXIT=2$DO 90 J=1,NC$DO 80 I=1,NMBE$Z=0.$DO 70 L=1,NK
70      Z=Z+CI(L)*FLOAT(JQR(J,L))*JQR(I,L)
80      A(I,J)=Z
90      A(J,J)=A(J,J)+CX(J)$DO 110 I=1,NC$Z=0.$DO 100 J=1,NMBE
100     Z=Z-A(J,I)*EPS(J)
110     V(I)=Z$DO 140 I=1,NC$DO 130 J=I,NC$Z=0.$DO 120 K=1,NMBE
120     Z=Z+A(K,I)*A(K,J)
130     B(I,J)=Z
140     U(I)=B(I,I)$ITS=ITS+1
150     IF(Q .EQ. 0.) GO TO 170$Q1=Q+1.$DO 160 I=1,NC
160     B(I,I)=U(I)*Q1
170     DO 180 I=1,NC
180     S(I)=V(I)$CALL FACT(B,NC,S,D,1)$IF(IFAIL .EQ. 1)RETURN
        VW=0.$DO 190 I=1,NC$VW=VW+V(I)*S(I)
        IF(ABS(S(I)).GT.TOL) IEXIT=1$IF(IFIX(S(I)) .EQ. -1.)S(I)=-.9999
190     CT(I)=CX(I)*(1.+S(I))$IF(IEXIT .EQ. 2)GO TO 225
        IF(VW .GT. 0.)GO TO 200$IFAIL=2$RETURN
200     DQ=0.$IF(Q .EQ. 0.)GO TO 220$DO 210 I=1,NC
210     DQ=DQ+S(I)*S(I)*U(I)
220     DQ=VW+Q*DQ
225     DO 250 I=1,NK$IF(KEY(I))250,230,230
230     CI(I)=BABS(I)$DO 240 J=1,NMBE
240     CI(I)=CI(I)*CT(J)**JQR(J,I)
250     CONTINUE$UN=0.$DO 270 I=1,NMBE$EPS(I)=CT(I)-TT(I)
        DO 260 J=1,NK
260     EPS(I)=EPS(I)+FLOAT(JQR(I,J))*CI(J)
270     UN=UN+EPS(I)*EPS(I)$IF(IEXIT .EQ. 2)GO TO 410$DU=UO-UN
        IF(DQ .GE. 0.)GO TO 280$IFAIL=2$RETURN
280     IF(ITS .LT. 100)GO TO 290$IFAIL=3$RETURN
290     IF(DU .GE. 0.25*DQ)GO TO 370$Z=2.*VW-DU$Y=0.5
        IF(Z .GT. 0.)Y=VW/Z$IF(Y .GT. 0.5)Y=0.5$IF(Y .LT. .1)Y=0.1
        IF(Q .NE. 0.)GO TO 360
        IF(NC .EQ. 1)GO TO 330$NM1=NC-1$DO 320 I=1,NM1$IP1=I+1
        DO 320 J=IP1,NC$W=-B(J,I)$IF(J .EQ. IP1)GO TO 320$JM1=J-1
        DO 310 K=IP1,JM1
310     W=W-B(J,K)*B(K,I)
320     B(J,I)=W
330     TR=0.$DO 350 I=1,NC$W=1./D(I)$IF(I .EQ. NC)GO TO 350
        IP1=I+1$DO 340 K=IP1,NC
340     W=W+B(K,I)*B(K,I)/D(K)
350     TR=TR+W*U(I)$Y=2.*Y$Q=1./TR$QC=Q
360     Q=Q/Y$IF(DU)150,150,380
370     IF(DU .LE. 0.75*DQ)GO TO 380$Q=Q*0.5$IF(Q .LT. QC/4.)Q=0.
```

```
330     FR=1.;DO 390 K=1,NC;W=CX(K)*(1.+FR*S(K))
        IF(W .GT. 0.)GO TO 390;FR=-0.9/S(K)
390     CONTINUE;IF(FR .EQ. 1.)GO TO 410;DO 400 K=1,NC
400     CX(K)=CX(K)*(1.+FR*S(K));NEG=NEG+1;IF(NEG .GT. 4)RETURN
        GO TO 5
410     UO=UN;DO 420 K=1,NC
420     CX(K)=CT(K);GO TO (60,430),IEXIT
430     RETURN;END
        SUBROUTINE FACT(B,N,S,D,JFAIL);DIMENSION B(N,N),S(N),D(N),
        1TITLE(20);COMMON JINP,JOUT,AL10,LARS,TOL,TOLU,ACCM,NF,NRUN,
        2TITLE,IFAIL;D(1)=B(1,1);IF(D(1))30,30,10
10      IF(N-1)40,20,40
20      S(1)=S(1)/D(1);RETURN
30      IFAIL=JFAIL;RETURN
40      DO 50 K=2,N
50      B(K,1)=B(1,K)/D(1);DO 100 I=2,N;D(I)=B(I,I);IM1=I-1
        DO 60 K=1,IM1
60      D(I)=D(I)-B(I,K)*B(I,K)*D(K);IF(D(I))30,30,80
80      IP1=I+1;IF(IP1 .GT. N)GO TO 100;DO 90 J=IP1,N;Z=B(I,J)
        DO 85 K=1,IM1
85      Z=Z-B(I,K)*B(J,K)*D(K)
90      B(J,I)=Z/D(I)
100     CONTINUE;DO 110 J=2,N;JM1=J-1;DO 110 K=1,JM1
110     S(J)=S(J)-B(J,K)*S(K);S(N)=S(N)/D(N);J=N-1
120     JP1=J+1;S(J)=S(J)/D(J);DO 130 K=JP1,N
130     S(J)=S(J)-B(K,J)*S(K);J=J-1;IF(J .GE. 1)GO TO 120;RETURN;END
        SUBROUTINE FUNCT(NK,NMBE,NC,LP,JQR,BABS,T,CONC,CX,CI,U,KEY,
        1CB,STEPS);DIMENSION JQR(NMBE,NK),TITLE(20),BABS(NK),CI(NK),
        2KEY(NK),T(NMBE,LP),CONC(NMBE,LP),CB(NK,LP),STEPS(NMBE,LP),
        3CX(NMBE);COMMON JINP,JOUT,AL10,LARS,TOL,TOLU,ACCM,NF,
        1NRUN,TITLE,IFAIL;U=0.;NF=NF+1;DO 300 IP=1,LP;DO 140 I=1,NMBE
140     CX(I)=CONC(I,IP);DO 152 I=1,NK;IF(KEY(I))152,146,146
146     W=BABS(I);DO 149 J=1,NMBE
149     W=W*CX(J)**JQR(J,I);CI(I)=W
152     CB(I,IP)=CI(I);DO 170 I=1,NMBE;EPS=CX(I)-T(I,IP);DO168 J=1,NK
168     EPS=EPS+FLOAT(JQR(I,J))*CI(J);STEPS(I,IP)=EPS
170     U=U+EPS*EPS
300     CONTINUE;RETURN;END
        SUBROUTINE NEG(NK,N,NMN,NM,X,W,KEY,IVAR,CI);DIMENSION X(NMN),
        1W(NMN),KEY(NK),IVAR(N),CI(NK),TITLE(20);COMMON JINP,JOUT,AL10,
        2LARS,TOL,TOLU,ACCM,NF,NRUN,TITLE,IFAIL;T=1.;J=0;DO 10 I=1,N
        L=NM+I;XT=X(L)+T*W(L)*X(L);IF(XT .GT. 0.)GOTO 10
        T=-1./W(L);J=I
10      CONTINUE
        IF (J .EQ. 0)RETURN;IV=IVAR(J);KEY(IV)=-NRUN*2;CI(IV)=0.
        IFAIL=-1;IF(J .EQ. 1)GO TO 20;J1=J-1;DO 15 I=1,J1;L=NM+I
15      X(L)=X(L)+T*W(L)*X(L)
20      N1=N-1;IF(J .EQ. N)RETURN;DO 30 I=J,N1;L=NM+I;LP=L+1
        IVAR(I)=IVAR(I+1)
30      X(L)=X(LP)+T*W(LP)*X(LP);RETURN;END
```

```
      SUBROUTINE STATS(NK,NMBE,LP,JQR,T,CONC,CB,U,JPR,KPR,LPR,STEPS,
     1JK,NK1)$INTEGER PLUS,BLANK,SYM,PT$DIMENSION JQR(NMBE,NK),
     2T(NMBE,LP),CONC(NMBE,LP),CB(NK,LP),LPR(5),JPOP(8),CLIM(8),
     3SYM(40),PT(116),TITLE(20),STEPS(NMBE,LP),JK(NK1)
      COMMON JINP,JOUT,AL10,LARS,TOL,TOLU,ACCM,NF,NRUN,TITLE,IFAIL
      DATA PLUS,BLANK,SYM/1H+,1H ,1HA,1HB,1HC,1HD,1HE,1HF,1HG,1HH,
     11HI,1HJ,1HK,1HL,1HM,1HN,1HO,1HP,1HQ,1HR,1HS,1HT,1HU,1HV,1HW,1H
     2,1HY,1HZ,1H1,1H2,1H3,1H4,1H5,1H6,1H7,1H8,1H9,1H+,1H-,1H.,1H*,
     31H=/
2     FORMAT(/I4,1P11E10.2,(/5X,11E10.2))
10    FORMAT(' ARITHMETIC MEAN ',1PE12.4,' MEAN DEVIATION ',E12.4,
     1  ' STANDARD DEVIATION ',E12.4//' VARIANCE ',E12.4,' MOMENT
     2COEFFICIENT OF SKEWNESS ',0PF10.2,'MOMENT COEFFICIENT OF KURTO
     3IS',F10.2)
19    FORMAT(/' OBSERVED CHI-SQUARE IS: ',F10.2,' R FACTOR= ',F12.6)
20    FORMAT(//' MASS BALANCE EQUATION ',I2)
21    FORMAT(I4,116A1)
22    FORMAT(//' PLOTS OF FORMATION PERCENTAGES '/)
24    FORMAT(/' RESIDUALS PLOT '/'   -3 SD',14X,'-2 SD',14X,'-1 SD',
     116X,'0',17X,'1 SD',15X,'2 SD',13X,'3 SD'/)
25    FORMAT(/5X,'0',49X,'50',48X,'100'/5X,A1,10(9X,A1)/1X,119A1)
      NR=8$NTOT=LP*NMBE$W=FLOAT(NTOT)$SD=SQRT(U/W)$CLIM(1)=-1.150*SD
      CLIM(2)=-0.675*SD$CLIM(3)=-0.319*SD$CLIM(4)=0.$CLIM(5)=0.319*SD
      CLIM(6)=0.675*SD$CLIM(7)=1.150*SD$CLIM(8)=SD/ACCM$DO 108 I=1,NR
108   JPOP(I)=0$AM=0.$DM=0.$VAR=0.$COSQ=0.$COKU=0.$RDEN=0.
      IF (JPR .EQ. 1) WRITE(JOUT,24)$DO 110 I=1,NK1
110   JK(I)=1$DO 114 J=1,116
114   PT(J)=BLANK$DO 200 IP=1,LP$DO 115 I=1,NMBE$JDINE=JK(I)
115   PT(JDINE)=BLANK$DO 116 J=2,116,19
116   PT(J)=PLUS$DO 130 I=1,NMBE$TT=T(I,IP)$EPS=STEPS(I,IP)
      DO 119 K=1,NR$IF(EPS-CLIM(K))118,118,119
118   JPOP(K)=JPOP(K)+1$GO TO 120
119   CONTINUE$JPOP(NR)=JPOP(NR)+1
120   AM=AM+EPS$RDEN=RDEN+TT*TT$DM=DM+ABS(EPS)$EPSS=EPS*EPS
                VAR=VAR+EPSS$COSQ=COSQ+EPS*EPSS$COKU=COKU+EPSS*EPSS
      J=IFIX(EPS/SD*19.+59.5)$IF(J .LT. 2)J=2$IF(J .GT. 116)J=116
      JK(I)=J
130   PT(J)=SYM(I)
200   IF(JPR .EQ. 1)WRITE (JOUT,21)IP,PT$AM=AM/FLOAT(NTOT)
      DM=DM/FLOAT(NTOT)
      VAR=VAR/W$COSQ=COSQ/(FLOAT(NTOT)  *VAR*SD)
      COKU=COKU/(FLOAT(NTOT)*VAR*VAR)
      WRITE(JOUT,10)AM,DM,SD,VAR,COSQ,COKU$OBSCH=0.$R1=-CLIM(NR)
      DO 350 K=1,NR$EXPOP=W/8.$OBFR=FLOAT(JPOP(K))/W
      RAPP=((FLOAT(JPOP(K))-EXPOP)**2)/EXPOP$R1=CLIM(K)
350   OBSCH=OBSCH+RAPP$RFACT=SQRT(U/RDEN)$WRITE(JOUT,19)OBSCH,RFACT
      IF(KPR .EQ. 0)GO TO 395$DO 380 IP=1,LP
380   WRITE(JOUT,2)IP,(T(J,IP),J=1,NMBE),(CONC(J,IP),J=1,NMBE),
      1(CB(J,IP),J=1,NK)
395   L=0$DO 400 I=1,5
```

```
400       L=L+LPR(I)$IF(L .GE. 1)WRITE(JOUT,22)$DO 410 I=1,116
410       PT(I)=BLANK$DO 480 I=1,NMBE$IF(LPR(I) .EQ. 0)GO TO 480
          WRITE(JOUT,20)I$WRITE(JOUT,25)(PLUS,K=1,130)$DO 470 IP=1,LP
          TS=T(I,IP)$DO 430 K=1,NK1$JVASU=JK(K)
430       PT(JVASU)=BLANK
          PT(2)=PLUS$PT(102)=PLUS$DO 460 J=1,NK
          K=IFIX(CB(J,IP)*FLOAT(JQR(I,J))*100./TS+2.5)$IF(K .LT. 2)K=2
          IF(K .GT. 116)K=116$JK(J)=K
460       PT(K)=SYM(J)$K=IFIX(CONC(I,IP)*100./TS+2.5
          1)$JK(NK1)=K$PT(K)=SYM(NK1)
470       WRITE(JOUT,21)IP,PT
480       CONTINUE$RETURN$END
          SUBROUTINE CALC(NK,N,NMBE,NC,IP,JQR,CONC,IVAR,A,EPS,CB,CI,NPNC,
          1LP,NN,NM,NMN,V,STEPS)$DIMENSION TITLE(20),JQR(NMBE,NK),
          2A(NMBE,NPNC),
          3EPS(NMBE),CONC(NMBE,LP),CB(NK,LP),CI(NK),IVAR(N),V(NMN),
          3STEPS(NMBE,LP)$COMMON JINP,JOUT,AL10,LARS,TOL,TOLU,ACCM,
          4NF,NRUN,TITLE,IFAIL
          DO 10 J=1,NK
10        CI(J)=CB(J,IP)$DO 30 I=1,NMBE
30        EPS(I)=STEPS(I,IP)$DO 60 J=1,NC$DO 50 I=1,NMBE$Z=0.
          DO 40 L=1,NK
40        Z=Z+CI(L)*FLOAT(JQR(J,L)*JQR(I,L))
50        A(I,J)=Z
60        A(J,J)=A(J,J)+CONC(J,IP)$DO 70 J=1,N$JPNC=J+NC$IV=IVAR(J)
          DO 70 I=1,NMBE
70        A(I,JPNC)=CI(IV)*FLOAT(JQR(I,IV))$DO 85 I=1,NC$Z=0.
          DO 80 J=1,NMBE
80        Z=Z-A(J,I)*EPS(J)$NNAI=NN+I
85        V(NNAI)=Z
          DO90I =1,N$IPNC=I+NC$IPNM=I+NM
          DO90J =1,NMBE
90        V(IPNM)=V(IPNM)-A(J,IPNC)*EPS(J)$RETURN$END
          SUBROUTINECHOLS(N,NC,NM,NMN,NPNC,LP,B,BT,S,IEXIT,NK,NMBE,X,
          1W,IVAR,BABS,C)
          DIMENSION B(NPNC,NMN),BT(NMN,NPNC),S(NMN),TITLE(20),X(NMN),
          1W(NMN),IVAR(N),BABS(NK),C(NMBE,LP)
          COMMON JINP,JOUT,AL10,LARS,TOL,TOLU,ACCM,NF,NRUN,TITLE,IFAIL
          NN=0$DO150IP=1,LP$DO145I=1,NC$I1=I-1$L=NN+I$DO140J=I,NPNC
          ST=B(J,L)$IF(I1.EQ.0)GOTO 120$DO110K=1,I1$KANN=K+NN
110       ST=ST-BT(KANN,J)*BT(KANN,I)
120       XT=ST$IF(J.NE.I)GOTO135$IF(XT.GT.0.)GOTO130
          IFAIL=4$RETURN
130       BT(L,I)=1./SQRT(XT)$GOTO 140
135       BT(L,J)=XT*BT(L,I)
140       CONTINUE
145       CONTINUE
150       NN=NN+NC$DO200I=1,N$I1=I-1+NM$IL=I+NC$L=NM+I
          DO 200 J=I,N$JL=J+NC$ST=B(JL,L)$DO 160 K=1,I1
160       ST=ST-BT(K,JL)*BT(K,IL)
```

```
400     L=L+LPR(I)$IF(L .GE. 1)WRITE(JOUT,22)$DO 410 I=1,116
410     PT(I)=BLANK$DO 480 I=1,NMBE$IF(LPR(I) .EQ. 0)GO TO 480
        WRITE(JOUT,20)I$WRITE(JOUT,25)(PLUS,K=1,130)$DO 470 IP=1,LP
        TS=T(I,IP)$DO 430 K=1,NK1$JVASU=JK(K)
430     PT(JVASU)=BLANK
        PT(2)=PLUS$PT(102)=PLUS$DO 460 J=1,NK
        K=IFIX(CB(J,IP)*FLOAT(JQR(I,J))*100./TS+2.5)$IF(K .LT. 2)K=2
        IF(K .GT. 116)K=116$JK(J)=K
460     PT(K)=SYM(J)$K=IFIX(CONC(I,IP)*100./TS+2.5
        1)$JK(NK1)=K$PT(K)=SYM(NK1)
470     WRITE(JOUT,21)IP,PT
480     CONTINUE$RETURN$END
        SUBROUTINE CALC(NK,N,NMBE,NC,IP,JQR,CONC,IVAR,A,EPS,CB,CI,NPNC,
        1LP,NN,NM,NMN,V,STEPS)$DIMENSION TITLE(20),JQR(NMBE,NK),
        2A(NMBE,NPNC),
        3EPS(NMBE),CONC(NMBE,LP),CB(NK,LP),CI(NK),IVAR(N),V(NMN),
        3STEPS(NMBE,LP)$COMMON JINP,JOUT,AL10,LARS,TOL,TOLU,ACCM,
        4NF,NRUN,TITLE,IFAIL
        DO 10 J=1,NK
10      CI(J)=CB(J,IP)$DO 30 I=1,NMBE
30      EPS(I)=STEPS(I,IP)$DO 60 J=1,NC$DO 50 I=1,NMBE$Z=0.
        DO 40 L=1,NK
40      Z=Z+CI(L)*FLOAT(JQR(J,L)*JQR(I,L))
50      A(I,J)=Z
60      A(J,J)=A(J,J)+CONC(J,IP)$DO 70 J=1,N$JPNC=J+NC$IV=IVAR(J)
        DO 70 I=1,NMBE
70      A(I,JPNC)=CI(IV)*FLOAT(JQR(I,IV))$DO 85 I=1,NC$Z=0.
        DO 80 J=1,NMBE
80      Z=Z-A(J,I)*EPS(J)$NNAI=NN+I
85      V(NNAI)=Z
        DO90I =1,N$IPNC=I+NC$IPNM=I+NM
        DO90J =1,NMBE
90      V(IPNM)=V(IPNM)-A(J,IPNC)*EPS(J)$RETURN$END
        SUBROUTINECHOLS(N,NC,NM,NMN,NPNC,LP,B,BT,S,IEXIT,NK,NMBE,X,
        1W,IVAR,BABS,C)
        DIMENSION B(NPNC,NMN),BT(NMN,NPNC),S(NMN),TITLE(20),X(NMN),
        1W(NMN),IVAR(N),BABS(NK),C(NMBE,LP)
        COMMON JINP,JOUT,AL10,LARS,TOL,TOLU,ACCM,NF,NRUN,TITLE,IFAIL
        NN=0$DO150IP=1,LP$DO145I=1,NC$I1=I-1$L=NN+I$DO140J=I,NPNC
        ST=B(J,L)$IF(I1.EQ.0)GOTO 120$DO110K=1,I1$KANN=K+NN
110     ST=ST-BT(KANN,J)*BT(KANN,I)
120     XT=ST$IF(J.NE.I)GOTO135$IF(XT.GT.0.)GOTO130
        IFAIL=4$RETURN
130     BT(L,I)=1./SQRT(XT)$GOTO 140
135     BT(L,J)=XT*BT(L,I)
140     CONTINUE
145     CONTINUE
150     NN=NN+NC$DO200I=1,N$I1=I-1+NM$IL=I+NC$L=NM+I
        DO 200 J=I,N$JL=J+NC$ST=B(JL,L)$DO 160 K=1,I1
160     ST=ST-BT(K,JL)*BT(K,IL)
```

```
      XT=ST$IF(J.NE.I)GO TO 190
      IF(XT.GT.0)GO TO 180$IFAIL=5$RETURN
180   BT(L,IL)=1./SQRT(XT)$GO TO 200
190   BT(L,JL)=XT*BT(L,IL)
200   CONTINUE
      NN=0$DO 230 IP=1,LP$L=NN+1$S(L)=S(L)*BT(L,1)
      IF(NC .EQ. 1)GO TO 230$DO 220 I=2,NC$L=NN+I$I1=I-1
      ST=S(L)$DO 210K=1,I1$KL=NN+K
210   ST=ST-BT(KL,I)*S(KL)
220   S(L)=ST*BT(L,I)
230   NN=NN+NC
      DO250I=1,N$L=NM+I$I1=L-1$IPNC=I+NC$ST=S(L)
      DO 240K=1,I1
240   ST=ST-BT(K,IPNC)*S(K)
250   S(L)=ST*BT(L,IPNC)
      DO270II=1,N$I=N-II+1$L=NM+I$I1=I+1
      IPNC=I+NC$ST=S(L)$IF(I.EQ.N)GO TO265$DO260K=I1,N
      KANC=K+NC$KANM=K+NM
260   ST=ST-BT(L,KANC)*W(KANM)
265   ST=ST*BT(L,IPNC)$W(L)=ST$S(L)=X(L)+ST*X(L)$ITANK=IVAR(I)
      BABS(ITANK)=S(L)
270   IF(ABS(ST).GE.TOL) IEXIT=1
275   NN=NM$DO300IP=1,LP$DO295I=1,NC
      II=NC-I+1$
      L=NN-I+1$ST=S(L)$DO280J=1,N$JANC=J+NC$JANM=J+NM
280   ST=ST-BT(L,JANC)*W(JANM)$IF(I.EQ.1)GO TO 290
      I1=II+1$KL=L$DO285K=I1,NC$KL=KL+1
285   ST=ST-BT(L,K)*W(KL)
290   ST=ST*BT(L,II)$W(L)=ST$S(L)=X(L)+ST*X(L)
      KP=LP-IP+1$C(II,KP)=S(L)
295   IF(ABS(ST).GE.TOL)IEXIT=1
300   NN=NN-NC$RETURN$END
      SUBROUTINE DOUT3(M,N,NMBE,X,JQR,IVAR,SD,U,KEY,COCO,BABS,
     1MODEL,NM,NMN)$INTEGER SYM$DIMENSION IVAR(N),SD(N),COCO(N,N),
     2X(NMN),SYM(40),
     3KEY(M),BABS(M),JQR(NMBE,M),TITLE(20)$COMMON JINP,JOUT,AL10,LAR
     4,TOL,TOLU,ACCM,NF,NRUN,TITLE,IFAIL$DATA SYM/1HA,1HB,1HC,1HD,1H
     5,1HF,1HG,1HH,1HI,1HJ,1HK,1HL,1HM,1HN,1HO,1HP,1HQ,1HR,1HS,1HT,
     61HU,1HV,1HW,1HX,1HY,1HZ,1H1,1H2,1H3,1H4,1H5,1H6,1H7,1H8,1H9,1H
     7,1H-,1H.,1H*,1H=/
100   FORMAT('1'///' THIS MODEL IS ACCORDING TO YOUR TRIAL NO$ ',I3,
     14X,20A4/)
101   FORMAT('THE DATA FAILED TO FIT ACCORDING TO THIS MODEL - NEVER
     1MIND, TRY A DIFFERENT MODEL OR A DIFFERENT SET OF GUESS VALUES
     2 FAIL CODE IS$ ',I2)
107   FORMAT(' REFINEMENT CONVERGED SUCESSFULLY-CONGRATULATIONS!
     1DONOT BE TOO THRILLED,TRY DIFFERENT GUESS VALUES AND CHECK
     2THE CONSISTENCY')
108   FORMAT('+',35X,I4,' ITERATIONS',I4,' FUNCTION CALLS',
     1' SUM OF SQUARES = ',1PE17.9/   32X,'    VALUE    STD. DEVIATI
```

```
      2 LOG BETA     STD. DEVIATION'/46X,'(REL. PERCENT)')
109   FORMAT(7H BETA (,A1,3H)  ,7I2)
110   FORMAT('+',23X,'SORRY,I TRIED MY BEST,BUT THIS BETA WAS REJECT
      1 IN   CYCLE',I4)
113   FORMAT('+',23X,' CONSTANT',1PE13.5,10X,0PF12.5)
114   FORMAT('+',23X,' REFINED ',1PE14.5,0PF10.2,2F12.5)
115   FORMAT(1HO,'MATRIX OF CORRELATION COEFFICIENTS RHO I,J'//4H
      1),WRITE (JOUT,100) MODEL, TITLE,IF (IFAIL) 7,6,7
116   FORMAT(I4,11F10.3/5X,11F10.3)
117   FORMAT(6HO  J  ,I5,10I10/5X,10110/)
7     WRITE (JOUT,101) IFAIL,GO TO(16,16,16,9,9,9,9,9),IFAIL
8     WRITE(JOUT,107)
9     WRITE(JOUT,108) NRUN,NF,U,K=1,DO 13 I=1,M
      IF(KEY(I).EQ. (-1))GO TO 13,WRITE(JOUT,109)SYM(I),(JQR(J,I),J=
      1NMBE),J=KEY(I)+3,IF(KEY(I) .LT. (-2))J=1,GOTO(10,13,11,12),J
10    J=-KEY(I)/2),WRITE(JOUT,110)J,GO TO 13
11    XD=ALOG(BABS(I))/AL10
      WRITE(JOUT,113) BABS(I),XD,GO TO 13
12    KANM=K+NM,XL=ALOG(X(KANM))/AL10,SDL=SD(K)/100./AL10
      WRITE(JOUT,114) X(KANM),SD(K),XL,SDL,K=K+1
13    CONTINUE,IF(N .EQ. 1)RETURN
130   WRITE(JOUT,115),DO 15 I=2,N,IM=I-1
15    WRITE (JOUT,116) IVAR(I),(COCO(I,J),J=1,IM)
      WRITE(JOUT,117) (IVAR(J),J=1,IM)
16    RETURN,END
      SUBROUTINE MAMIN(NK,N,NMBE,NC,NPNC,NMN,LP,Q,GC,S,U,V,W,X,B,ST,
      1T,IVAR,SIGMA,A,BB,BABS,CI,KEY,JQR,CX,TT,HX,EPS,SS,CD,MAXIT,IP
      2N,STEPS),DIMENSION A(NMBE,NPNC),BB(N,N),B(NPNC,NMN),C(NMBE,LP
      3T(NMBE,LP),CB(NK,LP),BT(NMN,NPNC),TITLE(20),BABS(NK),CI(NK),
      4KEY(NK),STEPS(NMBE,LP),SIGMA(N),X(NMN),S(NMN),U(NMN),V(NMN),
      5W(NMN),IVAR(N),CX(NMBE),TT(NMBE),HX(NMBE),EPS(NMBE),JQR(NMBE,
      COMMON JINP,JOUT,AL10,LARS,TOL,TOLU,ACCM,NF,NRUN,TITLE,IFAIL
      NC1=NC+1,NM=LP*NC,NM1=NM+1,Y=1.
1     K=0,DO 2 IP=1,LP,DO 2 I=1,NC,K=K+1
2     X(K)=C(I,IP),DO 3 I=1,N,K=K+1,IVENK=IVAR(I)
3     BABS(IVENK)=X(K),CALL FUNCT(NK,NMBE,NC,LP,JQR,BABS,T,C,CX,CI,
      1SS,KEY,CB,STEPS),NF=NF-1
5     IEXIT=2,DO 10 J=NM1,NMN,V(J)=0.,DO 10 I=NC1,NPNC
10    B(I,J)=0.,NN=0,DO 30 IP=1,LP,IQP=IP
      CALL CALC(NK,N,NMBE,NC,IQP,JQR,C,IVA
      1R,A,EPS,CB,CI,NPNC,LP,NN,NM,NMN,V,STEPS),DO 20 I=1,NC,L=NN+I
      DO 19 J=I,NPNC,Z=0.,DO 18 K=1,NMBE
18    Z=Z+A(K,I)*A(K,J)
19    B(J,L)=Z
20    U(L)=B(I,L),DO 25 I=1,N,L=NM+I,IPNC=I+NC,DO 25 J=IPNC,NPNC,Z=0
      DO 23 K=1,NMBE
23    Z=Z+A(K,IPNC)*A(K,J)
25    B(J,L)=B(J,L)+Z
30    NN=NN+NC,DO 40 I=NC1,NPNC,L=I-NC+NM
40    U(L)=B(I,L)
```

```
60      NRUN=NRUN+1;ITYPE=1;DO 70 K=1,100,5
70      IF(NRUN .EQ. K)ITYPE=2;IF(ITYPE .EQ. 2)Q=0.
90      IF(Q .EQ. 0.)GO TO 110;Q1=Q+1.;L=0;DO 95 IP=1,LP
        DO 95 I=1,NC;L=L+1
95      B(I,L)=U(L)*Q1;DO 100 I=1,N;L=NM+I;IANC=I+NC
100     B(IANC,L)=U(L)*Q1
110     DO 120 L=1,NMN
120     S(L)=V(L);CALL CHOLS(N,NC,NM,NMN,NPNC,LP,B,BT,S,IEXIT,NK,NMBE,
        1X,W,IVAR,BABS,C);IF(IFAIL .NE. 0)RETURN;IF(ITYPE .EQ. 2)GO TO
        2600;VW=0.;DO 330 I=1,NMN
330     VW=VW+V(I)*W(I);IF(VW .GT. 0.)GO TO 335;IFAIL=6;GO TO 405
335     DQ=0.;IF(Q .EQ. 0.)GO TO 345;DO 340 I=1,NMN
340     DQ=DQ+W(I)*W(I)*U(I)
345     DQ=VW+Q*DQ;CALL FUNCT(NK,NMBE,NC,LP,JQR,BABS,T,C,CX,CI,SSP,
        1KEY,CB,STEPS);DS=SS-SSP;IF(DS/SS .GT. TOLU)IEXIT=1
        IF(IEXIT .EQ. 2)GO TO 405;IF(DQ .GE. 0.)GO TO 390;IFAIL=7
        GO TO 405
390     IF(NRUN .LT. MAXIT)GO TO 400;IFAIL=8;GO TO 405
400     IF(DS .GE. 0.25*DQ)GO TO 590;Y=0.5;Z=2.*VW-DS
        IF(Z .GT. 0.)Y=VW/Z;IF(Y .GT. 0.5)Y=0.5;IF(Y .LT. 0.1)Y=0.1
        IF(Q .NE. 0.)GO TO 580
405     CALL INVER(N,NC,NM,NMN,NPNC,LP,BT,U,TR)
        Z=SQRT(SSP/FLOAT((NMBE-NC)*LP-N))*100.;DO 560 I=1,N
        IANM=I+NM;IFNC=I+NC;A(1,I)=SQRT(BT(IANM,IFNC))
560     SIGMA(I)=A(1,I)*Z;DO 570 I=1,N;IPNC=I+NC;DO 570 J=1,I;JANM=J+N
570     BB(I,J)=BT(JANM,IPNC)/A(1,I)/A(1,J);IF(IEXIT .EQ. 2)GO TO 600
        Y=2.*Y;Q=1./TR;QC=Q
580     Q=Q/Y;IF(DS)90,90,600
590     IF(DS .LE. 0.75*DQ)GO TO 600;Q=Q*0.5;IF(Q .LT. QC/4)Q=0.
600     IF(IPRIN .EQ. 0)GO TO 605
601     FORMAT('0CYCLE',2I4,'FUNCTION CALCULATED, U=',1PE17.9/
        1 'MARQUART PARAMETER',E17.9/22X,'   VALUE      REL.SHIFT')
602     FORMAT('                BETA (',I2,')',1P2E13.5)
        WRITE(JOUT,601)NRUN,NF,SS,Q;DO 603 I=1,N;L=NM+I
603     WRITE(JOUT,602)IVAR(I),X(L),W(L)
605     IF(ITYPE .EQ. 2)GO TO 700;J=1;NN=0;DO 608 IP=1,LP;FR=1.
        DO 606 K=1,NC;NNAK=NN+K
        IF(S(NNAK) .GT. 0.)GO TO 606;FR=-0.99/W(NNAK);J=2
606     CONTINUE;IF(FR .EQ. 1.)GO TO 608;DO 607 K=1,NC;L=NN+K
607     X(L)=X(L)*(1.+FR*W(L))
608     NN=NN+NC
609     CALL NEG(NK,N,NMN,NM,X,W,KEY,IVAR,CI);SS=SSP
        IF(IEXIT .EQ. 2 .OR. IFAIL .NE. 0)GO TO 620;GO TO (610,1),J
610     DO 615 I=1,NMN
615     X(I)=S(I);GO TO 5
620     K=0;DO 630 IP=1,LP;DO 630 I=1,NC;K=K+1
630     C(I,IP)=X(K);RETURN
700     SSP=0.;FR=1.;DO 703 K=1,N;L=NM+K;XT=X(L)+FR*W(L)*X(L)
        IF(XT .GT. 0.)GO TO 703;FR=-0.99/W(L)
703     CONTINUE;IF(FR .EQ. 1.)GO TO 709;DO 706 K=1,N;L=NM+K
```

```
      W(L)=FR*W(L)$ITANK=IVAR(K)
706   BABS(ITANK)=X(L)+W(L)*X(L)
709   J=0$DO 740 IP=1,LP$DO 710 K=1,NMBE$TT(K)=T(K,IP)
710   CX(K)=C(K,IP)$DO 715 K=1,NC$KAJ=K+J
715   CX(K)=X(KAJ)$CALL MQ (NC,NK,NMBE,SQ,KEY,CI,BABS,JQR,CX,TT,EPS
      1A,V,U,S,B,HX,ET)$IF(IFAIL .NE. 0)RETURN$SSP=SSP+SQ
      DO 720 K=1,NC$J=J+1
720   X(J)=CX(K)$DO 730 K=1,NMBE$C(K,IP)=CX(K)
730   STEPS(K,IP)=EPS(K)$DO 740 K=1,NK
740   CB(K,IP)=CI(K)$IF(SSP .LT. SS)GO TO 790$DO 750 K=1,N
      L=NM+K$W(L)=W(L)*0.5$IV=IVAR(K)
750   BABS(IV)=BABS(IV)-W(L)*X(L)$GO TO 700
790   DO 800 K=1,N$NMAK=NM+K$IAK=IVAR(K)
800   X(NMAK)=BABS(IAK)$SS=SSP$GO TO 5$END
      SUBROUTINE INVER(N,NC,NM,NMN,NPNC,LP,BT,D,TR)$DIMENSION BT(NM
      1NPNC),D(NMN)$NN=0$DO 450 IP=1,LP$DO 445 I=1,NC$IL=I+NN
      IF(I .EQ. NC)GO TO 420$I1=I+1$DO 415 J=I1,NC$J1=J-1$JL=J+NN
      Z=0.$DO 410 K=I,J1$KANN=K+NN
410   Z=Z-BT(KANN,J)*BT(IL,K)
415   BT(IL,J)=Z*BT(JL,J)
420   DO 440 J=1,N$JPNC=J+NC$Z=0.$DO 425 K=I,NC
425   Z=Z-BT(KANN,JPNC)*BT(IL,K)$IF(J .EQ. 1)GO TO 435$J1=J-1
      DO 430 K=1,J1$KANM=K+NM$KANC=K+NC
430   Z=Z-BT(KANM,JPNC)*BT(IL,KANC)
435   L=NM+J
440   BT(IL,JPNC)=Z*BT(L,JPNC)
445   CONTINUE
450   NN=NN+NC$IF(N .EQ. 1)GO TO 500$N1=N-1$DO 470 I=1,N1$IL=I+NM
      I1=I+1$DO 470 J=I1,N$J1=J-1$JL=J+NM$JPNC=J+NC$Z=0.$DO460K=I,J1
460   Z=Z-BT(KANM,JPNC)*BT(IL,KANC)
470   BT(IL,JPNC)=Z*BT(JL,JPNC)
500   NN=0$TR=0.$DO 530 IP=1,LP$DO 520 I=1,NC$IL=NN+I$Z=0.
      DO 510 K=I,NPNC
510   Z=Z+BT(IL,K)*BT(IL,K)
520   TR=TR+Z*D(IL)
530   NN=NN+NC$DO 550 I=1,N$IL=NM+I$DO 550 J=1,N$JL=NM+J$JPNC=J+NC
      Z=0.$DO 540 K=JPNC,NPNC
540   Z=Z+BT(IL,K)*BT(JL,K)$IF(J .EQ. I) TR=TR+Z*D(IL)
550   BT(IL,JPNC)=Z$RETURN$END
```

Instruction for feeding input data :

Card 1 : Title of system (e.g. Eu^{3+}-Aspartic acid pH 5.0)

Card 2 : Gives the following constants

LARS NK N MAXIT IPRIN NMBE NC JPR KPR

where LARS = 1; IPRIN = 1; MAXIT = 99; JPR = 1; KPR = 1

e.g. in Metal-Ligand titration with a model that includes β_1, β_2, β_3 NK = 5, as shown below:

NK is total number of formation constant

(1) M + L ML (1:1)

(2) M + 2L ML_2 (1:2)

(3) M + 3L ML_3 (1:3)

(4) M + Mu MMu (1:1)

(5) M + B MB (1:1)

(M = Metal, L = Ligand, Mu = Murexide, B = Buffer)

N = Number of formation constants to be determined e.g. K of the first 3 equations given above are unknown, therefore N = 3.

NMBE : Total number of mass balance equation; NMBE = 4 in the above system

(No. of Mass Balance Equation = Total No.of Reactants(L,B,M,Mu)

NC : No. of unknown free concentration (L_f and B_f in the above system)

Card 3 : Reaction Temperature in degree centrigrade.

Card 4 : Contains a certain number of zeroes equal to the number of known free concentration values (e.g. 2 zeroes corresponding to known M_f and Mu_f in the above system)

Card 5 to Card 9 : Provides values of known (NK-N) and unknown formation constants (N) and values of key (e.g. key = 0 if the corresponding formation constants is to be kept constant; key = 1 if it is to be varied)

Stoichiometry is given as follows :

Consider equation (1) and (5) given in Card 2. Guess value of β in equation (1) is say 5.0×10^2 the value of metal-buffer stability constant is known to be say 7.0 then one gives :

Value of β	Power of 10	L	B	M	Mu	key
5.0	2	1	0	1	0	1
7.0	0	0	1	1	0	0

(while giving the order of reactants, known free concentration should be in the last column, Mu here)

Card 10 : TOTC (initial total concentration of reactants in millimoles (concentration of stock solution x initial volume taken in the cuvette)) followed by a number of zeroes according to Card 4, then comes ADDC (concentration of titrants e.g. ligand and buffer only, ADDC = 0 for M and Mu here) TOTC and ADDC values are given in the same order as given in the stoichio-

Card 11 : Titration points are fed in as follows :

LUIGI TITRE EMF

where LUIGI = 0 for continuation of titration point within a titration set

LUIGI = some positive number between 1 and 9 for the end of the titration set

LUIGI = some negative number between 1 and 9 for the end of all titration points.

Between each titration set cards like Card 10 are given.

TITRE : Volume of titrants in ml is given in the same order as given in stoichiometry. In the present case only ligand and buffer are being added at each titration point, but we give the same value of titre for M and Mu also (See statement 119 in the subroutine DINP of the given programme, ADDC = 0 for M and Mu).

EMF : Known concentration (M and Mu here) in p scale again in the same order as in Card 5.

Output gives the refined values of β, standard deviation of each determined values of β and concentration of all species (Total, free, and complex species at each point).